281 809

UNIVERSITY OF CALIFORNIA

SCRIPPS INSTITUTION OF OCEANOGRAPHY

VISIBILITY LABORATORY

Visibility Laboratory
University of California
Scripps Institution of Oceanography
San Diego 52, California

A STUDY OF THE FACTORS AFFECTING THE SIGHTING OF SURFACE VESSELS FROM AIRCRAFT

William Hadley Richardson

June 1962

Bureau of Ships
Contract NObs-72092

SIO REFERENCE 62-13

Project S F001 05 01

PREFACE

This study was done at the Visibility Laboratory, Scripps Institution of Oceanography, University of California, San Diego, by Mr. Richardson outside of working hours as his thesis for the degree of Master of Science in Engineering from the University of California, Los Angeles. Although the study was done at no cost to the Laboratory contracts, it is pertinent and of interest to the program of the Laboratory and, as such, is presented as a Laboratory report.

S. Q. Duntley
Director
Visibility Laboratory

ACKNOWLEDGEMENTS

The author wishes to express his gratitude to the U. S. Coast Guard and to Doctor Joseph H. Engel, Operations Evaluation Group, U. S. Navy, for making the data used herein available in readily digestible form.

The Coast Guard Air Station, San Diego, and especially Captain R. E. McCaffery, Commander D. H. Lucius, Commander E. M. Kirschner and Lieutenant Commander J. H. Tooley have been extremely helpful with comments on the work and with interpretive assistance.

The U. S. Navy Electronics Laboratory, San Diego, has been very generous with its cooperation and support in this study.

TABLE OF CONTENTS

Page

Page

ABSTRACT OF THE THESIS

A Study of the Factors Affecting the Sighting
of Surface Vessels from Aircraft

by

William Hadley Richardson

A collection of 3,465 detailed reports of sightings of surface vessels from aircraft of the U. S. Coast Guard are analyzed by probit analysis to determine visual thresholds and measures of variance of the thresholds. Each of seventeen conditions affecting the sighting range is studied separately to determine its effect. Empirical functions are developed to describe the threshold effects of each of the eleven following conditions in decreasing order of importance: (1) meteorological visibility, (2) altitude of aircraft, (3) ship size, (4) height of major swells, (5) cloud cover, (6) wind velocity, (7) relative bearing of target, (8) sun altitude, (9) relative bearing of sun, (10) wake size, and (11) wind azimuth. Thresholds are developed for the six following discrete conditions in decreasing order of importance: (12) visual aid, (13) range determination method, (14) type of observing unit, (15) time of day, (16) observer, (17) station. In each case, tables of probit results and graphs are included. Only wind azimuth is found to have an insignificant effect. Classification of data is made by mechanical card sorter, probit

analysis by electronic computer and the remainder of the calculations by desk calculator. Measures of precision are listed and χ^2, F and t tests are used at the 0.05 level. A table of factors for each condition is included to allow forecasting of sighting thresholds and explanation of use for any probability level. A random selection of sightings is made in order to supply conditions for use of these factor tables as a demonstration of forecasting and as a test of the reliability of the data and of the forecasting method. Suggestions for further study are made.

1.0 Purpose

The purpose of this study is to determine, from given data, the factors affecting the sighting of surface vessels from aircraft and to evaluate the factors and to develop a method of forecasting the sighting of surface vessels under particular circumstances.

2.0 Discussion of the Problem

2.1 Origin

The initial impetus toward the final results in this project came from the work of the Visibility Laboratory, Scripps Institution of Oceanography, University of California, and from the idea that an empirical study and analysis of actual sightings of targets would be of assistance in the Laboratory's research into vision, visibility, perception and recognition theory. The first opportunity to develop this idea came with the discovery (1956) of a series of reports of the sighting of submarines by aircraft, made under the supervision of Captain Dayton Brown, U.S.N.R., Retired, U. S. Navy Electronics Laboratory. A preliminary study of this data indicated the feasibility of statistical analysis, although there were some disadvantages inherent in the data. For example an insufficient number of conditions were reported and, most important, the data were classified under national security acts. The classification could not be removed. Since precisely this type of study had been chosen as a thesis project, the security difficulty was frustrating. However, enough work was done in the study cited to demonstrate the possibilities of extending such an investigation. It should be noted here that the implications of this initial work were borne out by the eventual conclusions presented in this paper.

At about the time that the security aspect of the first material was becoming rather discouraging, there was a fortunate development

(1958) in that a similar project was reported to have been completed recently by the U. S. Coast Guard (Appendix U and V). Investigation showed that it was a very thorough reporting of practically all of the factors affecting visibility of surface craft, that could be readily determined by a trained observer. The reports covered almost 10,000 sightings of surface craft from both surface and air craft.

The results of this project had been given to the Operations Evaluation Group, U. S. Navy, for analysis. A visit to the Group (1958) elicited the assistance of Dr. J. H. Engel, Deputy Director. He explained the scope of the Group's work and was kind enough to turn over an abstract of the data on IBM cards. From his description of their work, it appeared that more could be done than they had planned. Thus emerged the possibility of developing the Coast Guard data into this thesis.

The Operations Evaluation Group has made an internal report of their study of the data, but this material has not been released. It is sufficient to say that the approach was different from that of the study presented herein, and there is a marked difference between results, in general, and between interpretations in several cases.

2.2 Approach to the Study

The original goal of the study was a statistical analysis of the various factors affecting sighting of ships from aircraft and determination of the effect of these factors on the sighting range, thus the sighting range became the dependent variable in the relationships and the factors affecting it became the independent variables. After consideration of time and facilities available, and the appropriate scope of the study, it was decided to analyze first the sighting range in terms of each variable in turn, and then to determine which variables had significant effects. The data would not be analyzed further unless required for a satisfactory completion of the study within the stated limits. Furthermore it was decided that detailed consideration of the interaction of subclassifications of the variables would be beyond the scope of such a study. Finally, there did not seem to be a place for consideration of visibility theory at this stage of development.

The statistical concepts to be used were originally planned to be central tendency, and variance. The variation of these measures with changes in each variable were to be determined. The work was to be done on an automatic desk calculator, leaving a more thorough computer investigation for a later study based on the results of this one. Such a preliminary development had been made for the abandoned Brown data (Section 2.1) and had indicated the probable value of this approach.

2.3 Development of the Approach

While preliminary processing of the data was proceeding (1960), there was a requirement in the psychophysics research of the Vision Branch, Visibility Laboratory, for a computer treatment by probit analysis of perceptual threshold experiments. In this application a visual threshold is that point at which there is an arbitrary probability of seeing a given target. A probit analysis program (Section 2.4) was made for the Burroughs 220 computer based on a previously developed automatic calculator method of the author. A consideration of this program indicated that it would be suitable for a study of the Coast Guard data, and it was immediately evident that a threshold study of the data would be superior to, and more useful than, a straight mean and standard deviation study. It would have been intellectually uneconomical not to use the fine tool (probit analysis) that was at hand. So the standard statistical approach and the desk calculator were relinquished in favor of probit analysis on the high speed computer.

2.4 Probit Analysis

The probit analysis method comes from several diverse sources. Essentially it is a method of fitting distribution functions to weighted data obtained from experiments. Early phases of its development were motivated by the requirement for the determination of kill dosages of insecticides. The probit method is based mathematically on the maximum likelihood method for estimation of parameters. The analysis was developed principally by Fisher (8),* Garwood (10), and Finney (7), among others to be mentioned later. The transformation from experimental frequencies to normal deviates was introduced by Hazen (11), and Whipple (24) by graphical means and later developed analytically, as now used in probit analysis, by Wright (25) and Gaddum (9), apparently independently. The weighting method involved in the transformation of experimental frequencies is due to Muller (17) and was rigorously developed by Urban (21). Bliss (1 and 2) was responsible for the name "probit" and for a general description of the process.

In the development of the probit analysis method, equations of estimation were derived by the use of the maximum likelihood method. A likelihood function was set up which was proportional to the product of the probabilities of empirical ratios of number of responses to number of presentations of stimuli. Taking the

* Parenthesized numbers following authors' names refer to the corresponding numbers in the bibliography.

logarithm of this function simplified development and did not change the character of the process. The logarithm of the likelihood function was then maximized with respect to the two unknown parameters, threshold and -dard deviation, by equating the partial derivatives to zero. The result was a system of two simultaneous equations which could lead to determining the unknown parameters mentioned above. The simultaneous system generally could not be solved by direct methods but could be solved approximately by iteration after expanding in Taylor's series and using trial values of the parameters. The solution of the equations was further simplified by substituting for the threshold and standard deviation their equivalents in terms of the slope and intercept of the linear transformation from the stimulus domain to the normal domain, since the new trial parameters could be found readily, either graphically, or analytically by the method of least squares, or other fitting method. The solution of the transformed system of simultaneous equations was then formulized after introduction of a device called the working probit, which further simplified the formulation.

The probit analysis method is adaptable to many experimental problems involving cumulative quantal data. The method is in use in psychophysical research at the University of Michigan and the University of California. It has been adapted for desk calculator use by Kincaid and Blackwell (13), and by the author (18); to digital computers by Moldauer and Kincaid (16) for MIDAC, by Lamphiear and Wendel (14) for IBM 650, and by the author for

Burroughs 220 (future publication) and CDC 1604 and IBM 7090 (future publication).

The adaptation used in this project is that of the author for the Burroughs 220 (future publication) which in turn is based on his adaptation for desk calculators (18). Given cumulative positive responses to stimuli over the range of the stimuli, ratios or empirical probabilities are calculated and transformed to abscissas of the normal distribution function, normal (0,1), that is with mean of zero and standard deviation of one. Finney (7) uses a 5-biased normal distribution, normal (5,1), to avoid negative abscissas. The resulting abscissa is called the probit, hence the name of the method. In the digital computer treatment negative abscissas are no disadvantage so the 5-bias is not used, though the liberty is taken of calling this abscissa a probit also, since the use is the same. The probit which has been determined is termed the empirical probit. A trial linear transformation function of the form $y = a + bx$ to transform from the experimental domain to the normal domain is determined, in this method, by the method of least squares. The resulting probits, y, corresponding to the experimental stimulus points, x, are termed trial probits. Having determined the trial probits for the range of stimuli, the weighting factor is applied to account for the instability of the empirical probabilities toward the tails of the distribution function. All of the requirements are now available for the solution of the maximum likelihood system. The solution is facilitated by the introduction

of the working probit, sometimes and incorrectly called the corrected probit, which allows a simply calculated, next approximation to the parameters of the transformation function. Approximate values of the threshold and standard deviation are determined directly from the parameters and are used to make a χ^2 test of the relation between the empirical frequency ratio and the ratio calculated from the threshold and standard deviation. If the test shows a significant difference, the transformation parameters are used as corrected trial parameters to reenter the process in order to improve the results by iteration. The computer application used in this project continues iteration until an acceptable χ^2 value results or until the process begins to diverge. If an acceptable χ^2 value results, the final approximation of the threshold and standard deviation are recorded.

The flow of the computation is shown in Appendix W.

It may be of interest that the computer process requires a computation time of 2 to 3 seconds, since card input of data is folded into the computation. Print-out time is about 30 seconds since a Soroban teletype printer is used. Use of an IBM 407 printer would cut overall problem time to about 5 seconds.

3.0 Discussion of the Analysis Process

3.1 Sorting

The initial step in processing the mass of data was to separate the air sightings from the 10,000 cards that included both air and surface sightings. This was done on an IBM mechanical card sorter and the cards were sorted both by type of observing vehicle and by observer to assure that no surface sightings were included in the 3,465 cards, each of which documented an air sighting. This sorting was done before the decision was made to use probit analysis. The data were next sorted to classify them for a standard statistical analysis. This sort was with respect to the dependent variable, sighting range. The range of the variable was checked and it appeared that the last class should include 22 miles and more, since any further classes would contain too few sightings for reliable analysis. This procedure was very convenient: the optimum number of classes from the standpoint of both reliability and practicality is usually taken as from ten to fifteen; thus, using an increment of two miles from zero to twenty-two miles, there were twelve classes.

3.2 Counting and Tabulating

The card sorter was equipped with a counter and the next procedure was to sort each class of the dependent variable into classes of an independent variable and then rerun each class of the independent variable to determine the count. Here the number of classes does not depend on statistical theory but on a logical division of the ranges of the independent variable so as to give useful results in the case of a continuous type variable. Some of the independent variables were inherently broken down into discrete classes as in the case of the visual aids used. The result of this sort and count on the seventeen independent variables was tabulated and produced seventeen frequency matrices.

3.3 Arranging for Probit Analysis

One more processing step remained before the data could be presented to the computer. Probit analysis treats cumulative distribution functions and not Gaussian frequency functions. A distribution matrix was compiled with each class of the independent variable becoming a distribution function vector with respect to the sighting range. In other words, the sighting range then became the independent variable for probit purposes, and the frequency within the class of the independent variable became the dependent variable, or distribution function of the sighting range. This resulted in 147 probit problems.

In sorting and counting on the independent variables, cards coded for no-report-entry or anomalous entry were tabulated and given a balancing check against the over-all count. They were also included in the probit analysis of the variable as an extra class, but no significance was noted other than that, as sighting conditions become more difficult, observers tend to be more meticulous (which was inferred from the lower proportion of faulty cards).

The data were ready for computer manipulation at this point.

3.4 Computer Processing and Problems in the Probit Analysis

The data were now punched into cards for entry to the computer. The original classification was followed, each sighting range increment of two miles becoming a point determining the distribution. In general this gave twelve points on the abscissa for even numbered miles. The distribution functions were found to be of the log-normal type, considered to be a result of the exponential attenuation of radiance and contrast. The computer program provided for both normal and log-normal distributions. The input data called for a selection of log-normal analysis and the computation was started on this basis. Apparently a major task in the processing had been completed and the results of the computation were ready for analysis of effects and trends. Unfortunately this proved not to be the case.

The computer output consists of the parameters of the probit transfer function, the threshold, the fiducial limits, the standard deviations of the data, threshold, standard deviation and parameters, and last, but far from least, the χ^2 measure of goodness of fit.

An examination of the χ^2 measure showed that only a little over half of the functions were fitted at the 0.05 level, which had been selected as the acceptable criterion. The unacceptable functions were checked and end points in the tails of the distributions, that showed very small numbers in the frequency table, were stripped out. This is usual procedure in probit analysis, since it does not affect the results, and the instability in the tails may affect the

χ^2 measure, not the essential character of the distribution. Reruns were made of the unacceptable data sets and, while there was a marked gain in production, there was still about a quarter of the sets that were not acceptable.

It was at this point that what had been noticed as an interesting sidelight in the data counting became a matter of crucial importance: it had been evident in the sorting and counting that observers tend to estimate, or round off, to multiples of five, and the stacks in these bins were disproportionately high. It was now evident that, with the relatively fine definition of a two mile increment in sighting range, this tendency was introducing an extraneous scallop in the distribution functions.

An obvious method of removing this scallop was to increase the increment in the sighting range so that the data divisions were located at points where the data character was consistent, such as on multiples of five miles. Here the sorting on even miles might have been a possible handicap, for the only alternative to resorting and recounting the basic card deck was to choose the divisions of the existing sort that included the multiples of five miles. This course was decided for trial, and all of the data sets were set up again with abscissa points at zero, four, ten, fourteen and twenty miles, since these included the five mile divisions. The results of this run were gratifying, for only about a tenth of the problems were not acceptable at the 0.05 level and most of these were acceptable at the 0.01 level. This last level was not considered acceptable and

the tail points with very few numbers were stripped out. Most of these were equivalent to probabilities of less than 0.01 and in no case as much as 0.03. It is of interest to note here that many of the acceptable problems included probabilities of less than 0.01, which is not usually expected. A rerun was made of the stripped problems and, out of those that might be expected to give good results, only three remained unacceptable at the 0.05 level. That is, the few others remaining had less than six sightings to a problem.

While one can solve for any probability threshold in probit analysis, depending on the needs of the analysis, in this study the 0.5 threshold is found. This is also known as the "50% threshold," or the "mean threshold." It is the point at which the probability of sighting is 0.5, or that point at which an observer is as likely to see as not to see an object. The conversion of the 0.5 threshold to a threshold of any other probability is given later.

3.5 Development of the Produced Data

3.5.1 Tables

The computer-processed results are tabulated (Appendices A through P) to show the initial data and the probit analysis parameters: threshold (T), standard deviation of the distribution (s), standard deviation of the threshold (s_T) and the chi-square measure of goodness of fit (χ^2). Where a small probability tail value is dropped, it is shown in parenthesis.

The mean standard deviation ($\bar{s}$), the standard deviation of the standard deviations (s_s), the standard deviation of the mean standard deviation ($s_{\bar{s}}$) were also added to the tables.

3.5.2 Graphical Display

The thresholds are plotted on graph paper, in a linear plot or in a logarithmic plot if this appears appropriate. (Appendices B through P). This procedure aids in determining the type of empirical function to be fitted to the data. Where a sine or cosine type curve appears suitable, double plotting is used to facilitate visual interpretation. In this case the original plot is made and the supplement or complement of the angle is used to plot the corresponding thresholds on the same abscissa axis.

3.5.3 Fitting Empirical Functions

After a survey of the data graphs, empirical functions are fitted to the threshold data using standard least square methods of fit. In the case of parabolic functions, Cholesky's method (19) of reduction of matrices is used in the solution of the normal least square equations. This method greatly facilitates the solution of simultaneous linear systems. It is described by Salvadori and Baron (19). The simplest function is chosen which gives a high correlation coefficient and preserves the character of the data. These functions are added to the tables along with a factor function (f) which is the empirical function normalized to the normal range which will be described in the section on the general distribution of sightings (Section 4.1). Functional threshold values are then calculated and added to the graphs for comparison purposes.

3.5.4 Testing for Significance

Maximum and minimum functional threshold values are tested to determine whether or not the effect of the variable is significant. The t test for difference of two means is used, based on Student's t distribution. The only case of insignificant effect is that of wind azimuth which is to be discussed in detail in that section.

3.5.5 Notes on Results

It is very important to keep in mind that, while the threshold T is in the linear domain and dimensioned in nautical miles, s , s_T , $\bar{s}$, $s_{\bar{s}}$ are in the logarithmic domain and are dimensionless constants in this application. χ^2 , t and F also apply to the logarithmic domain.

To use the standard deviation as a probability tool in determining a threshold of other than 0.5, the following relationship holds:

$$T(p) = T e^{-D(p)s} .$$

where $T(p)$ is the threshold for the desired cumulative probability p .

T is the threshold which is always for a $p = 0.5$ in this study.

$D(p)$ is the normal deviate for the probability p .

s is the standard deviation.

The reason for the negative exponent in the above relationship is that these are reverse distribution functions; the distribution function is monotonically decreasing in the positive abscissa direction.

The above formula is specialized and, if the user is working in other units than nautical miles, T must be converted to the new units in order to compute $T(p)$. The s is not converted in any way.

It is interesting to note the extreme sensitivity of the probit analysis technique in conjunction with the χ^2 test. Twenty of the problems, not acceptable on the first run, are made acceptable by removing the very small numbers in the extreme tails of the distributions. In nineteen of the problems, this change results in an average reduction of χ^2 from 10.253 to 1.894 while there is an average absolute change of only 0.00965 of the value of the threshold. This result definitely indicates the inherent stability and excellence of the method. In the one remaining problem, removing the small tail number proportionally changes the threshold 0.186 while reducing χ^2 from 72.157 to the magnitude of 10^{-11}. It is surely a coincidence with the criterion of acceptance that this one reading is 0.05 of the twenty readings in this category.

4.0 The Analysis: Discussion of Graphs and Tables

In this section a detailed discussion is made, where appropriate, of the input data to, and results of, the probit analysis. In particular, comments are made on the graphical evidence and empirical function determination. The empirical threshold function, T(.); the normalized threshold or factor function, f(.); and the correlation coefficient, r are stated in this section. Any other significant observations are included with each variable treated.

The mean of the computed standard deviations is entered in the appendix tables for information and possible use, since the standard deviations of the thresholds appear generally level enough so that the mean standard deviation might well be used through the range of most of the variables.

4.1 General Distribution (See Appendix A)

In this case all records that have sighting ranges are lumped together and a distribution set up. The data shows a typically log-normal character. The probit calculation gives a threshold of 6.599 nautical miles with a χ^2 of 4.308, which is acceptable at the 0.05 level.

This threshold for all sightings is based on 3,465 sightings taken on the Atlantic and Pacific coasts from Puerto Rico to Alaska and should be a representative measure of central tendency of the class of all sightings of surface vessels from aircraft. This conclusion is borne out by the estimate of the coefficient of variation of the threshold, 0.0015. Hence this threshold range, 6.599 miles, is taken as the standard reference range in this study and is used as the normalizing range where normalization is carried out, as in the development of the threshold factors. This range is called the "normal range," T_N, and is so marked on the graphs.

4.2 Meteorological Visibility (Appendix B)

Meteorological visibility is defined as follows by the U. S. Weather Bureau (23): "... the greatest distance toward the horizon that prominent objects such as mountains, buildings, towers, etc., can be seen and identified by the normal eye, unaided by special optical devices, such as binoculars, telescopes, glare eliminators, goggles, etc., and which distance must prevail over the range of more than half the horizon." Granting that this procedure does not present a rigorous measure of atmospheric turbidity, it is still the best one now in general use and is the one in which all observers are trained, have used, and that most will use for some time to come. However it should be noted that precise definitions of visibility have been formulated in terms of "meteorological range," a quantity that can be defined analytically, measured instrumentally and used in the solution of visibility problems.

The 0 - 1 mile visibility classification has only three sightings, one at six miles sighting range and two at zero miles. While the cumulative data are routinely introduced in the probit analysis, this classification, as might be expected, gives a T of the order of 10^{-11}, s of 10^{-38}, s_T of 10^{-42}. Any further consideration of this classification is ruled out. There is an apparent anomaly in the data for the classification of 10 - 19 miles visibility between the sighting ranges of ten and twenty miles. Numerous efforts with various combinations of input result in no convergence at the 0.05

level. The count has been rechecked and the only possible conclusion is that this is one of the things that sometimes happens. This is the only case in this study where the 0.05 acceptance criterion is relaxed. The data included for this classification in the appendix are acceptable at the 0.01 level with a χ^2 of 10.094 and are the best fit obtained. The next best fit is at a χ^2 of 15.837 which has a proportional difference of 0.00239 from the accepted threshold. Since the stability of the mean is established thus, and because of the fact that all other results group very closely about the accepted threshold, the number that appears in the table is accepted. This procedure is admittedly subjective reasoning to a certain extent but it is a considered judgment.

A plot on semi-logarithmic paper shows a distinct linearity of the type $T(V) = a + b \ln V$. A least square fit gives this equation:

$$T(V) = 3.476 \ln V - 2.064, \quad V = \text{Visibility}$$

$$f(V) = 0.527 \ln V - 0.313$$

$$r = 0.969$$, in the logarithmic domain.

The sighting range may well approach an asymptote as visibility increases, but there is insufficient evidence to determine this effect at this time.

A point of interest in the threshold table is the sharp and (at first thought) surprising drop in sighting range with unlimited visibility. It would appear that when an observer has no definite landmarks but good, clear air, he terms this condition "unlimited."

However, if he states visibility is 70 miles, he doubtless identifies an object at that known range. May we assume that the classification "unlimited" really means, "I think I can see a long way"? Meteorologists agree with this assumption and consider that a report of unlimited visibility should be taken to mean "more than fifteen miles."

4.3 Altitude (See Appendix C)

The data on this variable require discussion only in the 9,000 foot classification. No difficulty is involved in the solution of any of the other classes. The usual run at 9,000 feet including the multiples of five miles sighting range gives anomalous results. Previously, when run at increments of two miles, acceptable results had appeared, and even better results with respect to χ^2 had occurred on increments of four miles. This last interval is the number used. The irregularity results no doubt from only seven sightings at this altitude. The data shows a linear trend in a semi-logarithmic domain with a functional form of $T(A) = ae^{bA}$. The best fit function is:

$$T(A) = 5.385\, e^{0.116A}, \quad A = \text{altitude in 1000's of feet.}$$

$$f(A) = 0.816\, e^{0.116A}$$

$$r = 0.963, \text{ in the fitting domain.}$$

There is no apparent reason for the reverse trend from 2,000 to 4,000 feet, such as a general hemispheric tendency to a 3,000 foot haze layer. The linear plot shows close grouping about the fitted line. Hence no attempt is made to fit a cubic equation. This might be a matter for further investigation.

4.4 Ship Size (See Appendix D)

The data here appear unremarkable, and the probit analysis presents no difficulty, requiring reruns only where there are four and five tail sightings in the classes: less than 30 feet bright-colored; 30 to 60 feet bright colored.

It is in this variable that the only major criticism of the report form (Appendix V) arises. The dimension of the variable changes at 100 feet from length to tonnage. This discontinuity requires a transformation from tonnage to length. With the help of Fahey's catalog of U. S. Navy auxiliaries (6), a function is developed to effect this transformation. It appears that the list of auxiliaries is a representative cross-section of ships that a Coast Guard patrol would sight. The function adopted is:

$$L = 21.4 \ T_W^{1/3} - 16$$

where T_W is full load tonnage and L is length in feet. This function has a correlation coefficient of 0.985. (See Appendix D-3 and 4)

After transforming the data tonnages to length, the threshold data show a very decided linearity in the semi-logarithmic domain of the type $T(L) = a + b \ln L$. The best fit function is:

$$T(L) = 1.844 \ln L - 1.100, \quad L = \text{Length in feet}$$

$$f(L) = 0.280 \ln L - 0.167$$

$r = 0.982$

The effect of shading of target might be handled in a number of ways, but various trials show that a simple and satisfactory correction is to add 0.279 miles to the threshold for bright vessels and subtract 0.279 miles for dark vessels, both types under 100 feet. There is insufficient basis to apply this correction to larger targets. The correction is based on a fit made to the separate bright and dark classes.

4.5 Height of Major Swells (See Appendix E)

There is no need to comment on the data here other than to mention that mean swell height for the ten-feet-and-more classification is 15.381 feet and is so used in the fitting process. The probit analysis turns out well.

The data show a sufficient linear trend to adopt an empirical function of the $T(S) = a + bS$ type. The fit produced is:

$$T(S) = 6.170 + 0.239\ S\ , \quad S = \text{Swell height in feet}$$

$$f(S) = 0.935 + 0.0362\ S$$

$$r = 0.707$$

The correlation coefficient is not as large as would be desired, due mainly to the two highest values. Including these values might be questioned, in view of the few sightings in these classifications. However they show no anomalies, have $p(\chi^2)$ values of greater than 0.9 and 0.4 respectively, and they straddle the fitted line. It is considered better to retain them, lacking further evidence.

It may seem surprising that one sees objects better in higher swells, but there may be three causes for this. One is the relative motion of the object with respect to the water masses, which attracts attention. Another is that the higher swells break up the grazing reflection of the brighter horizon sky. A third perhaps is that the object is seen against a surface sloped toward the observer which may have some effect by giving a generally darker background rather than the horizon sky reflection. This same trend has been noticed by

Coast Guard observers.

4.6 Cloud Cover (See Appendix F)

No difficulty is encountered with this data or with the probit analysis. An inspection of the linear plot clearly indicates a parabolic fit of the form $T(C) = a + bC + cC^2$. The least square method gives:

$$T(C) = 7.069 + 2.871C - 4.717C^2, \quad C = \text{Cloud cover in decimal fraction}$$

$$f(C) = 1.071 + 0.435C - 0.715C^2$$

$$r = 0.903, \text{ in the linear domain}$$

The maximum value of this function, $T(0.304) = 7.506$ miles threshold, bears out informal Coast Guard impressions that an observer sees best with about one-third cloud cover. This may be a result of diminution of surface glare and glitter with enough direct lighting remaining to give good contrasts.

4.7 Wind Velocity (See Appendix G)

The one sighting of 45 - 49 knots is disregarded. At 50 knots and greater there are only four sightings. The probit analysis is good until the 50 knot results are inspected carefully. Here the parameters of the probit transfer equation are of an entirely different magnitude and character from the rest of the family. Since there are so few sightings (and this is an extremely erratic threshold of low dependability: $S_T = 0.43$ in the log domain) it is rejected. The other two erratic points are accepted. There is no clear reason for their rejection.

The accepted thresholds, when plotted, indicate a parabolic trend of the type $T(WV) = a + bWV + c(WV)^2$. The best fit is:

$$T(WV) = 5.488 - 0.142\ WV - 0.002673(WV)^2$$

WV = Wind velocity in knots

$$f(WV) = 0.832 + 0.0214\ WV - 0.000405(WV)^2$$

$$r = 0.531$$

Here the correlation coefficient is lower than desirable, due to the two erratic points included. However, the empirical function is the only simple function typical of the trend of the data. The maximum value of the function, $T(26.6) = 7.378$ miles indicates the best seeing is where the meteorologists say a breeze becomes a gale between 27 and 28 knots, or between force six and force seven winds on the Beaufort scale. This conclusion is reasonable since in this

velocity range the surface becomes very disturbed and spray and foam appear. This condition explains the different character of the variable, WV , from that of swell height.

4.8 Relative Bearing of the Target (See Appendix H)

This variable is also termed "clock code" in the report form (See Appendix V). The data show very few sightings in the rear field of view. This sighting lack raises the question of the practicality of designing patrol planes with tail observations a major factor.

The probit analysis gives good results although the character of the few sightings at seven o'clock defeats efforts to determine an acceptable threshold. The low number of sightings to the rear and their somewhat erratic behavior make it tempting to discard them. However, double plotting shows the data are consistent in character and follow a cyclic pattern of the type $T(B) = a + b \cos B$. The best fit function is:

$$T(B) = 6.046 + 0.808 \cos B$$

$$B = \text{Relative bearing or } 30 \cdot (\text{clock code}) \text{ degrees}$$

$$f(B) = 0.916 + 0.122 \cos B$$

$$r = 0.697$$

Again, the relatively low r is the result of the erratic rear sightings. However, a polar plot of this function shows an apparently less erratic trend to the rear.

4.9 Sun Altitude (See Appendix I)

Here the only case demanding comment is that at 90 degrees where there are only six sightings. The probit analysis does not give an acceptable fit and this classification is disregarded. Otherwise the probit analysis is normal.

A survey of the plotted thresholds indicates an empirical function of the type $T(SA) = a + b \sin(SA)$, and the least square method produces:

$$T(SA) = 7.795 - 1.564 \sin(SA), \quad SA = \text{Sun altitude: } 0^\circ \angle SA \angle 90^\circ$$

$$f(SA) = 1.208 - 0.238 \sin(SA)$$

$$r = 0.915 \text{ in the fitting domain}$$

Thus, it appears that seeing deteriorates with increasing sun altitude. This conclusion seems reasonable since a low sun results in stronger internal contrasts in the target while a high sun gives a flatter lighting.

4.10 Relative Bearing of Sun (See Appendix J)

This bearing is with respect to the target. The data here is worthy of comment in that the total number of sightings in each classification of bearing alternate in magnitude with the high number applying to the classifications containing the four major divisions of the circle, multiples of 90 degrees. There is no probit trouble and every problem develops acceptably the first time.

Double plotting of the data (as in Section 3.5.2) clearly indicates an empirical cyclic function of the type $T(SB) = a + + \cos(\pi - SB)$. The character of the data necessitates the phase shift. The fitting process gives:

$$T(SB) = 7.043 + 0.342 \cos(\pi - SB), \quad SB = \text{Sunbearing in degrees}$$

$$f(SB) = 1.067 + 0.0518(\pi - SB)$$

$$r = 0.987 \text{ in the fitting domain}$$

This conclusion shows, as might be expected, that an observer sees better with the sun behind him as he looks at the target. However, the change from minimum to maximum of 6.701 miles to 7.385 is not as great as one might expect.

The question may be raised why the minimum threshold is greater than the normal range. Does one expect, on the basis of this behavior, always to see better than the normal range? Examination of the

data leads to the explanation that in total overcast, cloud cover of 1.0, relative bearing of sun with respect to target is frequently not reported and under these overcast conditions the threshold is much less than the normal range.

A further point of interest is that the alternate classifications with low numbers of sightings, mentioned above in the first paragraph, are also the classifications having the larger thresholds. Perhaps this distribution means that those who are meticulous in noting exact bearing, rather than the nearest 90 degree direction, are also more meticulous and alert in their search operation.

4.11 Proportional Wake Size (See Appendix K)

This is the last of the conditions that lead to a continuous type threshold function and, in effect, the least important. The choice of proportional instead of actual wake size was due, doubtless, to plan rather than fortune. This proportional measure automatically rules out such aberrations as might result from large slow ships with little wake in comparison with small fast vessels leaving large wakes. The effect here is small though significant statistically.

The data appears good as is proven by no failures on the first probit runs. A survey of the plotted thresholds indicates an exponential curve approaching a non-zero asymptote. The type curve is $T(WS) = a + be^{c(WS)}$. Taking the asymptote, $T(WS) = a$, to be the threshold of the classification defined as greater than twice the length of the vessel, the following function develops:

$$T(WS) = 7.295 - 1.066e^{-1.284(WS)}, \quad WS = \text{Wake size, as a multiple of ship length}$$

$$f(WS) = 1.105 - 0.162e^{-1.284(WS)}$$

$$r = 0.920 \text{ in the fitting domain}$$

The correlation is even better in the linear domain so no attempt is made to determine the asymptote analytically, a doubtful procedure at best with as few data points as are available here.

4.12 Wind Azimuth (See Appendix L)

It is unfortunate that the definition of wind direction as an azimuth was prescribed in the report form (see Appendix V). It seems very unlikely that wind azimuth would show a significant effect on thresholds of sightings, whose azimuths must be assumed to be more or less random. A much better and more valuable definition would be wind bearing with respect to target, in the same manner as sun direction is defined.

The data show no anomalies, and the first probit run gives a total success with excellent χ^2 values.

The plotted thresholds exhibit an undistinguished scatter about the normal range. A fit of $y = a$ type produces $a = 6.556$. A t test shows that this distribution is not significantly different from the normal range and a χ^2 test shows the points normally distributed about the normal range with $0.95 \angle p(\chi^2) \angle 0.98$. It is necessary to disregard any effect of this condition.

4.13 Visual Aid (See Appendix M)

This is the first of the conditions that must be treated discretely, and it has the greatest effect, considering the spread between the high and low thresholds. Binoculars show a great advantage from a threshold standpoint, but this must be a questionable advantage when only 0.01 of the sightings are made with them. The interpretation might well be that, <u>if</u> an observer sees a target with binoculars, he sees it farther away. Probably a more factual interpretation is that observers do not consider binoculars valuable as a search aid.

The difference between no visual aid and the use of sunglasses is very important however. Many people feel that, since sunglasses protect the eyes from glare and strong light and are more restful, they are an aid to vision. The advantage of eye relief is evidently outweighed by the attenuation of contrast in the colored lens and the consequent threshold reduction. A t test shows a strong significance here and it is necessary to accept the definite difference between using and not using sunglasses. The results are tabulated:

	T	f
Binoculars	8.908	1.350
No aid	6.637	1.002
Sunglasses	6.265	0.949

4.14 Range Determination Method (See Appendix N)

The results of this probit analysis are somewhat surprising. It had not been considered that the means by which sighting range was determined after the sighting would have any effect on the threshold. However, the following explanations may be worth considering. If an observer estimates the sighting range with radar, the inference is that he has his radar activated prior to sighting and picks up the target on it, thereby having a strong clue as to where to look. His advantage over the uninformed observer is obvious. The other explanation, possibly valid, is that while time-distance checks (calculating distance by speed, and time to reach target) are quite accurate, and this is borne out by the threshold developed, the unaided observer tends to underestimate distances. A tabulation of results follows:

	T	f
Radar	8.611	1.298
Time-distance	6.629	1.001
Estimate	6.147	0.923

4.15 Type of Observing Aircraft (See Appendix P)

The results here are interesting and may well measure the effectiveness of the types of sighting craft. However missions and method of operation should be considered. Considering operating altitude, the measure of effectiveness becomes weaker. The operating altitudes are not normally distributed but are more nearly log-normal. The log normal means are computed and the following table shows probit results with a consideration of altitude added:

Type	T	f	Mean Altitude	T(Altitude) (Expected)	T/T(Alt.)
Patrol	6.694	1.014	1278	6.247	1.072
Utility	5.836	0.884	1083	6.107	0.956
Helicopter	4.836	0.733	606	5.778	0.836

While this analysis is not too precise, the T/T(Alt.) measure is slightly more generous to the utility plane and the helicopter than is the f measure. Again, a consideration of missions might alter these indications.

4.16 Time of Day (See Appendix P)

This condition is defined for day, twilight, and night, since sun altitude takes care of lighting variation during the day. The usefulness of the thresholds of this condition are open to question since the t test at the 0.05 level shows a significant difference between day and twilight but not between day and night. The thresholds for twilight and night may be taken as the same. However the populations sampled may be different. At night it is probable that many of the sightings are of lights, not ships as in daytime. In view of the day-twilight significance, the factors are tentatively accepted. This subject merits further study.

The computed values are tabulated as follows:

	T	f
Day	6.614	1.002
Night	5.583	0.846
Twilight	5.496	0.833

4.17 Observer (See Appendix Q)

Here the pilot and copilot appear to observe equally well, and this is confirmed by the t test with a p(t) of 0.920. There is a significant difference between pilot-copilot and bow lookout. This might seem unusual unless one considers the situation of the bow-lookout and his excellent view almost straight down. It is a great temptation to concentrate on the area directly under him when he realizes he sees better there. As far as the waist lookout is concerned, he would be expected to see less well than the pilot-copilot since he is looking to the side. The data from the section on relative bearing of the target shows that at 90 degrees he would expect to have a threshold at about 6.2 miles. He is still seeing less than this, though perhaps not significantly so.

A table of thresholds and factors follows:

	T	f
Pilot	6.603	1.0006
Copilot	6.616	1.002
Waistlookout	5.853	0.887
Bowlookout	5.553	0.841

The low number of three sightings by the tail lookout reinforces the previously inferred suggestion that this search position might well be abandoned. Tail observations were not considered here.

4.18 Station (See Appendix R)

The data are presented herein but no analysis was attempted. There are too many extraneous influences, such as local weather and local operating procedures and policies, to permit analysis of the effects within the restricted scope of this study.

There is certainly a fertile field here for cultivation by a full scale operations research study.

One small scale operations study was carried out after a number of very odd quantities showed up in the card sorting. These were such reports as a bearing of 540 degrees, a sighting range of 85 miles, cloud cover of 1.40 and so on. Curiosity suggested pulling out these cards to see what they might have in common. It was first found that they all come from the same station. A further investigation showed that they were all made on the same day, 1 January 1956. The reader is left to his own inference.

4.19 Tabular Extract of Threshold Factors (See Appendix S)

The factors (thresholds normalized to normal range) are included in Appendix S and need no comment.

5.0 The Test (See Appendix T)

The original plan was to present the preceding analysis of the sighting data as the complete study. It became a matter of curiosity to see if the normalized thresholds could be used to forecast sighting thresholds. The results of this curiosity are so gratifying that they are included as a test of the process and as a demonstration of the possibilities that further and more detailed work may develop.

o

5.1 Description

The entire deck of cards recording air sightings were disarranged by sorting on the second digit of the wind azimuth number, a classification that should result in no pattern. Then 20 cards were drawn at approximately equal increments of distance through the length of the deck. This procedure should give a random assortment of sightings and a survey of the reconstituted records shows this to be apparently true. (See Appendix T - 3 ff.)

The factors corresponding to the conditions of a particular sighting are taken from the factor tables in Appendix S and the product of all of these and the normal range give the calculated threshold for that sighting. This technique is followed without consideration, at this stage, of the reported range. If a condition is not reported, it is omitted, which is essentially judging that the expected value of this condition pertained at the time of the sighting.

5.2 The Results (See Appendix T)

The results of the twenty computations are plotted on the graph against the reported value. A mean line is included, as is the ideal line. If the forecast were perfect, the computed points would be expected to be normally distributed about the ideal line. As it results, a χ^2 test shows the points are normally distributed about the mean line with a $p(\chi^2)$ between 0.90 and 0.95.

The correlation coefficient, 0.695, shows the strength of the trend. The coefficient is not expected to be high for the computed points are forecasted thresholds, and sightings based on the conditions determining the forecast should vary normally with resepct to the threshold.

These results suggest strongly that thresholds can be effectively forecasted by proper consideration of the conditions affecting sighting at the time.

6.0 Conclusions

6.1 General Observations

The limited scope of this study precludes detailed study of all the inter-relations suggested by the work on the data. Some of the deficiencies are that dependence of variables is treated only superficially; trends of sub-classes of the conditions are not determined; complete study of the few anomalies occurring in the computations are not possible at this time. However it appears that the study indicates a positive method of forecasting sightings and sighting probabilities. Further, it would seem that, until more conclusive information is available, the factor table as it stands might well be a valuable tool in forecasting.

It is not possible to estimate the total number of possible sightings in any particular case, since sightings not made generally cannot be reported. In a standard analysis of variance procedure the missed sightings would lead to an obviously erroneous result. However one must assume that these missing possibilities are accounted for, to a certain extent, in probit analysis which considers, in fitting a curve to the data, the character of the distribution function as well as the numerical values of the frequencies. This assumption is further reinforced when the characteristics of the log-normal distribution are reviewed. In a normal distribution the missed sightings would result in a cumulative probability of less than one at zero range which infers that it would be possible,

technically, to compute some sightings at negative range. This situation is not true in the log-normal case for the cumulative probability at zero range must be one.

It is possible that further development of the probit analysis method will allow accounting for these missed sightings.

6.2 Value of the Study

This study is expected to be of value in vision and visibility research as a factual basis for checking theoretical studies.

The matter herein should be of use to the Coast Guard and Navy in refining search procedures and methods as defined in the "National Search and Rescue Manual" (22).

The study should also be of use in any operational research involving searching and visibility at sea.

6.3 Further Studies Suggested

The most apparent future project is a similar analysis of the sightings from surface craft and a comparison with these results.

There is a fertile field for anyone interested in the psychological study of the choice of values when estimating quantities and related fields. In some processes observers tend to prefer the number seven to eight, while in others, the reverse is true. It is understood that much research has been done on this subject, and this basic data should yield a mass of supportive evidence.

Further analysis of perturbations in the distributions other than those caused by choice of numbers would be desirable. The fact that, in distributions involving large numbers of sightings, high χ^2 values generally occur would indicate that in the limit these populations might wander from the log-normal.

Additional investigation would probably determine asymptotes at extremes of some of the variables, such as altitude and meteorological visibility.

Further investigation should be made of twilight and night sightings with perhaps a data collection program incorporated.

The odd curvature indicated by the altitude data is intriguing and suggests an attempt at determination of whether these two points of inflection are real or only coincidental vagaries. It might be that there is a haze layer or other condition generally existent which causes such an effect.

Further study should be made of the few erratic thresholds noted in the discussion to determine whether or not they are simple manifestations of probability theory.

Finally, one definite recommendation: the Coast Guard and other search agencies should give serious thought toward eliminating tail lookouts, since, as was noted above in Sections 4.8 and 4.17, the probability of stern sightings is close to zero.

BIBLIOGRAPHY

1. Bliss, C. I., "The method of probits," Science, 79, 38-9 (1934).
2. Bliss, C. I., "The method of probits - a correction," Science, 79, 409-10 (1934)
3. Cramer, H., The elements of probability theory, Wiley, New York, (1955).
4. Cramer, H., Mathematical methods of statistics, Princeton University Press, Princeton (1951).
5. Diamond, S., Information and error, Basic Books, New York (1959).
6. Fahey, J. C., The ships and aircraft of the United States Fleet, 6th ed., Ships and Aircraft, Washington (1954).
7. Finney, D. J., Probit analysis, 2nd ed., University Press, Cambridge, Eng. (1952).
8. Fisher, R. A., Appendix to C. I. Bliss, "The case of the zero survivors," Ann. Appl. Biol. 22, 164-5 (1935).
9. Gaddum, J. H., "Reports on biological standards. III. Methods of biological assay depending on a quantal response," Spec. Rep. Ser. Med. Res. County of London, No. 183 (1933).
10. Garwood, F., "The application of maximum likelihood to dosage-mortality curves," Biometrica, 32, 46-58 (1941).
11. Hazen, A., "Storage to be provided in impounding reservoirs for municipal water supply," Trans. Am. Soc. Civ. Engrs., 77, 1539-1669 (1914).

12. Hoel, P. G., Introduction to mathematical statistics, 2nd ed., Wiley, New York (1955).

13. Kincaid, W. M., and H. R. Blackwell, Application of probit analysis to psychophysical data. I. Techniques for desk computation, Report No. 2144-283-T, Vision Research Laboratories, University of Michigan, Ann Arbor (1958).

14. Lamphiear, D. E., and J. G. Wendel, Probit analysis program for IBM Type 650, Report No. 2144-1102-M, Vision Research Laboratories, University of Michigan, Ann Arbor (1957).

15. Lindquist, E. F., Design and analysis of experiments in psychology and education, Houghton Mifflin, Boston, (1953).

16. Moldauer, A. B., and W. M. Kincaid, Applications of probit analysis to psychophysical data. II. Techniques for the Michigan Digital Automatic Computer (MIDAC), Report No. 2144-289-T, Vision Research Laboratories, University of Michigan, Ann Arbor (1957).

17. Müller, G. E., "Über die Maassbestimmungen des Ortsinnes der Haupt mittels der Methode der richtigen und falschen Fälle," Pflüg. Arch. ges. Physiol., 19, 191-235 (1879).

18. Richardson, W. H., An adaptation of the method of probit analysis to psychophysical threshold data, SIO Reference 60-47, Visibility Laboratory, Scripps Institution of Oceanography, University of California, San Diego (1960).

19. Salvadori, M. G., and M. L. Baron, Numerical methods in engineering, Prentice-Hall, New York (1952).

20. Shaycroft, M. F., and J. W. Altman, _A procedure for evaluating graduate research on the basis of the thesis,_ American Institute for Research, Pittsburgh, Penna. (1955).

21. Urban, F. M., "Die psychophysichen Massmethoden als Grundlagen empirischer Messungen," _Arch. ges. Psychol._, 15, 261-355 (1909); continued 16, 168-227 (1910).

22. U. S. Coast Guard, _National search and rescue manual,_ CE-308, Departments of The Army, The Navy, The Air Force; The Treasury and The Air Coordinating Committee, Washington (1959).

23. U. S. Weather Bureau, _Circular N,_ 5th ed., p. 34.

24. Whipple, G. C., "The element of chance in sanitation," _J. Franklin Inst._, 182, 37-59 and 205-27 (1916).

25. Wright, S., "A frequency curve adapted to variation in percentage occurrence," _J. Am. Statist. Assoc._, 21, 162-178 (1926).

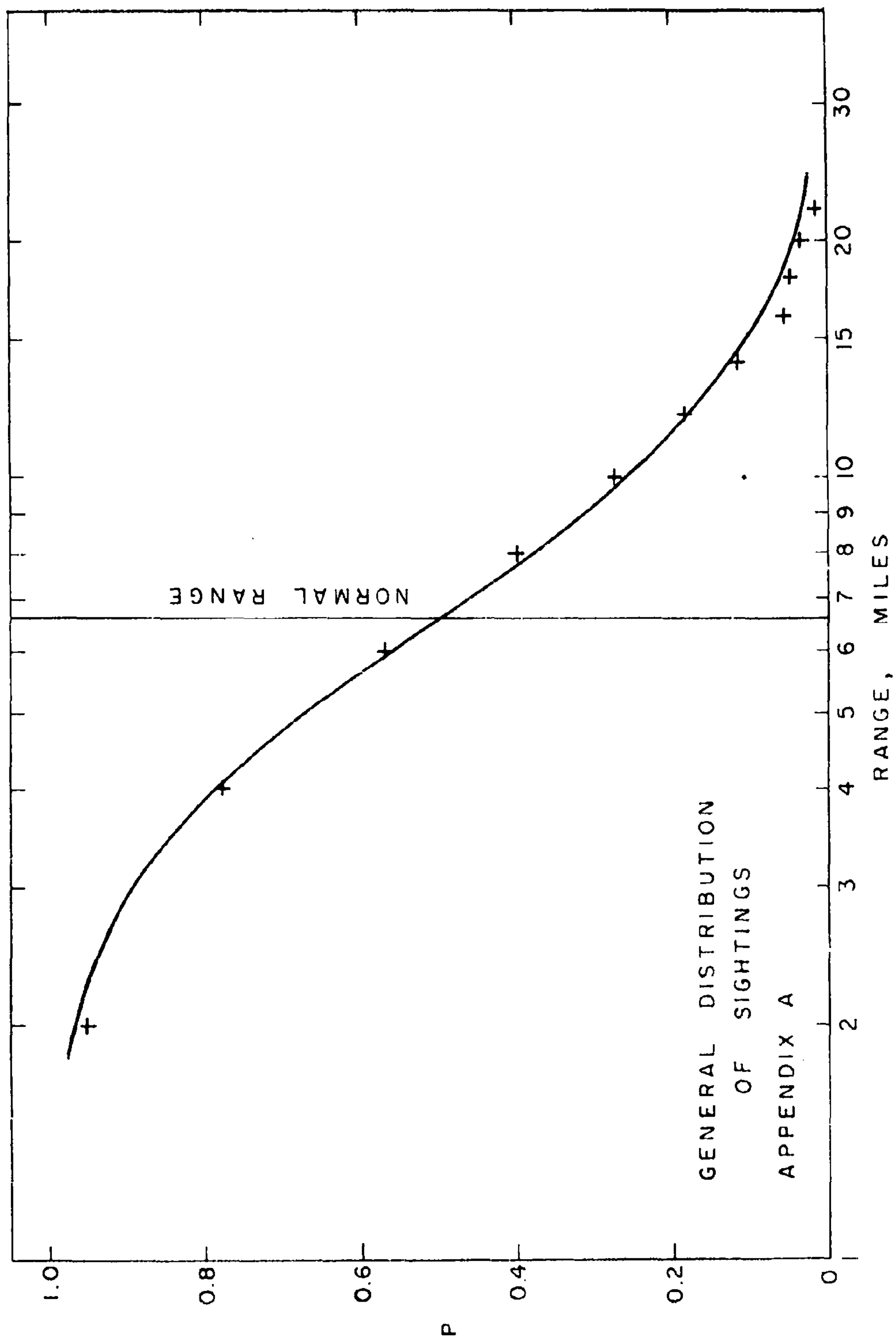

GENERAL DISTRIBUTION OF SIGHTINGS

APPENDIX A

APPENDIX A-2

ALL SIGHTINGS

	Range	Frequency
	0	3465
	4	2691
	10	948
	14	397
	20	109
T		6.599
S		0.65
S_T		0.0096
χ^2		4.308

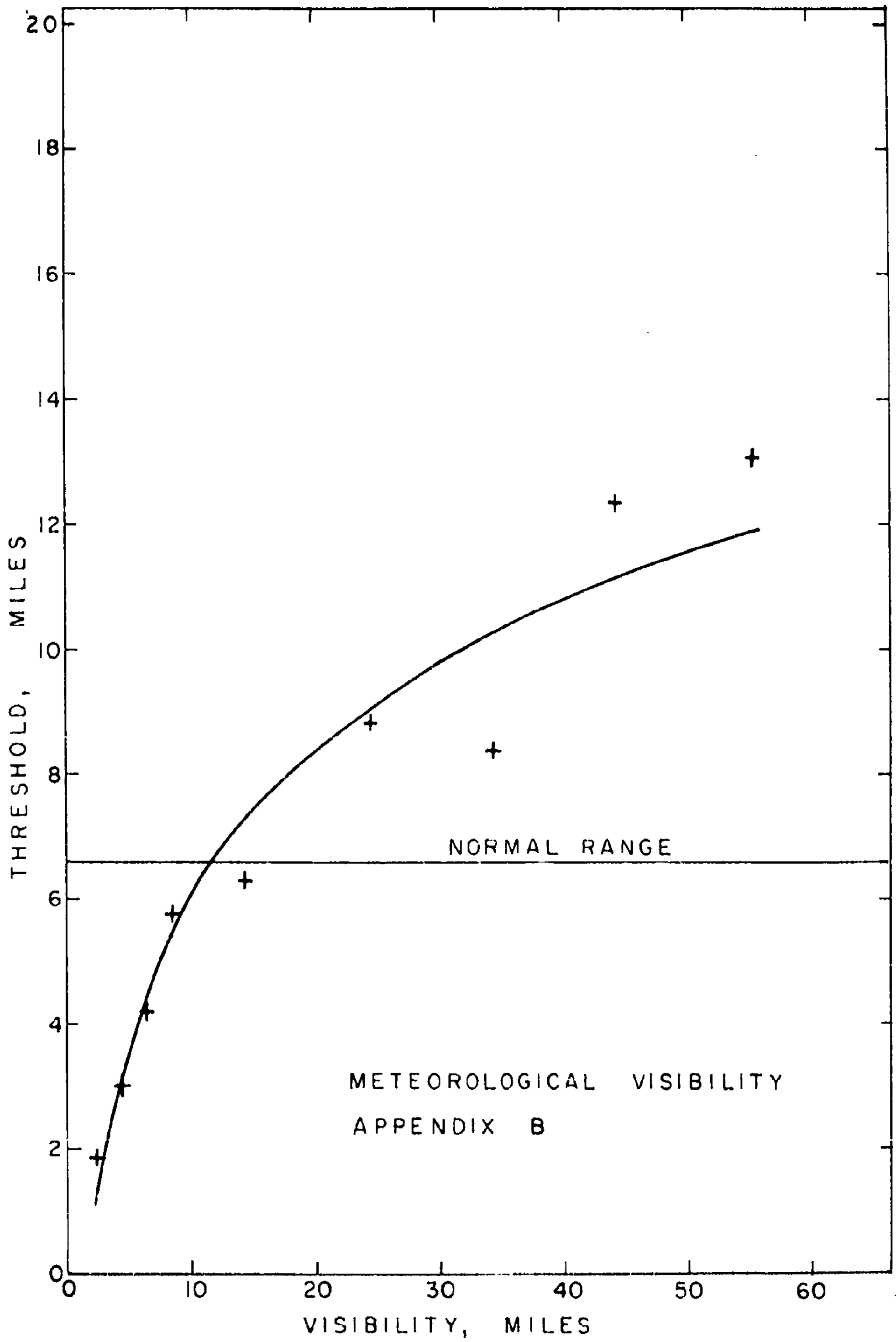

20
18
16
14
12
10
8
6
4
2
0
THRESHOLD, MILES
NORMAL RANGE
METEOROLOGICAL VISIBILITY
APPENDIX B
0
10
20
30
40
50
60
VISIBILITY, MILES

METEOROLOGICAL VISIBILITY (Miles)

Range (Miles)	0-1	2-3	4-5	6-7	8-9	10-19	20-29	30-39	40-49	50^+	Unlimited
0	3	63	148	144	163	1701	840	185	79	47	22
4	1	3	51	77	122	1344	751	147	71	43	20
10	0	0	5	1	3	373	376	85	49	30	12
14	0	0	3	0	0	96	173	53	38	23	8
20	0	0	1	0	0	15	39	18	19	13	2
T	(No	1.885	2.999	4.189	5.719	6.281	8.812	8.345	12.364	13.026	9.790
S	Fit)	0.33	0.70	0.61	0.53	0.54	0.61	0.81	0.83	0.83	0.71
S_T	-	0.064	0.099	0.070	0.095	0.012	0.017	0.044	0.064	0.084	0.11
χ^2	-	1.341	0.679	0.208	10^{-11}	10.094	3.233	4.869	0.884	0.181	1.457

$\bar{S}$ 0.650

S_s 0.15

$S_{\bar{s}}$ 0.048

$T(V) = 3.476 \ln V - 2.064$, V = Visibility (Miles)

Factor $= 0.627 \ln V - 0.313$

$r = 0.969$

APPENDIX B-2

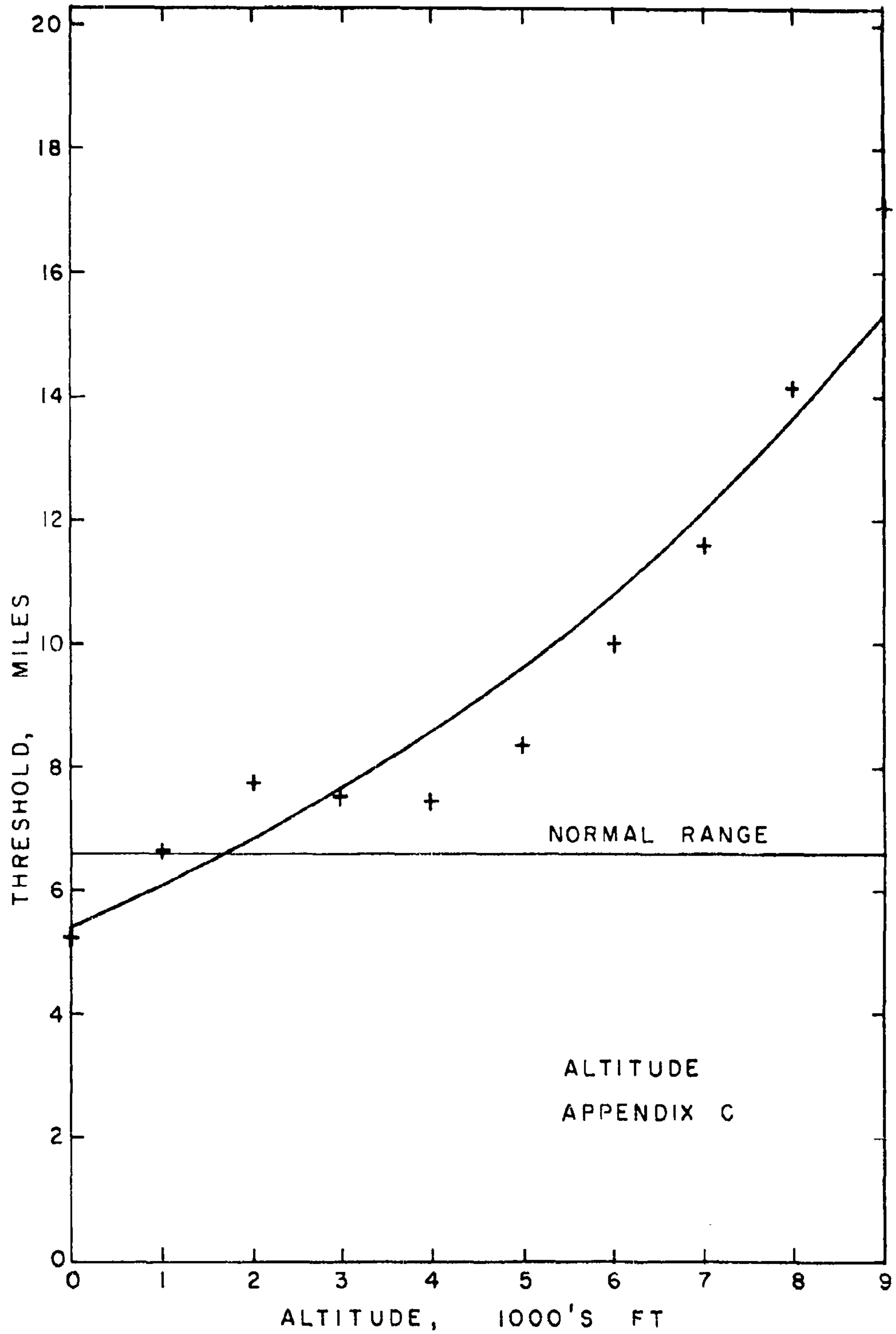
20
18
16
14
12
10
8
6
4
2
0
THRESHOLD, MILES
0
1
2
3
4
5
6
7
8
9
ALTITUDE, 1000'S FT
NORMAL RANGE
ALTITUDE
APPENDIX C

ALTITUDE (Feet)

Range (Miles)	0	1000	2000	3000	4000	5000	6000	7000	8000	9000
0	981	1453	492	135	97	65	48	8	26	7
4	639	1169	425	118	82	59	46	8	26	7
10	169	400	177	41	37	26	23	5	21	6
14	69	160	74	19	10	11	13	4	14	4
20	20	39	24	5	2	2	6	1	6	2
T	5.219	6.674	7.783	7.562	7.487	8.371	10.043	11.64	14.14	17.02
S	0.67	0.60	0.59	0.56	0.55	0.53	0.56	0.79	0.88	1.2
S_T	0.021	0.014	0.022	0.041	0.050	0.055	0.063	0.18	0.12	0.38
χ^2	0.465	5.070	1.398	0.0847	3.861	0.865	0.158	1.160	2.492	1.182

$\bar{S} = 0.698$

$S_s = 0.20$

$S_{\bar{s}} = 0.064$

$T(A) = 5.385\, e^{0.116A}$, A: Altitude (1000's of feet)

$f(A) = 0.816\, e^{0.116A}$

$r = 0.963$

APPENDIX C-2

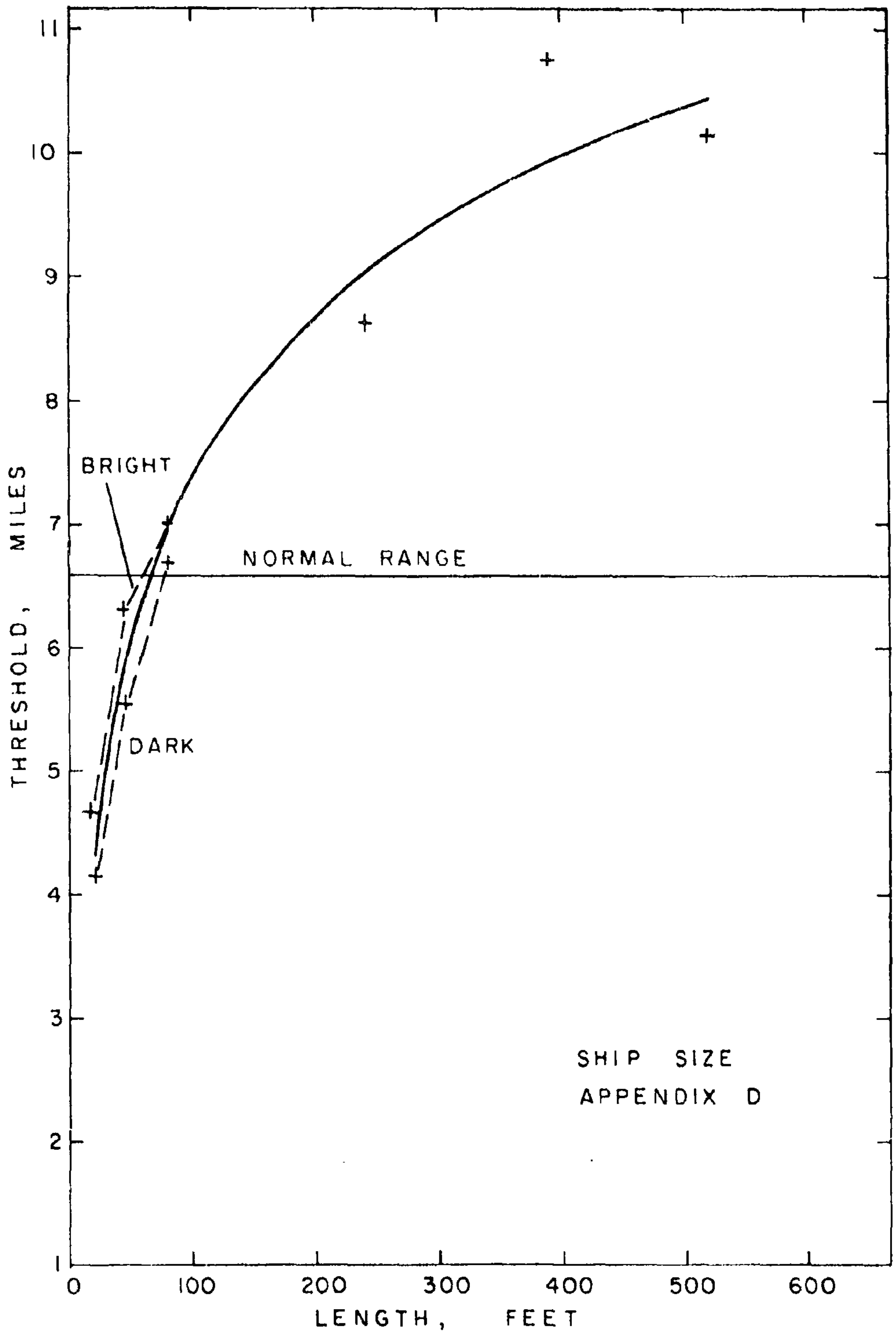
THRESHOLD, MILES
LENGTH, FEET
BRIGHT
DARK
NORMAL RANGE
SHIP SIZE
APPENDIX D
11
10
9
8
7
6
5
4
3
2
1
0
100
200
300
400
500
600

SHIP SIZE

Range (Miles)	Less than 30' Bright	Less than 30' Dark	30' - 60' Bright	30' - 60' Dark	60' - 100' Bright	60' - 100' Dark	500-5000T	5000-10000T	Over 10000T
0	475	269	753	297	172	127	356	414	310
4	295	141	603	227	152	103	320	389	288
10	42	18	154	30	41	33	157	251	167
14	4	3	49	5	10	11	65	132	94
20	0	0	5	0	0	2	21	48	31
T	4.658	4.154	6.305	5.548	7.018	6.669	8.619	10.743	10.104
S	0.61	0.56	0.52	0.45	0.46	0.56	0.57	0.58	0.59
S_T	0.028	0.041	0.018	0.028	0.034	0.045	0.024	0.021	0.025
χ^2	1.911	0.700	6.524	0.266	0.476	0.960	2.668	4.583	2.580

$\bar{S} = 0.544 \pm 0.053(S)$

$S_s = 0.053$

$S_{\bar{s}} = 0.017$

$T(L) = 1.844 \ln L - 1.100$, L: Ship size(feet)

$f(L) = 0.280 \ln L - 0.167$

$r = 0.982$

APPENDIX D-2

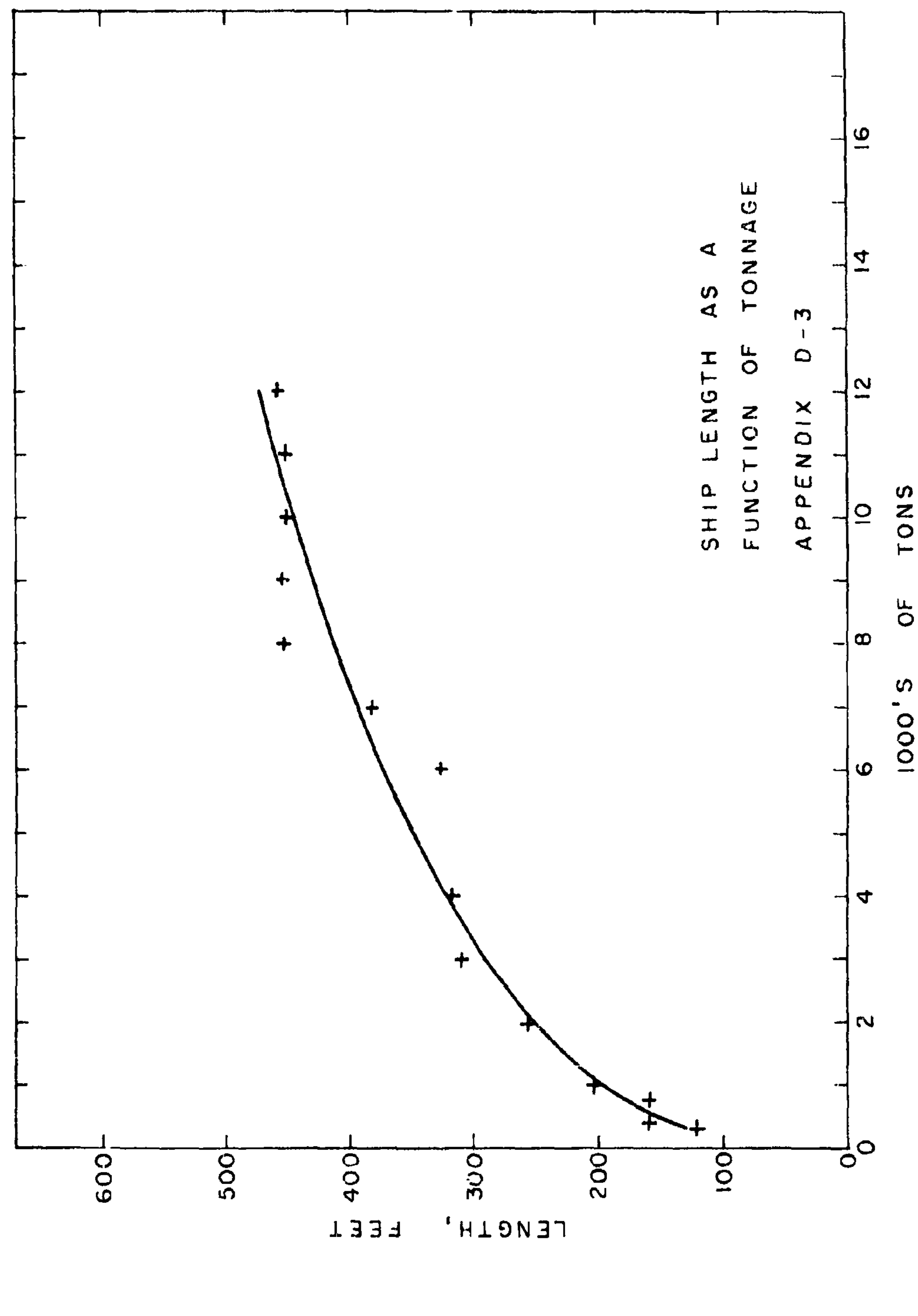
SHIP LENGTH AS A
FUNCTION OF TONNAGE
APPENDIX D-3
1000'S OF TONS
LENGTH, FEET
0
2
4
6
8
10
12
14
16
100
200
300
400
500
600

LENGTH AS A FUNCTION OF TONNAGE

Gross Tonnage	Mean Length (Feet)
300	120
750	158
1000	203
2000	257
3000	310
4000	319
6000	326
7000	382
8000	451
9000	464
10000	450
11000	450
12000	456

$$\text{Length} = 21.4\,(\text{Tonnage})^{1/3} - 16.0$$

$$r = 0.985$$

APPENDIX D-4

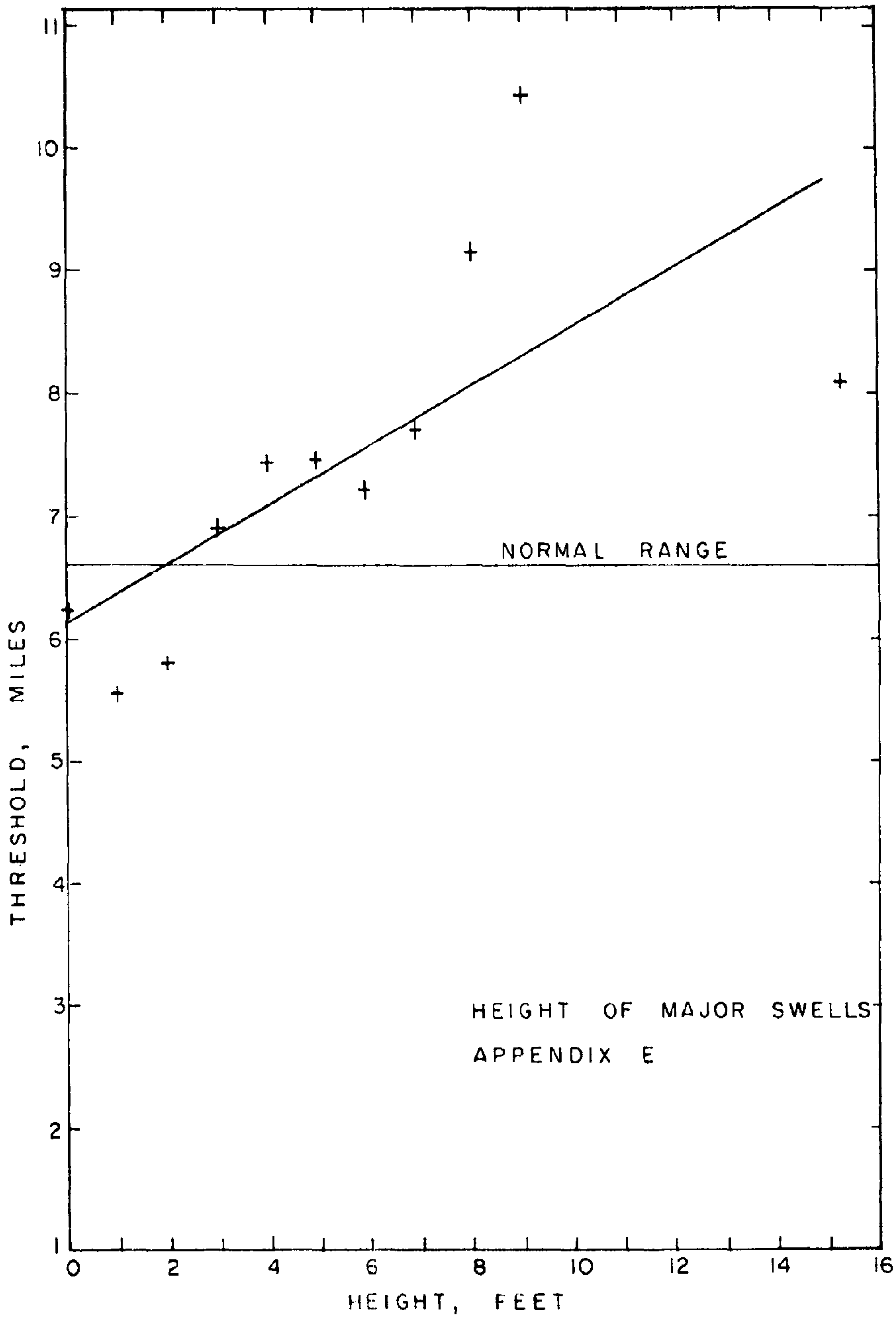
THRESHOLD, MILES
HEIGHT, FEET
NORMAL RANGE
HEIGHT OF MAJOR SWELLS
APPENDIX E
1
2
3
4
5
6
7
8
9
10
11
0
2
4
6
8
10
12
14
16

HEIGHT OF MAJOR SWELLS

Range (Miles)	0	1	2	3	4	5	6	7	8	9	10+
0	531	482	625	612	451	270	188	26	50	5	24
4	399	342	429	507	381	222	157	21	43	4	20
10	129	81	154	173	141	99	55	8	26	2	11
14	52	26	72	66	69	42	26	6	15	2	3
20	9	3	17	20	17	13	11	5	3	2	3
T	6.215	5.559	5.801	6.989	7.403	7.485	7.239	7.724	9.168	10.341	8.097
S	0.62	0.57	0.72	0.58	0.60	0.64	0.62	0.88	0.67	1.4	0.70
S_T	0.025	0.026	0.026	0.021	0.024	0.032	0.038	0.13	0.071	0.41	0.11
χ^2	5.989	4.153	6.549	0.827	1.549	2.491	0.289	0.951	3.888	0.250	2.072

$\bar{S} = 0.727$

$S_s = 0.23$

$S_{\bar{s}} = 0.068$

$T(S) = 6.170 + 0.239\,S$, S: Swell height (Feet)

$f(S) = 0.935 + 0.0362\,S$

$r = 0.707$

APPENDIX E-2

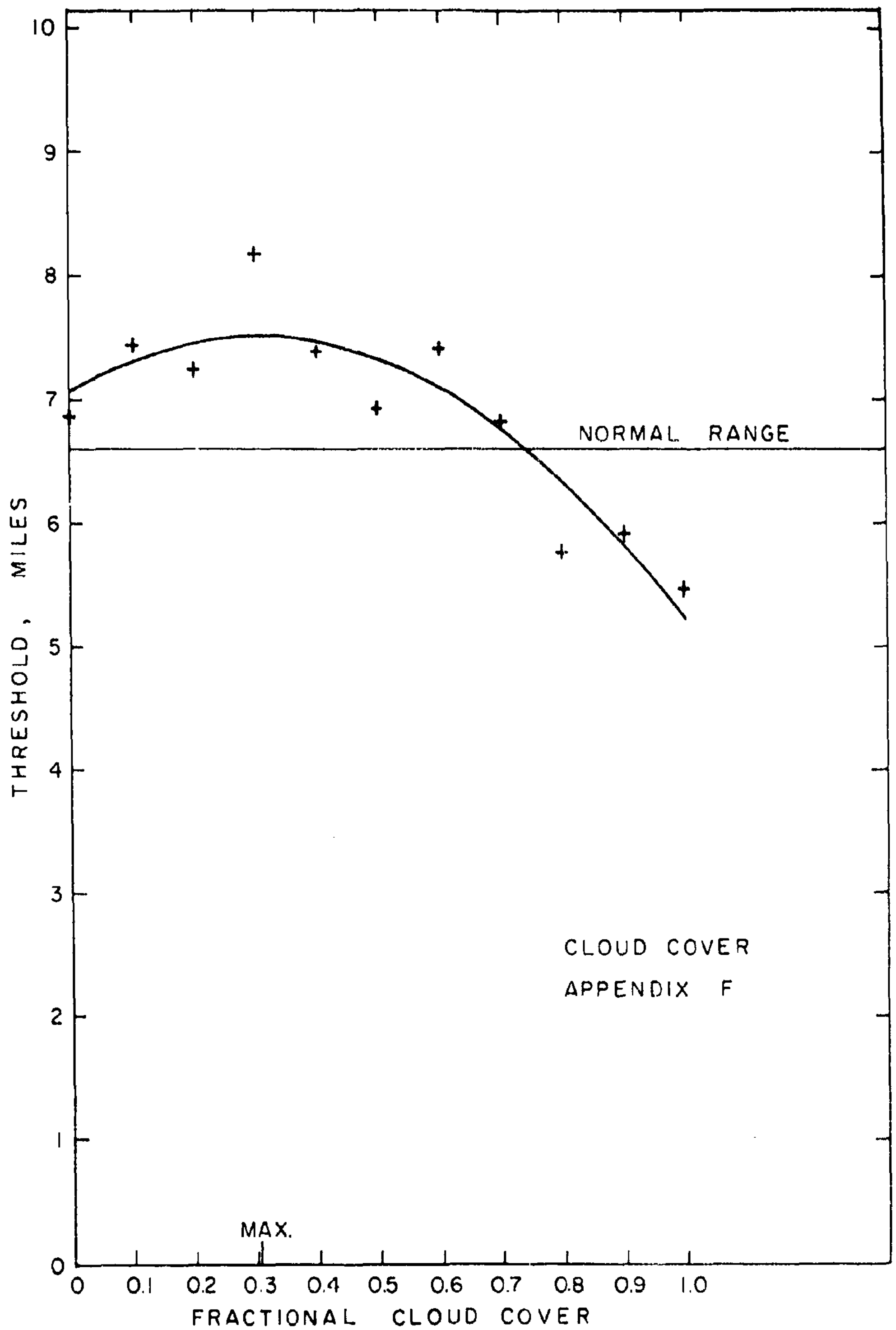
10
9
8
7
6
5
4
3
2
1
0
THRESHOLD, MILES
NORMAL RANGE
CLOUD COVER
APPENDIX F
MAX.
0
0.1
0.2
0.3
0.4
0.5
0.6
0.7
0.8
0.9
1.0
FRACTIONAL CLOUD COVER

FRACTIONAL CLOUD COVER

Range (Miles)	0	0.1	0.2	0.3	0.4	0.5	0.6	0.7	0.8	0.9	1.0
0	1041	345	182	156	139	197	110	124	182	244	690
4	822	293	148	136	115	153	95	98	128	181	475
10	320	112	62	58	45	62	32	33	40	50	122
14	131	46	25	35	23	29	15	20	15	14	43
20	31	16	8	8	8	15	4	5	5	3	5
T	6.884	7.444	7.229	8.191	7.398	6.920	7.405	6.809	5.761	5.904	5.471
S	0.66	0.59	0.63	0.61	0.65	0.72	0.56	0.66	0.66	0.57	0.63
s_T	0.018	0.027	0.040	0.040	0.045	0.043	0.047	0.051	0.046	0.035	0.023
χ^2	3.456	0.501	1.283	2.209	0.0604	0.523	0.0752	0.887	0.426	1.565	0.562

$\bar{S} = 0.631$

$S_s = 0.044$

$S_{\bar{s}} = 0.013$

$T(C) = 7.069 + 2.871C - 4.717C^2$, C: Cloud cover (Decimal fraction)

$f(C) = 1.07 + 0.435\ C - 0.715C^2$

$r = 0.903$

APPENDIX F-2

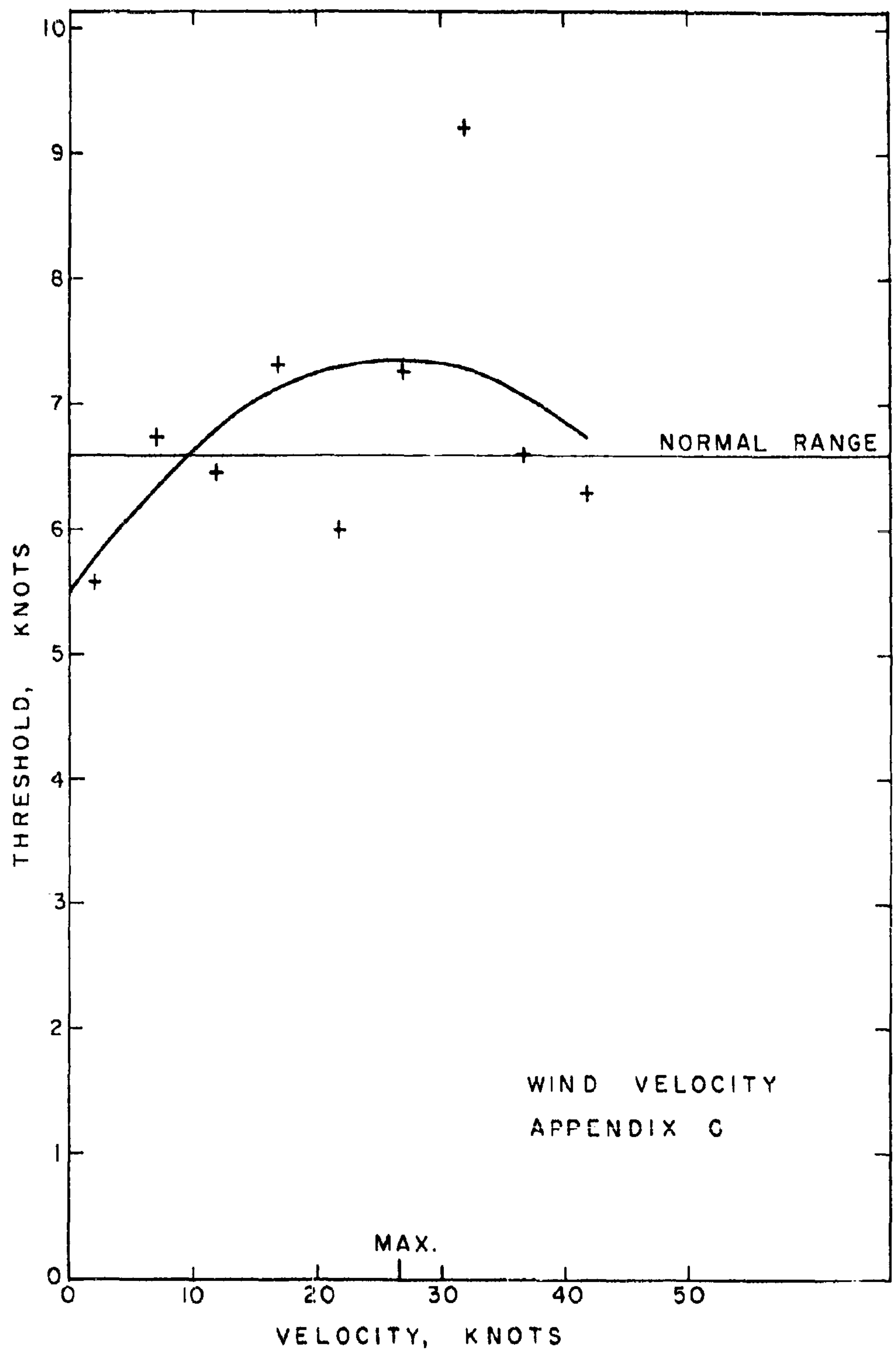
NORMAL RANGE
WIND VELOCITY
APPENDIX C
MAX.
THRESHOLD, KNOTS
VELOCITY, KNOTS
0
1
2
3
4
5
6
7
8
9
10
0
10
20
30
40
50

WIND VELOCITY (KNOTS)

Range	0-4	5-9	10-14	15-19	20-24	25-29	30-34	35-39	40-44	45-49	50+
0	396	1094	832	487	311	117	46	15	12	1	4
4	278	863	639	411	220	96	41	14	11	1	3
10	88	310	216	161	83	38	21	2	1	0	2
14	40	130	95	56	32	18	13	0	0	0	2
20	6	40	28	15	8	6	5	0	0	0	1
T	5.806	6.732	6.464	7.325	6.003	7.292	9.236	6.604	6.308	(No)	(No)
S	0.70	0.63	0.64	0.60	0.69	0.64	0.66	0.49	0.45	(Data)	(Fit)
S_T	0.033	0.017	0.020	0.022	0.036	0.050	0.073	0.11	0.12	—	*
χ^2	0.0603	2.383	1.161	3.945	4.233	0.160	0.130	0.593	0.802	—	*

$\bar{S} = 0.611$

$S_s = 0.081$

$S_{\bar{s}} = 0.027$

$T(WV) = 5.488 - 0.142WV - 0.002673(WV)^2$

WV: Wind velocity

$f(WV) = 0.832 + 0.0214WV - 0.000405(WV)^2$

$r = 0.531$

*Rejected on basis of entirely different type of curve from rest of family

APPENDIX G-2

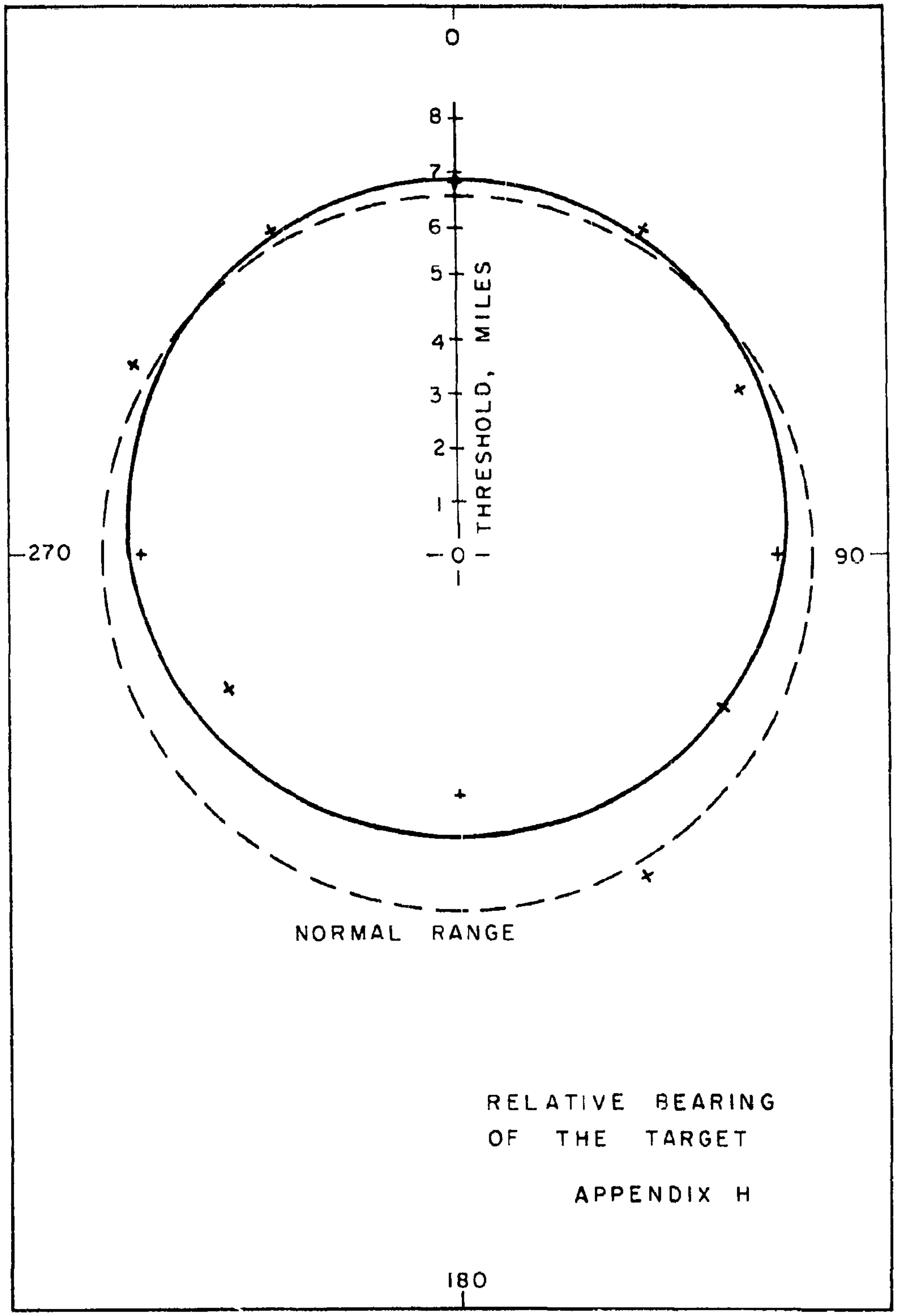
0
8
7
6
5
4
3
2
1
0
THRESHOLD, MILES
270
90
NORMAL RANGE
RELATIVE BEARING
OF THE TARGET
APPENDIX H
180

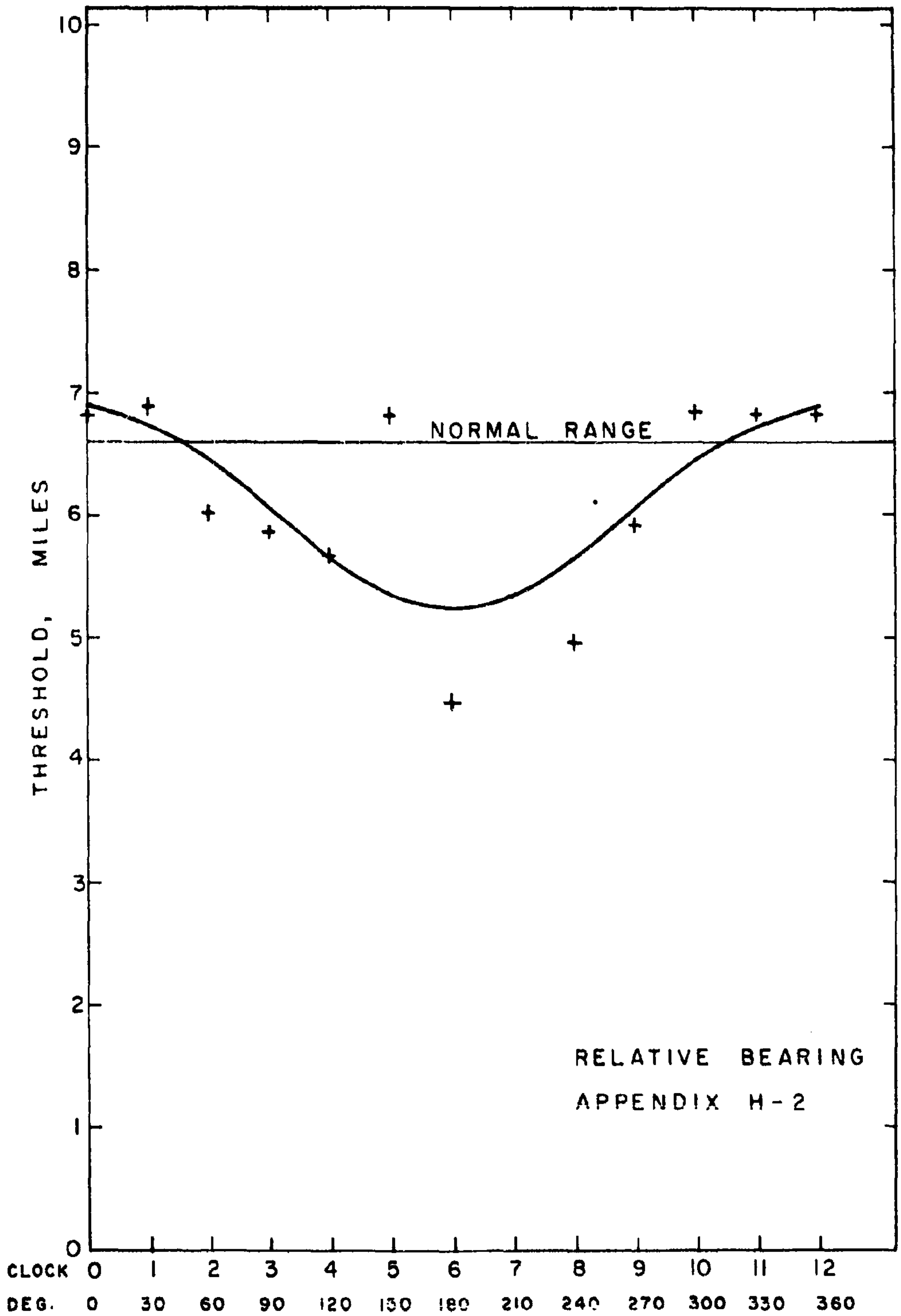
THRESHOLD, MILES
0
1
2
3
4
5
6
7
8
9
10
NORMAL RANGE
RELATIVE BEARING
APPENDIX H-2
CLOCK 0 1 2 3 4 5 6 7 8 9 10 11 12
DEG. 0 30 60 90 120 150 180 210 240 270 300 330 360

SIGHTING BEARING (CLOCK CODE)

Range (Miles)	1	2	3	4	5	6	7	8	9	10	11	12
0	530	450	271	31	6	5	6	15	192	365	529	764
4	427	327	198	22	5	3	4	10	138	299	419	580
10	154	109	57	6	2	1	3	0	44	101	153	255
14	65	46	20	2	2	0	0	0	17	37	67	105
20	17	13	7	0	1	0	0	0	1	15	23	25
T	6.892	6.056	5.899	5.674	6.804	4.466	(No)	4.972	5.922	6.982	6.816	6.814
S	0.61	0.66	0.62	0.62	0.50	2.425	(Fit)	0.70	0.66	0.59	0.64	0.73
S_T	0.023	0.029	0.035	0.10	0.17	0.86	-	0.12	0.044	0.027	0.024	0.022
χ^2	1.899	1.355	0.481	0.060	0.071	0.096	-	0.346	0.347	1.169	0.586	5.944

$\bar{S} = 0.80$

$S_s = 0.51$

$S_{\bar{s}} = 0.16$

$T(B) = 6.046 + 0.808 \cos B$, B: **Relative bearing on 30X (Clock Code)**

$f(B) = 0.916 + 0.122 \cos B$

$r = 0.697$

APPENDIX H-3

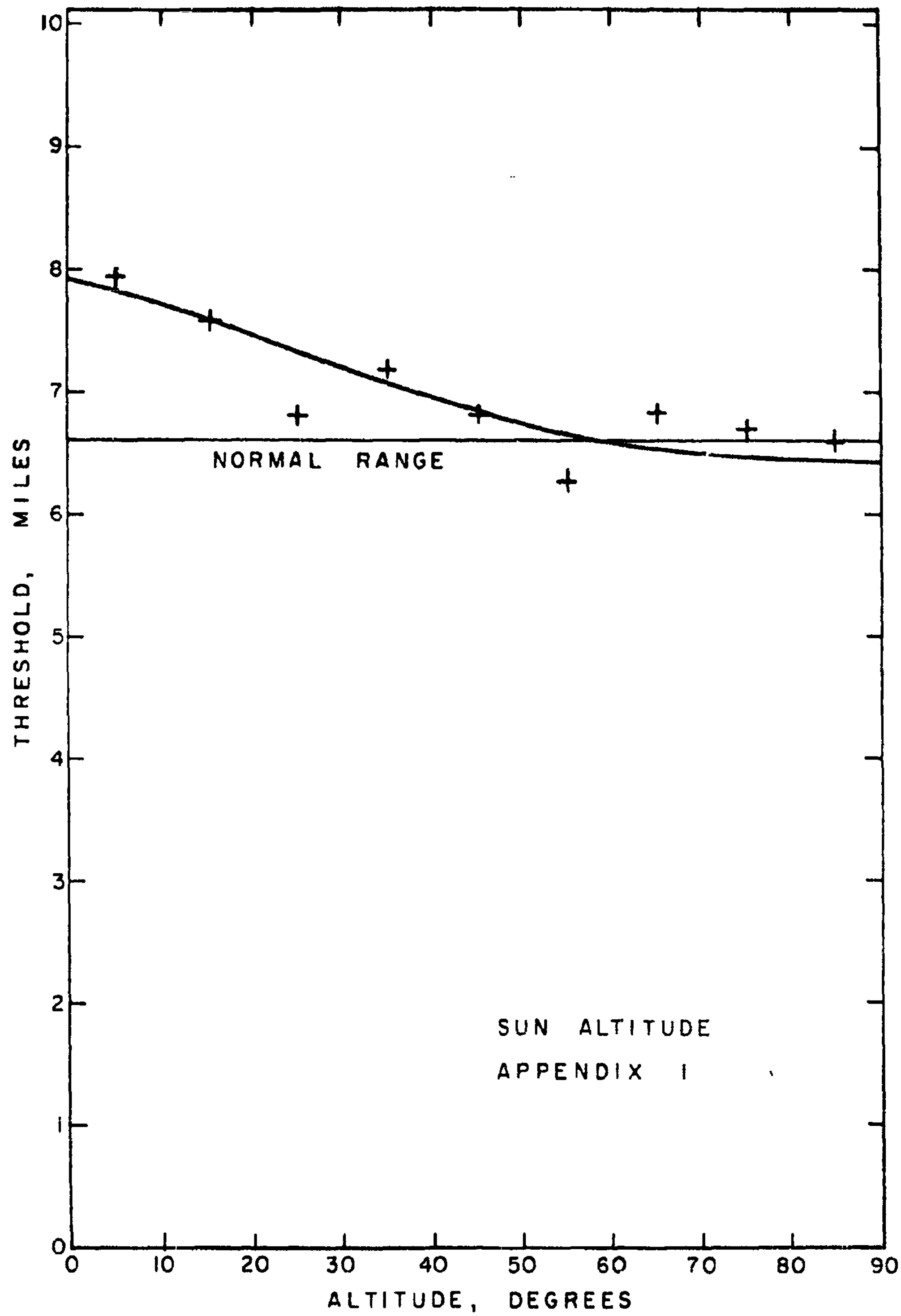
10
9
8
7
6
5
4
3
2
1
0
THRESHOLD, MILES
NORMAL RANGE
SUN ALTITUDE
APPENDIX I
0
10
20
30
40
50
60
70
80
90
ALTITUDE, DEGREES

SUN ALTITUDE (Degrees)

Range (Miles)	0	10	20	30	40	50	60	70	80	90
0	35	159	334	572	757	306	296	230	130	6
4	29	132	268	467	591	231	241	190	106	5
10	14	52	94	197	221	75	84	55	33	4
14	6	28	38	90	109	33	28	17	6	0
20	4	16	11	24	23	8	8	6	0	0
T	7.926	7.569	6.805	7.333	6.816	6.285	6.832	6.679	6.555	(No)
S	0.72	0.70	0.61	0.64	0.68	0.64	0.58	0.54	0.52	(Fit)
S_T	0.094	0.044	0.029	0.022	0.021	0.033	0.030	0.033	0.044	-
χ^2	0.506	0.884	0.723	5.083	0.0817	1.039	1.594	0.773	3.161	-

$\bar{S} = 0.626$

$S_s = 0.066$

$S_{\bar{s}} = 0.021$

$T(SA) = 7.975 - 1.564 \sin SA$, SA: Sun altitude degrees

$f(SA) = 1.208 - 0.238 \sin SA$

$r = 0.915$

APPENDIX I-2

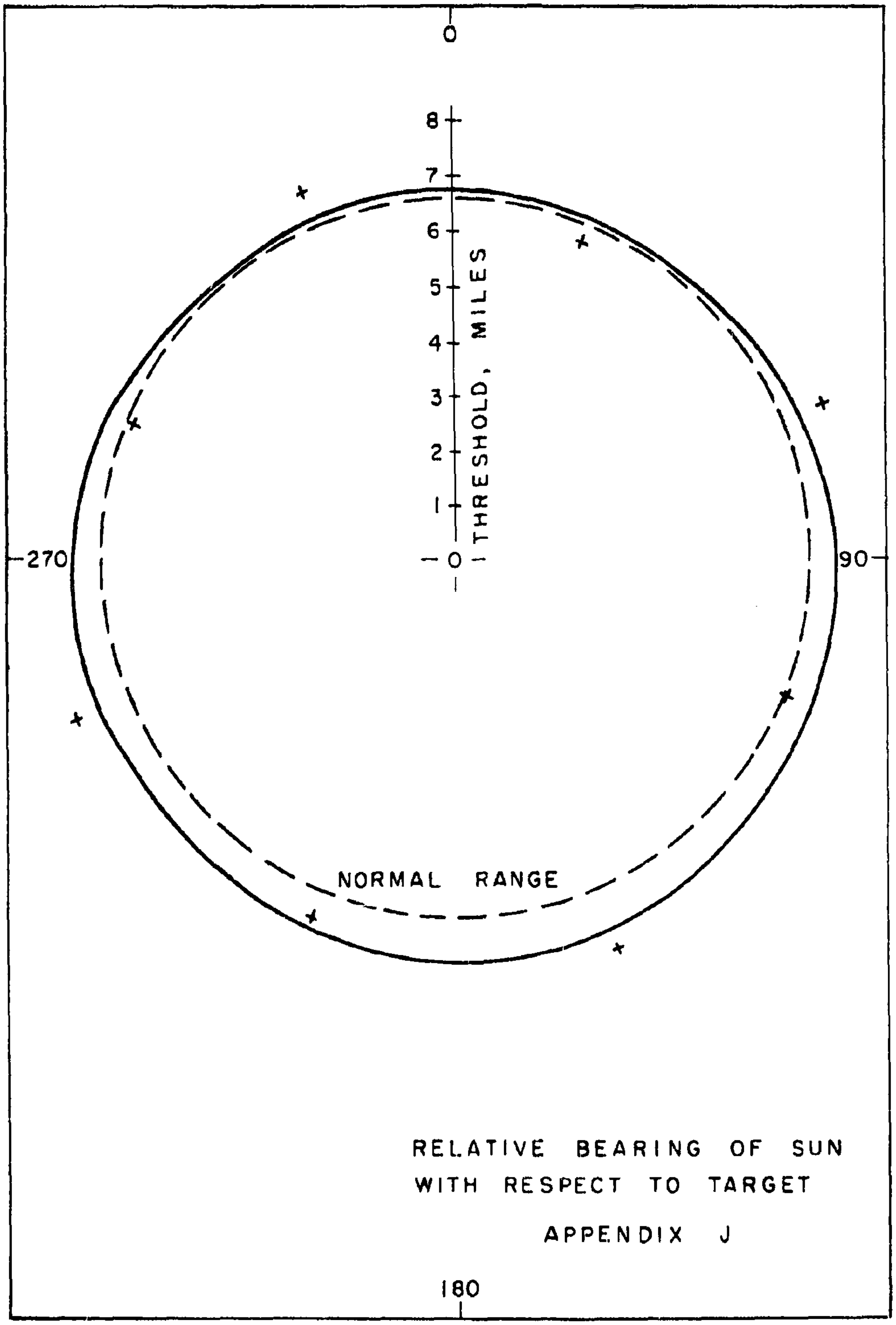

RELATIVE BEARING OF SUN WITH RESPECT TO TARGET

APPENDIX J

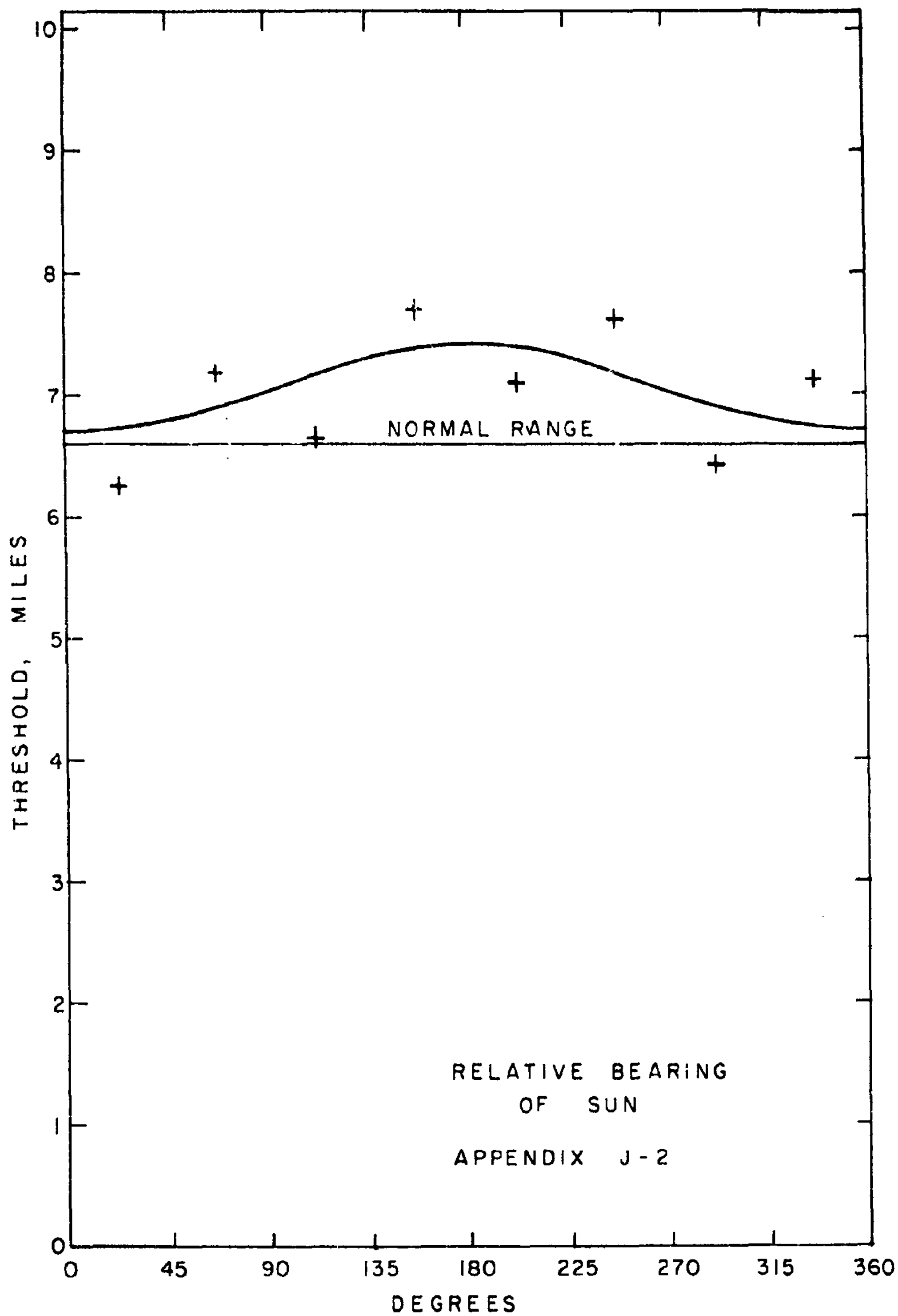
10
9
8
7
6
5
4
3
2
1
0
THRESHOLD, MILES
NORMAL RANGE
RELATIVE BEARING
OF SUN
APPENDIX J-2
0
45
90
135
180
225
270
315
360
DEGREES

RELATIVE BEARING OF SUN (Degrees)

Range (Miles)	0–45	45–89	90–134	135–174	180–224	225–269	270–314	315–359
0	572	208	398	209	593	194	422	286
4	428	180	307	168	487	155	325	242
10	149	66	112	81	178	67	108	85
14	56	28	52	45	79	25	43	36
20	12	13	14	15	20	11	13	6
T	6.253	7.397	6.624	7.700	7.089	7.600	6.427	7.220
S	0.64	0.67	0.66	0.72	0.60	0.62	0.63	0.56
S_T	0.023	0.034	0.028	0.040	0.021	0.038	0.027	0.029
χ^2	6.503	2.885	1.917	1.958	2.053	1.541	0.745	2.773

$\bar{S} = 0.64$

$S_s = 0.045$

$S_{\bar{s}} = 0.016$

$T(SB) = 7.043 + 0.342 \cos(\pi - SB)$, SB: Bearing of sun (Degrees)

$f(SB) = 1.067 + 0.0518 \cos(\pi - SB)$

$r = 0.987$

APPENDIX J-3

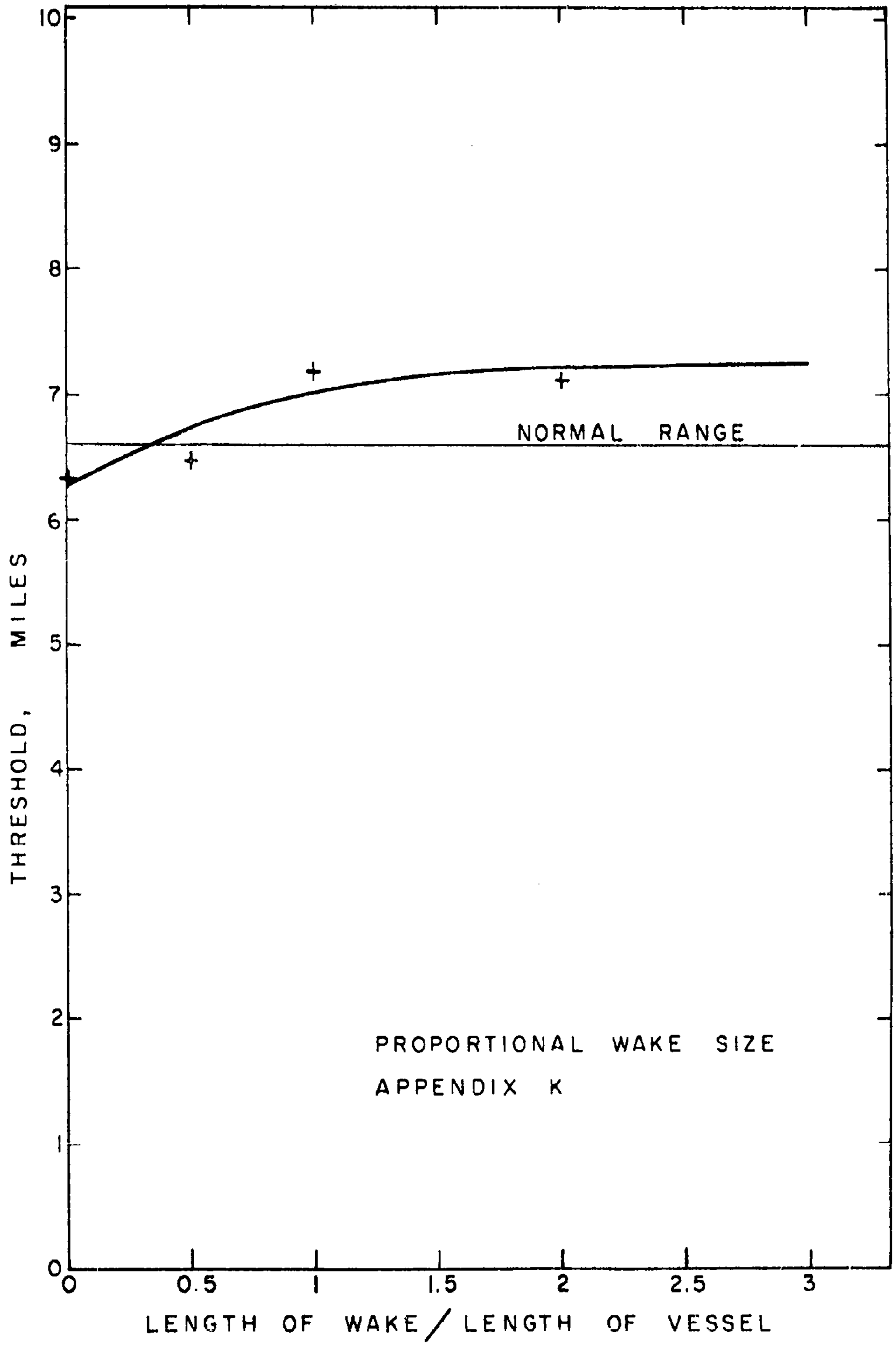

THRESHOLD, MILES
10
9
8
7
6
5
4
3
2
1
0
NORMAL RANGE
PROPORTIONAL WAKE SIZE
APPENDIX K
0
0.5
1
1.5
2
2.5
3
LENGTH OF WAKE / LENGTH OF VESSEL

PROPORTIONAL WAKE SIZE

Range (Miles)	0	0.5X	1.0X	2.0X	More than 2.0X
0	1769	410	385	353	370
4	1328	327	313	292	323
10	452	103	123	115	105
14	197	39	57	41	39
20	55	9	15	15	6
T	6.308	6.575	7.163	7.203	7.295
S	0.65	0.58	0.63	0.60	0.51
S_T	0.014	0.026	0.027	0.027	0.024
χ^2	4.826	1.073	2.189	2.284	1.943

$\bar{S} = 0.594 \pm 0.048 \ (S_s)$

$S_s = 0.048$

$S_{\bar{s}} = 0.017$

$T(W) = 7.295 - 1.066 \, e^{-1.284W}$, W: Wake size (Multiple of vessel length)

$f(W) = 1.105 - 0.162 \, e^{-1.284W}$

$r = 0.920$

APPENDIX K-2

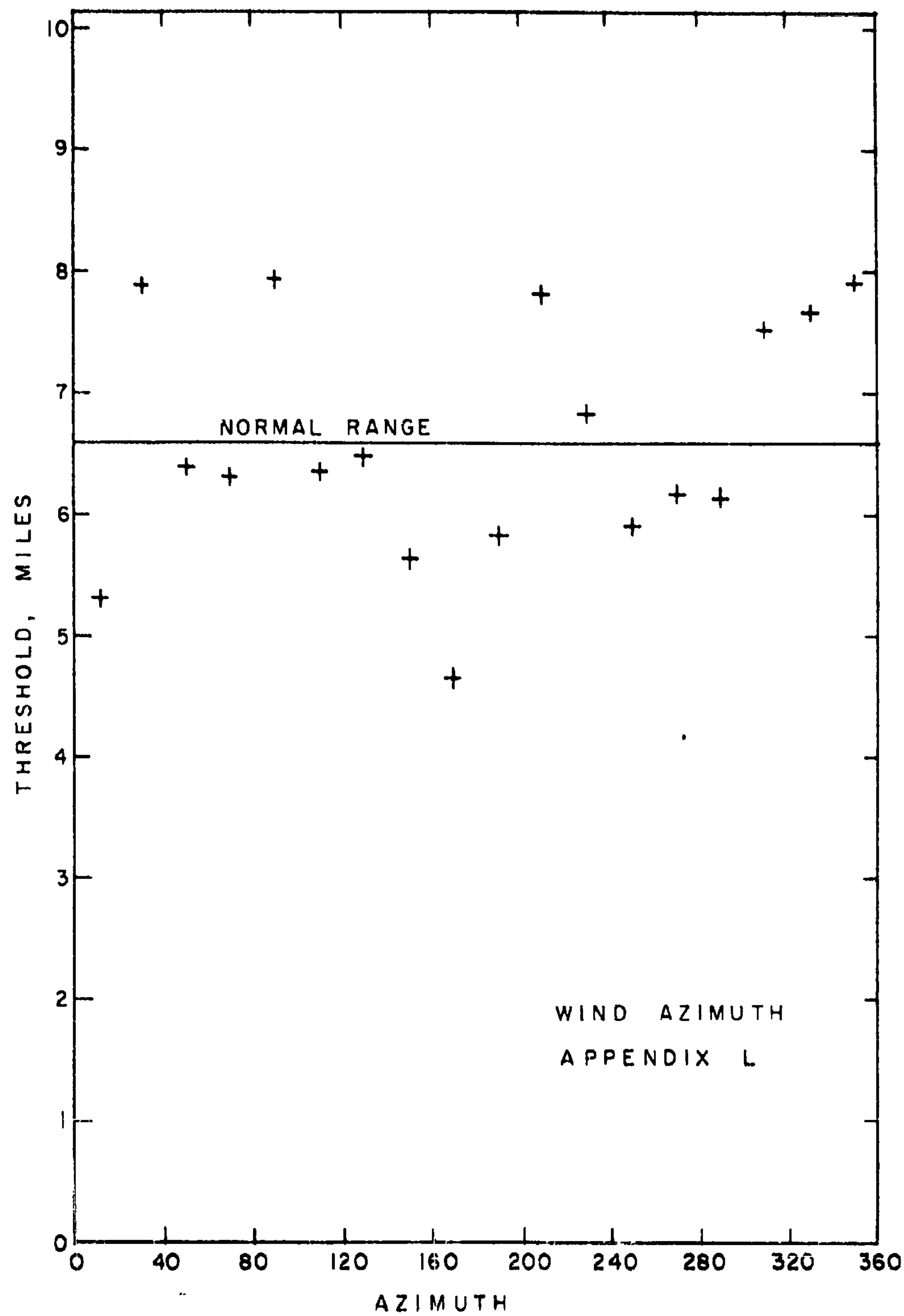
NORMAL RANGE
WIND AZIMUTH
APPENDIX L
THRESHOLD, MILES
AZIMUTH
0
1
2
3
4
5
6
7
8
9
10
0
40
80
120
160
200
240
280
320
360

WIND AZIMUTH (Degrees)

Range	0-19	20-39	40-59	60-79	80-99	100-119	120-139	140-159	160-179
0	199	84	140	170	352	95	180	114	83
4	129	73	118	137	301	72	145	79	51
10	41	33	33	50	137	24	39	24	6
14	15	12	15	19	61	10	15	9	1
20	4	2	3	6	19	5	4	1	0
T	5.311	7.881	6.886	6.880	7.939	6.362	6.467	5.646	4.652
S	0.69	0.55	0.54	0.61	0.62	0.67	0.56	0.64	0.51
S_T	0.048	0.052	0.042	0.041	0.027	0.061	0.038	0.058	0.062
χ^2	1.372	2.569	0.309	0.600	2.278	0.337	0.00344	3.183	0.113

No functions accepted

APPENDIX L-2

WIND AZIMUTH (Degrees)

Range (Miles)	180–199	200–219	220–239	240–259	260–279	280–299	300–319	320–339	340–359
0	189	88	97	126	444	291	371	150	105
4	135	78	79	93	334	219	311	125	90
10	40	28	24	25	105	63	136	53	40
14	17	13	13	10	41	35	51	28	18
20	3	5	4	2	12	6	16	10	6
T	5,821	7.807	6.840	5.914	6.194	6.189	7.540	7.676	7.921
S	0.64	0.67	0.61	0.60	0.63	0.63	0.60	0.66	0.62
S_T	0.044	0.051	0.054	0.051	0.027	0.034	0.026	0.044	0.049
χ^2	1.543	0.163	0.283	0.293	0.689	3.027	3.800	0.171	0.402
$\bar{S}$	0.614								
S_s	0.047								
$S_{\bar{s}}$	0.011								

APPENDIX L-3

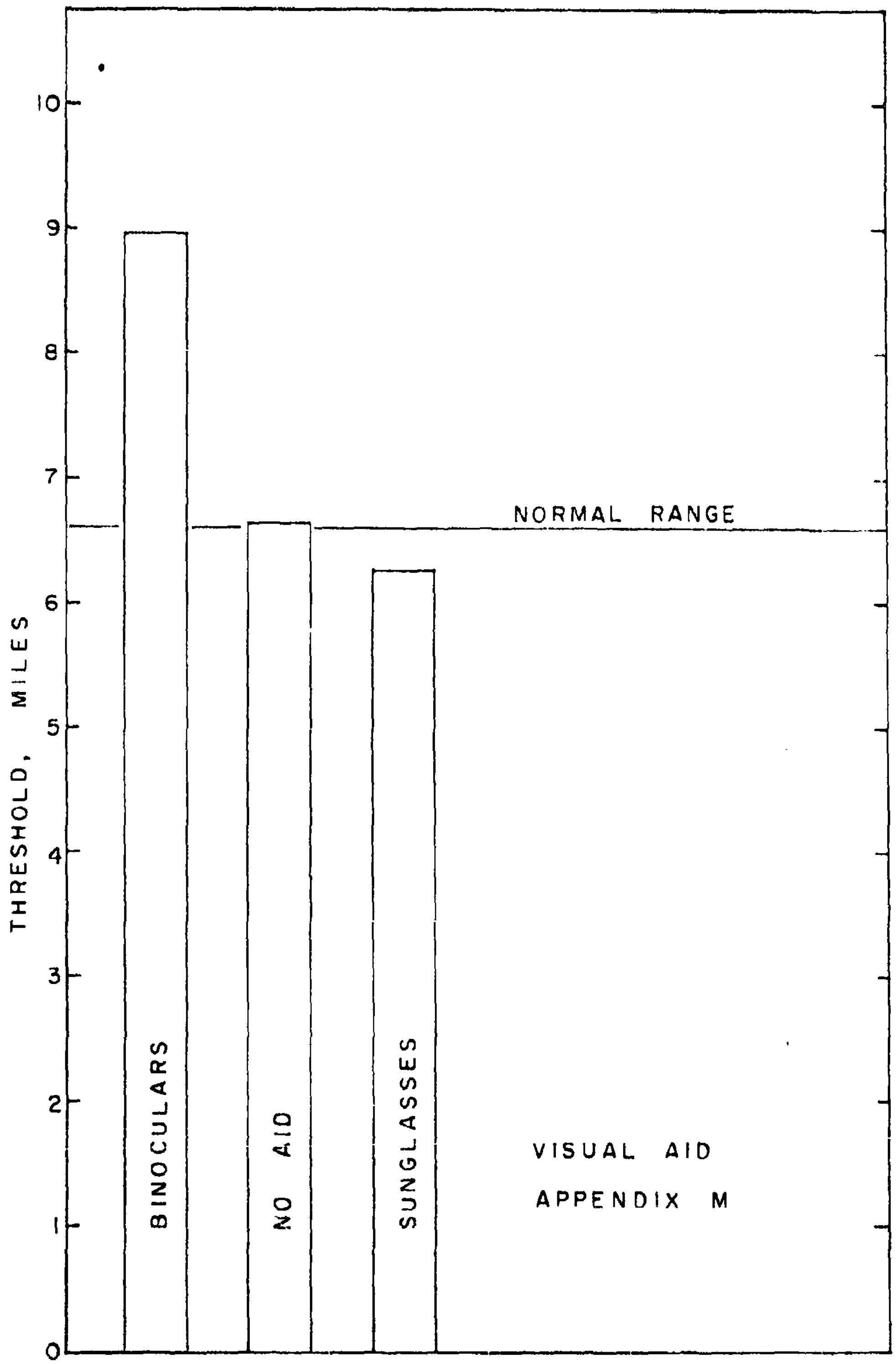
THRESHOLD, MILES
0
1
2
3
4
5
6
7
8
9
10
NORMAL RANGE
BINOCULARS
NO AID
SUNGLASSES
VISUAL AID
APPENDIX M

VISUAL AID

Range (Miles)	None	Binocular	Sun Glass
0	2812	36	561
4	2179	32	438
10	784	16	126
14	345	9	38
20	93	3	8
T	6.637	8.908	6.205
S	0.66	0.63	0.56
S_T	0.011	0.081	0.022
X^2	2.391	0.173	2.708
Factor	1.002	1.350	0.949

$\bar{S} = 0.617$

$S_s = 0.042$

$S_{\bar{S}} = 0.024$

APPENDIX M-2

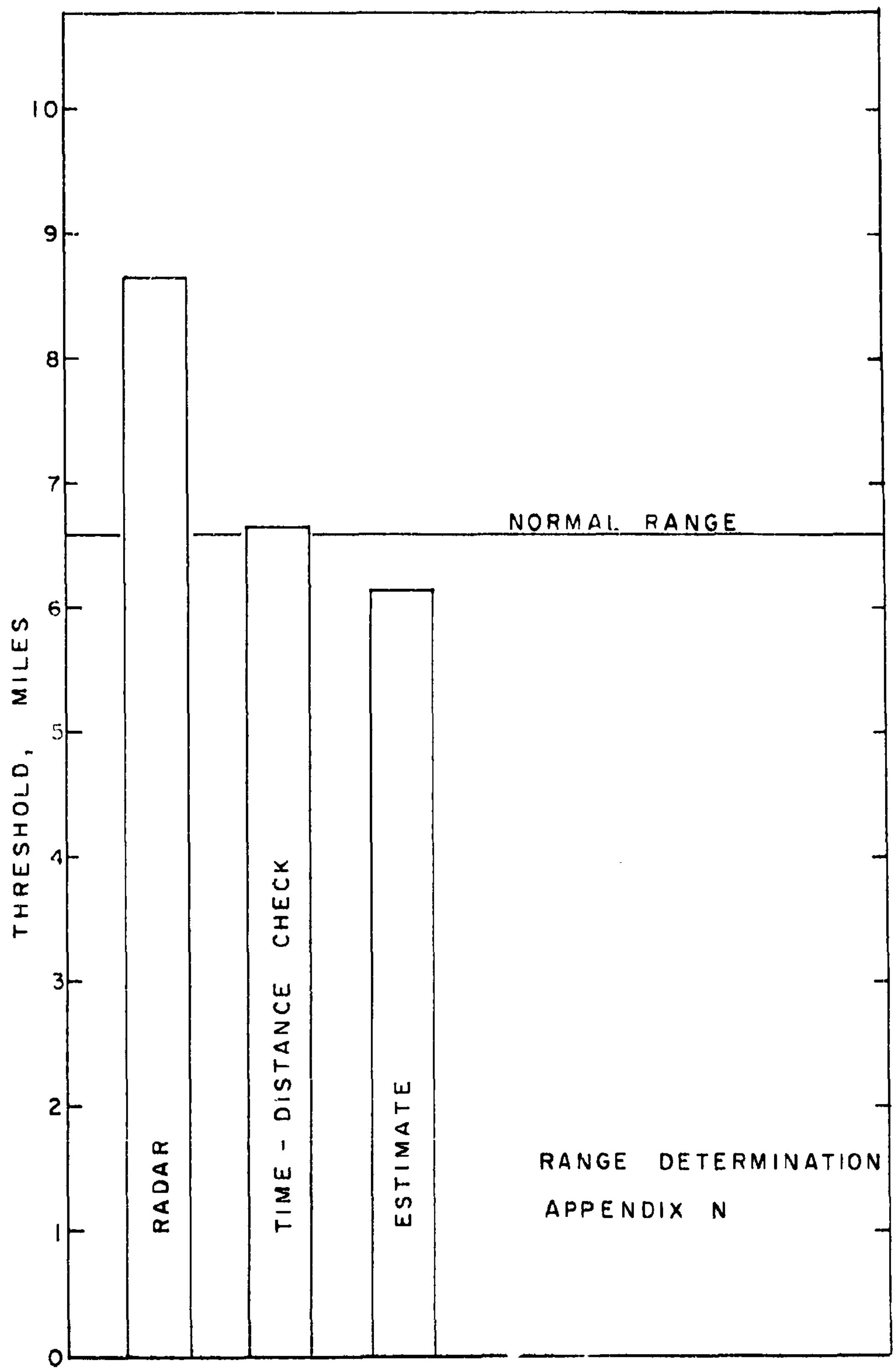
THRESHOLD, MILES
0
1
2
3
4
5
6
7
8
9
10
NORMAL RANGE
RADAR
TIME - DISTANCE CHECK
ESTIMATE
RANGE DETERMINATION
APPENDIX N

RANGE DETERMINATION METHOD

Range (Miles)	Radar	Time-Distance	Estimate
0	453	1336	1604
4	400	1053	1182
10	184	354	392
14	103	146	140
20	37	33	36
T	8.611	6.629	6.147
S	0.65	0.63	0.66
S_T	0.025	0.015	0.015
X^2	0.0106	0.988	4.470
Factor	1.298	1.001	0.923

$\bar{S} = 0.647$

$S_s = 0.012$

$S_{\bar{s}} = 0.0072$

APPENDIX N-2

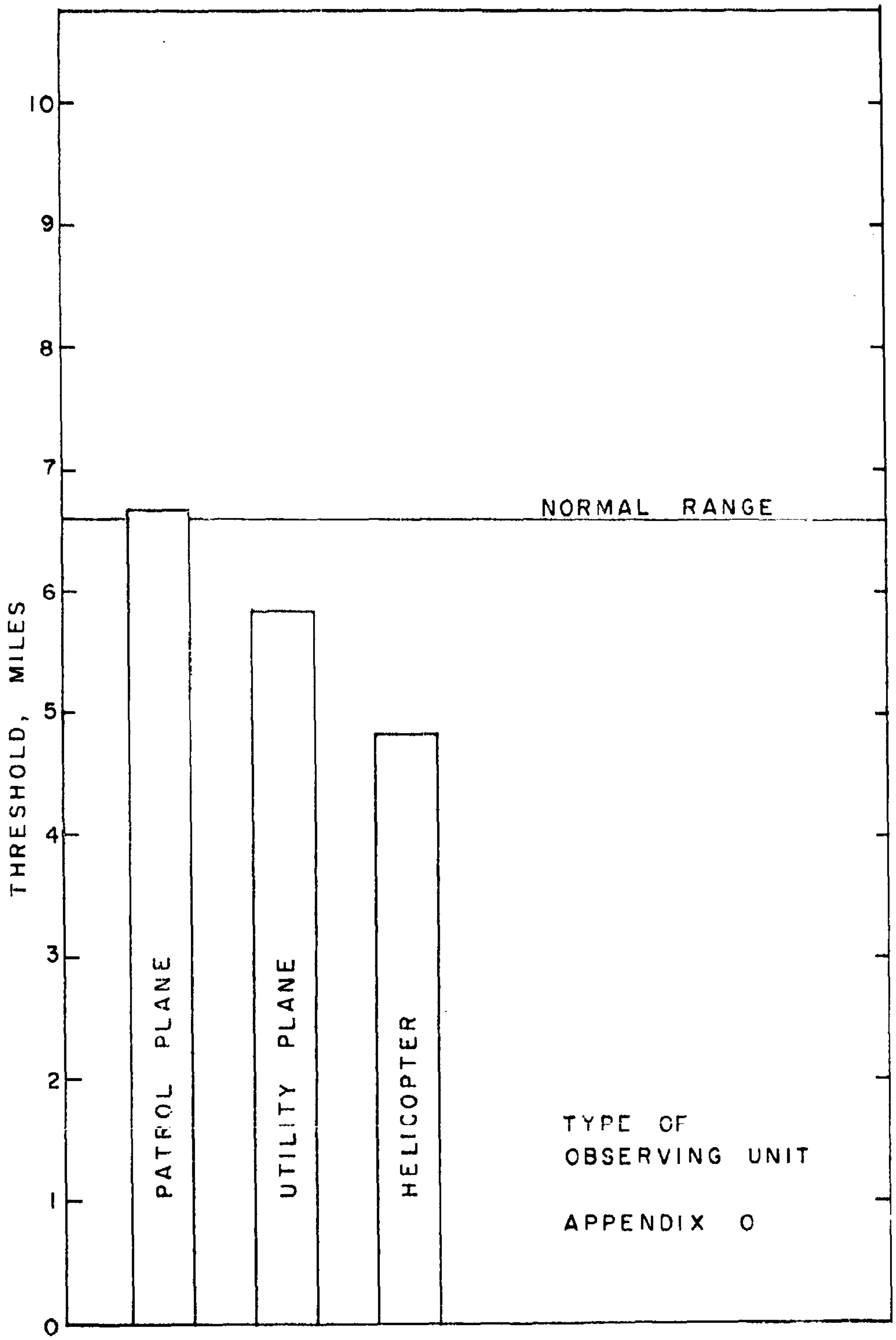
THRESHOLD, MILES
10
9
8
7
6
5
4
3
2
1
0
NORMAL RANGE
PATROL PLANE
UTILITY PLANE
HELICOPTER
TYPE OF OBSERVING UNIT

APPENDIX O

TYPE OF OBSERVING AIRCRAFT

Range (Miles)	Patrol	Utility	Helicopter
0	3138	165	113
4	2403	119	67
10	872	37	22
14	373	9	4
20	99	4	1
T	6.694	5.836	4.836
S	0.64	0.62	0.73
S_T	0.010	0.045	0.071
X^2	2.843	2.480	4.933
Factor	1.014	0.884	0.733

$\bar{S} = 0.663$

$S_s = 0.048$

$S_{\bar{s}} = 0.028$

APPENDIX 0-2

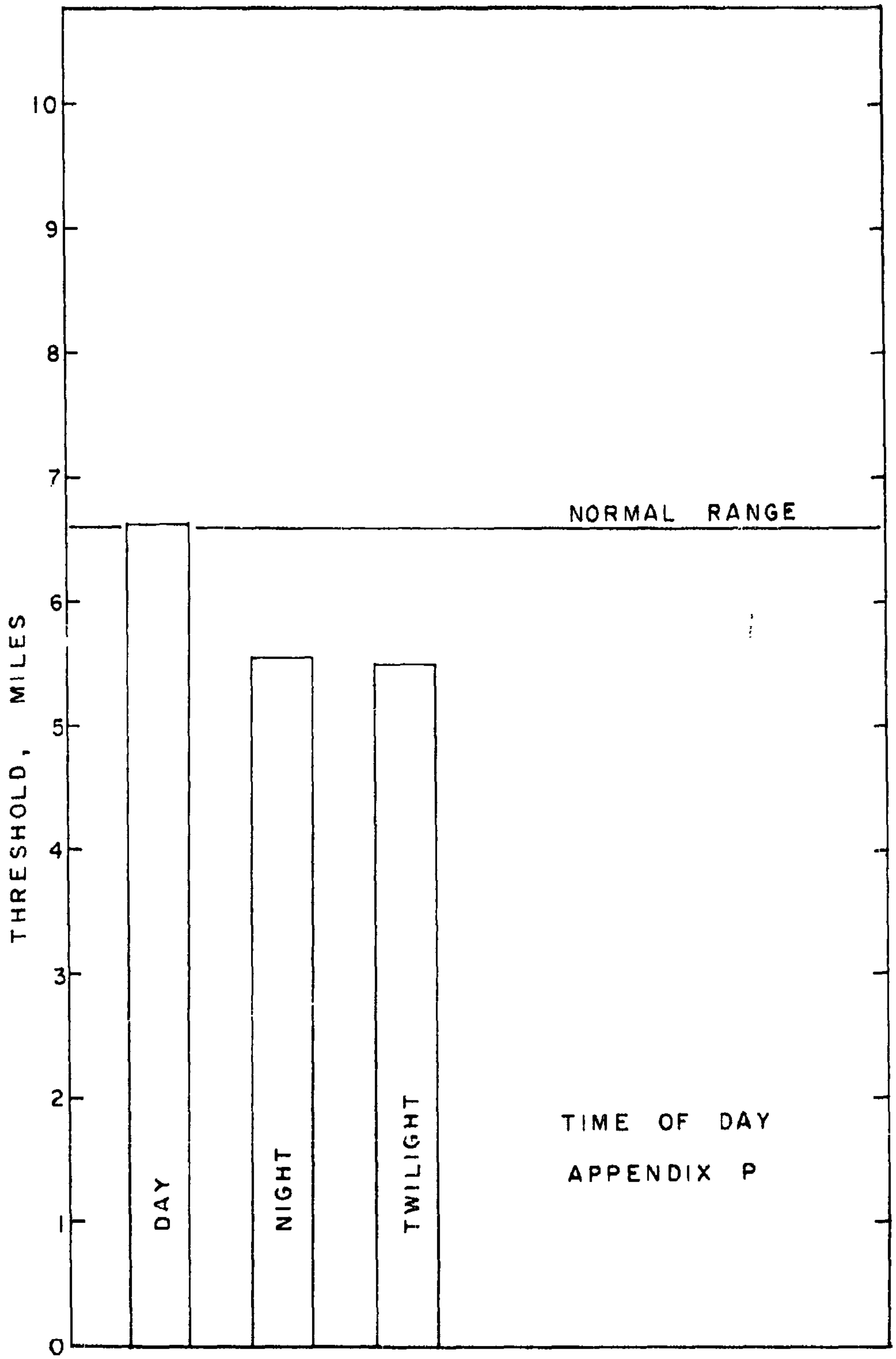
10
9
8
7
6
5
4
3
2
1
0
THRESHOLD, MILES
NORMAL RANGE
DAY
NIGHT
TWILIGHT
TIME OF DAY
APPENDIX P

TIME OF DAY

Range (Miles)	Day	Night	Twilight
0	3309	47	62
4	2579	32	45
10	917	10	9
14	388	4	1
20	105	2	0
T	6.614	5.583	5.496
S	0.67	0.71	0.51
$S_{\hat{T}}$	0.0096	0.098	0.007
X^2	5.770	0.145	1.381
Factor	1.002	0.846	0.833

$\bar{S} = 0.630$

$S_s = 0.086$

$S_{\bar{s}} = 0.050$

APPENDIX P-2

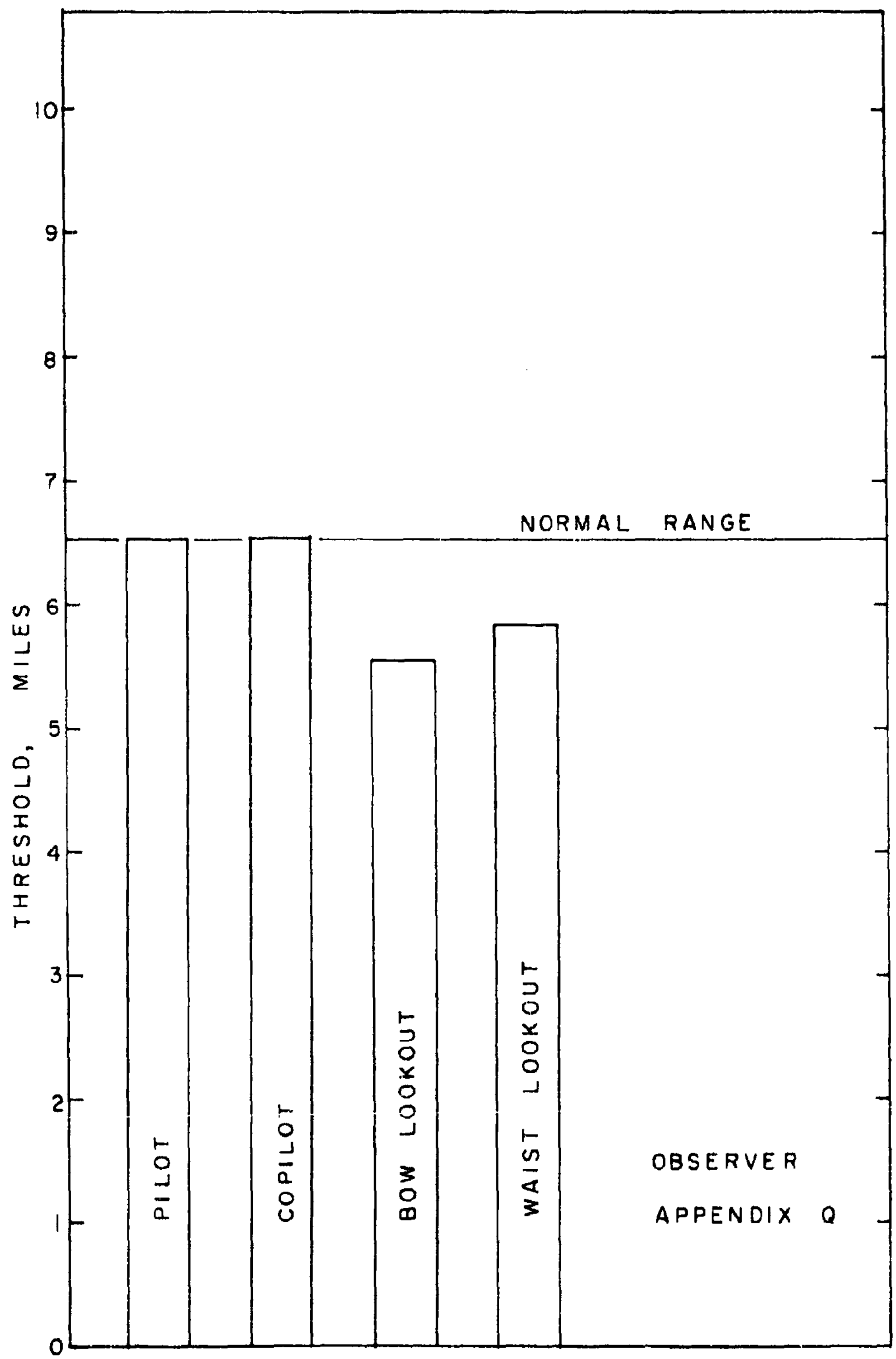
THRESHOLD, MILES
0
1
2
3
4
5
6
7
8
9
10
NORMAL RANGE
PILOT
COPILOT
BOW LOOKOUT
WAIST LOOKOUT
OBSERVER
APPENDIX Q

OBSERVER

Range (Miles)	Pilot	Copilot	Bow Lookout	Waist Lookout	Tail Lookout
0	1772	1452	59	122	3
4	1377	1140	40	82	2
10	494	382	13	34	1
14	192	170	4	15	0
20	42	51	0	7	0
T	6.603	6.616	5.553	5.853	(No)
S	0.64	0.63	0.68	0.80	(Fit)
S_T	0.013	0.015	0.085	0.079	-
X^2	5.184	0.997	0.501	0.588	-
Factors	1.0006	1.0026	0.841	0.887	-

$\bar{S} = 0.683$

$S_s = 0.063$

$S_{\bar{s}} = 0.034$

APPENDIX Q-2

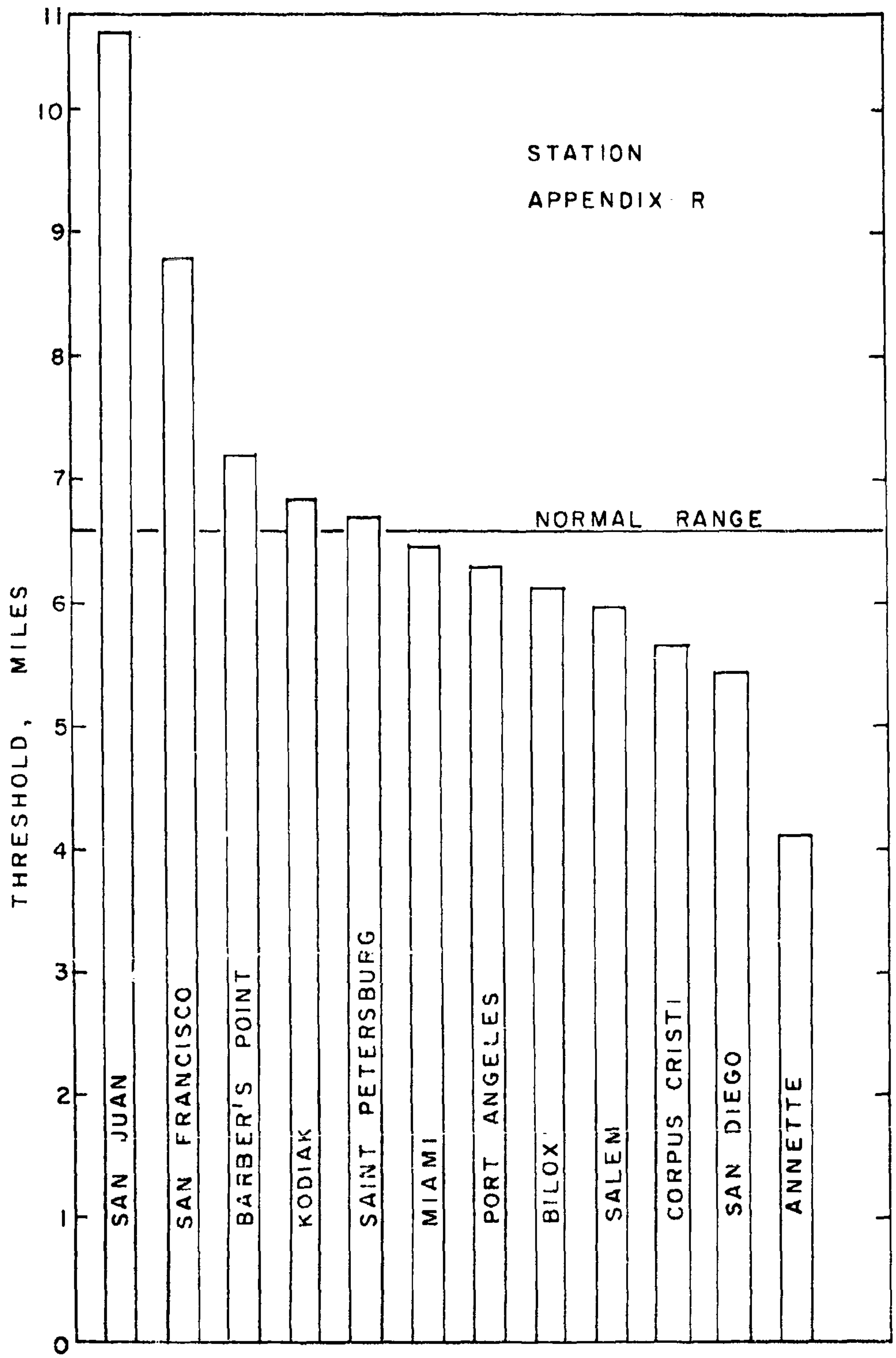
STATION
APPENDIX R
NORMAL RANGE
THRESHOLD, MILES
0
1
2
3
4
5
6
7
8
9
10
11
SAN JUAN
SAN FRANCISCO
BARBER'S POINT
KODIAK
SAINT PETERSBURG
MIAMI
PORT ANGELES
BILOXI
SALEM
CORPUS CRISTI
SAN DIEGO
ANNETTE

STATION

Range (Miles)	San Juan	San Francisco	Barber's Point	Kodiak	Saint Petersburg	Miami	Port Angeles	Biloxi	Salem
0	179	315	102	13	97	181	1533	276	112
4	167	292	84	10	77	140	1171	210	78
10	106	141	35	4	23	46	360	66	32
14	58	51	10	2	14	20	153	17	10
20	20	13	3	0	5	4	38	3	3
T	10.601	8.782	7.158	6.836	6.689	6.456	6.288	6.163	5.959
S	0.59	0.51	0.58	0.72	0.65	0.62	0.62	0.57	0.69
S_T	0.033	0.024	0.050	0.17	0.058	0.041	0.014	0.033	0.060
χ^2	2.317	3.098	2.122	0.00651	0.623	1.242	2.551	4.788	2.617
Factor	1.606	1.331	1.085	1.036	1.014	0.978	0.953	0.934	0.903

$\bar{S} = 0.613$

$S_s = 0.087$

$S_{\bar{s}} = 0.025$

APPENDIX R-2

STATION

Range (Miles)	Corpus Cristi	San Diego	Annette
0	80	218	62
4	63	141	32
10	8	46	5
14	1	27	1
20	0	7	1
T	5.654	5.393	4.119
S	0.43	0.77	0.61
S_T	0.052	0.050	0.093
X^2	0.81	1.449	0.186
Factor	0.857	0.817	0.454

APPENDIX R-3

TABLE OF FACTORS

	Ship Size		Range Method					
Tonnage (C)	Length	Factor		Factor	Clock Code	Factor	Length Wake / Length Ship	Factor
0.1	8	0.415	Estimate	0.923	0-12	1.039	0	0.954
0.5	16	0.609	Time-Distance	1.001	1-11	1.022	0.5	1.020
3	30	0.785	Radar	1.298	2-10	0.977	1.0	1.061
25	60	0.979			3-9	0.916	2.0	1.093
100	100	1.122			4-8	0.855		
1000	200	1.316			5-7	0.810		
3000	300	1.430			6	0.794		
7500	400	1.510						
15000	500	1.573						
25000	600	1.624						

APPENDIX S

TABLE OF FACTORS

Visual Aid	Factor	Time of Day	Factor	Altitude	Factor	Wind Velocity	Factor
Sunglasses	0.949	Twilight	0.833	0	0.816	0	0.832
None	1.002	Night	0.846	1K	0.916	5	0.929
Binocular	1.350	Day	1.002	2	1.029	10	1.006
				3	1.155	15	1.062
				4	1.297	20	1.098
				5	1.457	30	1.110
				6	1.637	40	1.040
				7	1.838	50	0.890
				8	2.064		
				9	2.318		
				10	2.608		

APPENDIX S-2

TABLE OF FACTORS

Major Swell Height	Factor	Fractional Cloud Cover	Factor	Meteorological Visibility	Factor	Relative Sun Bearing	Factor
0	0.935	0	1.071	2	0.052	0-360	1.015
1	0.971	0.1	1.100	5	0.535	30-330	1.021
2	1.007	0.2	1.130	10	0.901	60-300	1.041
3	1.044	0.3	1.137	15	1.114	90-270	1.067
4	1.080	0.4	1.131	20	1.266	120-240	1.093
5	1.116	0.5	1.110	30	1.479	150-210	1.112
6	1.152	0.6	1.075	40	1.631	180	1.119
7	1.139	0.7	1.025	50	1.749		
8	1.225	0.8	0.962				
9	1.261	0.9	0.884	Unlimited	1.484		
10	1.297	1.0	0.791				
15	1.478						

APPENDIX S-3

TABLE OF FACTORS

Sun Altitude	Factor	Observer	Factor	Observing Unit	Factor
0	1.208	Pilot	1.001	Patrol	1.014
10	1.167	Copilot	1.000	Utility	0.884
20	1.126	Bow L'kout	0.841	Helicopter	0.733
30	1.089	Waist L'kout	0.887		
40	1.055	Tail L'kout	(0.032)		
50	1.025				
60	1.001				
70	0.984				
80	0.974				
90	0.970				

APPENDIX S-4

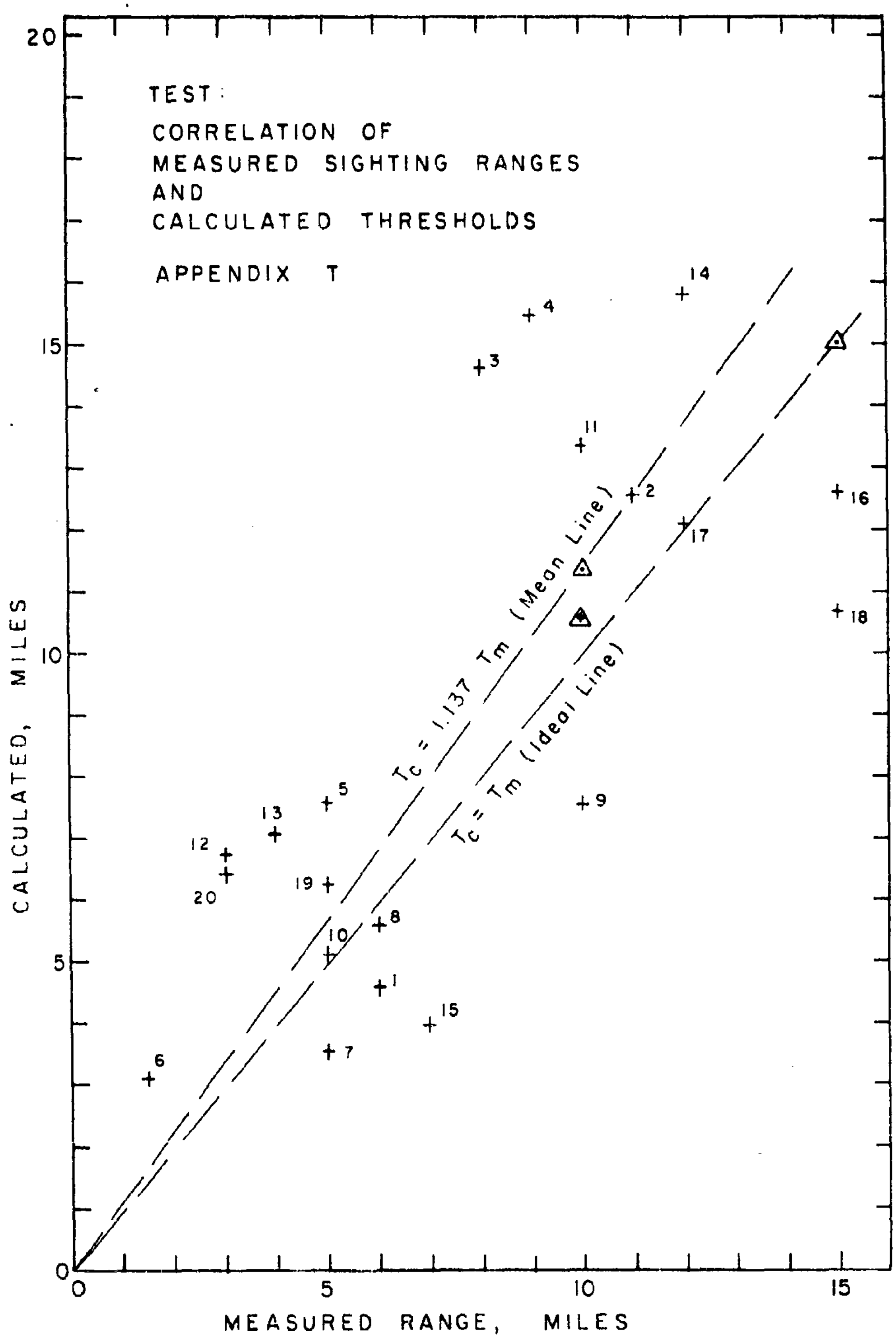
TEST:
CORRELATION OF
MEASURED SIGHTING RANGES
AND
CALCULATED THRESHOLDS
APPENDIX T
Tc = 1.137 Tm (Mean Line)
Tc = Tm (Ideal Line)
CALCULATED, MILES
MEASURED RANGE, MILES
0
5
10
15
20
1
2
3
4
5
6
7
8
9
10
11
12
13
14
15
16
17
18
19
20

TEST

T_D Data	T_C Calculated	Error $T_C - T_D$	T_D Data	T_C Calculated	Error $T_C - T_D$
6.0	4.561	- 1.439	10.0	13.351	+ 3.351
11.0	12.548	+ 1.548	3.0	6.725	+ 4.725
8.0	14.610	+ 6.611	4.0	7.075	+ 3.075
9.0	15.456	+ 6.456	12.0	15.787	+ 3.787
5.0	7.563	+ 2.563	7.2	3.979	- 3.221
1.5	3.102	+ 1.602	15.0	12.606	- 2.394
5.0	3.538	- 1.462	12.0	12.078	+ 0.078
6.0	5.497	- 0.503	15.0	9.649	- 5.351
10.0	7.517	- 2.483	5.0	6.250	+ 1.250
5.0	5.115	+ 0.115	3.0	6.430	+ 3.430

$r = 0.695$

APPENDIX T-2

TESTS

	1	Factor	2	Factor	3	Factor	4	Factor
Date	10 Jul 56	-	5 Dec 56	-	1 Sep 56	-	1 Jan 56	-
Source	Biloxi	-	San Juan	-	-	-	Miami	-
Type	30-60'	0.882	30-60'	0.882	30-60'	0.882	30-60'	0.882
	Bright	1.060	Bright	1.060	Bright	1.060	Bright	1.060
Range	6.0	-	11	-	8	-	9	-
Method	Est	0.923	Radar	1.298	Radar	1.298	Radar	1.298
Clock Code	9	0.916	10	0.977	0	1.039	11	1.022
Wake	2X	1.093	0	0.954	2X	1.093	0	0.954
Vis. Aid	Sun Gl.	0.949	None	1.002	Sun Gl.	0.949	None	0.949
Time Day	Day	1.002	Day	1.002	Day	1.002	Day	1.002
Altitude	2500	1.092	1200	0.939	1500	0.973	5300	1.511
Wind Vel.	10	1.006	12	1.028	10	1.006	25	1.104
Wind Az.	180	-	80	-	290	-	90	-
Swells	0	0.935	4	1.080	5	1.116	1	0.971
% Cloud	70	1.025	0	1.071	40	1.131	0	1.071
Visibility	10	0.901	25	1.373	20	1.266	20	1.266
Sun Brng.	270	1.067	100	1.075	035	1.024	015	1.031
Sun Alt.	80	0.974	60	1.001	45	1.040	45	1.040
Observer	Waist	0.887	Pilot	1.001	Pilot	1.001	Copilot	1.000
Obs. Unit	Patrol	1.014	Patrol	1.014	Patrol	1.014	Util.	0.884
Computed Threshold	4.561		12.548		14.610		15.456	

APPENDIX T-3

TEST

	5	Factor	6	Factor	7	Factor	8	Factor
Date	3 Apr 57	-	1 Aug 56	-	3 Oct 57	-	18 Mar 57	-
Source	-	-	Annette	-	Pt. Ang.	-	Pt. Ang.	-
Type	30-	0.609	30-60'	0.882	30-	0.609	10 KT+	1.624
	Bright	1.060	Dark	0.943	Bright	1.060	-	-
Range	5	-	1.5	-	5	-	6	-
Method	Est	0.923	Est	0.923	Est	0.923	Radar	1.296
Clock Code	1	1.022	2	0.977	3	0.916	12	1.039
Wake	2 X+	1.093	3X	1.093	0	0.954	0	0.954
Vis. Aid	None	1.002	None	1.002	Sun Gl.	0.949	Sun Gl.	0.949
Time Day	Day	1.002	Twi	0.833	Day	1.002	Day	1.002
Altitude	1500	0.973	800	0.896	700	0.886	400	0.856
Wind Vel.	8	0.975	5	0.929	3	0.890	3	0.890
Wind Az.	200	-	0	-	0	-	315	-
Swells	3	1.044	0	0.935	3	1.044	0	0.935
% Cloud	0	1.071	100	0.791	0	1.071	100	0.791
Visibility	30	1.479	15	1.114	15	1.114	8	0.755
Sun Brng.	135	1.118	-	-	170	1.116	-	-
Sun Alt.	50	1.025	-	-	80	0.974	-	0.974
Observer	Copilot	1.000	-	-	Copilot	1.000	Copilot	1.000
Obs. Unit	Patrol	1.014	-	-	Patrol	1.014	Patrol	1.014
Computed Threshold	7.563		3.102		3.538		5.497	

APPENDIX T-4

TEST

	9	Factor	10	Factor	11	Factor	12	Factor
Date	22 Mar 56	-	19 Sep 57	-	14 Oct 56	-	3 Apr 57	-
Source	Salem	-	Pt. Ang.	-	St. Pet.	-	-	-
Type	5 Oct-5KT	1.430	30-60'	0.882	5K-10K	1.510	30-60'	0.882
	-	-	Dark	0.943	-	-	Dark	0.943
Range	10	-	5	-	10	-	3	-
Method	Est	0.923	Est	0.923	Est	0.923	Radar	1.298
Clock Code	10	0.977	3	0.916	3	0.916	11	1.072
Wake	C	0.954	0.5X	1.020	1X	1.061	0.5X	1.020
Vis. Aid	None	1.002	Sun El.	0.949	-	-	None	1.002
Time Day	Day	1.002	Day	1.002	-	-	Day	1.002
Alt.	1000	0.916	100	0.826	-	-	1500	0.973
Wind Vel.	5	0.929	8	0.975	25	1.104	6	0.944
Wind Az.	110	-	220	-	20	-	135	-
Swells	2	1.007	3	1.044	11	1.333	3	1.044
% Cloud	0	1.071	0	1.071	-	-	1	1.074
Visibility	15	1.114	15	1.114	-	-	8	0.755
Sun Brng.	20	1.019	280	1.058	-	-	10	1.017
Sun Alt.	60	1.001	40	1.055	-	-	35	1.072
Observer	Pilot	1.001	Copilot	1.000	Pilot	1.001	Pilot	1.001
Obs. Unit	Utility	0.884	Patrol	1.014	Patrol	1.014	Patrol	1.014
Computed Threshold	7.517		5.115		13.351		6.725	

APPENDIX T-5

TEST

	13	Factor	14	Factor	15	Factor	16	Factor
Date	18 Sep 57	-	16 May 56	-	23 Feb 56	-	21 Dec 55	-
Source	Pt. Ang.	-	San Juan	-	Biloxi	-	Biloxi	-
Type	30-60'	0.882	500T-5KT	1.430	30-	0.609	5-10KT	1.510
	Dark	0.943	-	-	Dark	0.943	-	-
Range	4	-	12	-	7.2	-	15	-
Method	T-D	1.001	T-D	1.001	T-D	1.001	Est	0.923
Clock	2	0.977	11	1.022	11	1.022	12	1.039
Wake	0	0.954	0	0.954	0	0.954	2X	1.093
Vis.Aid	None	1.002	None	1.002	None	1.002	None	1.002
Time Day	Day	1.002	Day	1.002	Day	1.002	Day	1.002
Altitude	1500	0.973	2000	1.029	300	0.846	1500	0.973
Wind Vel.	14	1.051	6	0.944	14	1.051	15	1.062
Wind Az.	340	-	140	-	350	-	50	-
Swells	1	0.971	3	1.044	2	1.007	4	1.080
% Cloud	0	1.071	50	1.110	0	1.071	40	1.131
Visibility	15	1.114	20	1.266	15	1.114	10	0.901
Sun Brng.	210	1.112	180	1.119	20	1.019	350	1.017
Sun Alt.	50	1.025	40	1.055	70	0.984	50	1.025
Observer	Pilot	1.001	Pilot	1.001	Pilot	1.001	Copilot	1.000
Obs. Unit	Patrol	1.014	Patrol	1.014	Heli.	0.733	Patrol	1.014
Computed Threshold	7.075		15.787		3.979		12.606	

APPENDIX T-6

TEST

	17	Factor	18	Factor	19	Factor	20	Factor
Date	3 Jun 56	-	26 Mar 57	-	10 June	-	30 Aug 56	-
Source	San Juan	-	Pt. Ang.	-	Pt. Ang.	-	San Diego	-
Type	10KT+	1.573	10KT+	1.573	-	-	30-60'	0.882
	-	-	-	-	-	-	Dark	0.943
Range	12	-	15	-	5	-	3	-
Method	T-D	1.001	Est	0.923	Radar	1.298	T-D	1.001
Clock	12	1.039	12	1.039	12	1.039	11	1.022
Wake	2X	1.093	0	0.954	0	0.954	2X	1.093
Vis. Aid	None	1.002	None	1.002	None	1.002	None	1.002
Time Day	Day	1.002	Day	1.002	Day	1.002	Twi	0.833
Altitude	1000	0.916	1200	0.939	2000	1.029	500	0.866
Wind Vel.	20	1.098	5	0.929	5	0.929	11	1.017
Wind Az.	60	-	270	-	270	-	270	-
Swells	8	1.225	4	1.080	1	0.971	4	1.080
% Cloud	100	0.791	90	0.884	80	0.962	5	1.110
Visibility	12	0.986	15	1.114	8	0.755	12	1.029
Sun Brng.	270	1.067	15	1.018	0	1.015	90	1.067
Sun Alt.	60	1.001	40	1.055	40	1.055	30	1.089
Observer	Pilot	1.001	Pilot	1.001	Pilot	1.001	Pilot	1.001
Obs. Unit	Patrol	1.014	Patrol	1.014	Patrol	1.014	Patrol	1.014
Computed Threshold	12.078		9.649		6.258		6.430	

APPENDIX T-7

SIO Ref: 62-13

COPY

UNITED STATES COAST GUARD

ADDRESS REPLY TO:
COMMANDANT
U.S. COAST GUARD
HEADQUARTERS
WASHINGTON 25, D.C.

O
8 September 1955

OPERATIONS INSTRUCTION NO. 58-55

Subj: Sighting Data Report (Form CG-3627); instructions for

1. Purpose. To prescribe procedures which are required of aircraft and certain floating units relative to the preparation and submission of data collected in connection with the program for the collection of sighting data.

2. Objective. This program is designed to collect reports of 8-10,000 sightings of life rafts, emergency visual signals, small boats and vessels under many visibility and air and sea conditions.

3. Information. Presently available "Effective Visibility" tables do not include small boats and vessels with which the Coast Guard is commonly concerned, nor is the condition of air and sea taken into consideration. Therefore, in order to obtain more realistic tables on this important subject, the U. S. Navy, at the request of the Coast Guard, has agreed to evaluate (by use of Univac machines) sighting data collected by the Coast Guard and to derive empirical formulae from which curves for search, sweep width, and sighting effectiveness may be drawn. These results will ultimately be incorporated in a Coast Guard Search and Rescue Manual.

4. Action.

a. Floating units 83' in length and over and aircraft shall fill in subject form, which is self explanatory, on each sighting deemed to be advantageous to the program. Data must be complete for each sighting reported. Forms should be carried on all flights over water and on bridges of floating units ready for use as may be practicable.

b. Units shall submit forms to Commandant (O) in lots of 100 sighting reports.

5. Availability of Forms. An initial distribution of Form CG-3627 will be made in the near future to all aviation units and floating units 83' in length and over. The form will be included in the Catalog of Forms (CG 218) with source of supply "SC".

COPY

OPERATIONS INSTRUCTION NO. 58-55

6. Effective date. This instruction is effective upon receipt and will be canceled by separate instruction upon completion of the project.

H. C. PERKINS
By direction

Encl: (1) Sighting Data Report,
Form CG-3627

Dist. (SDL No. 61)
A: a,aabcd(5); efi(3); g.1.2.3. hjklmn(1)
B: C(15); eghi(5); jl(3); d(2); b(1)
C: A(5); bd(3)
D: NONE

TREASURY DEPARTMENT
U. S. COAST GUARD
CG-3627 (8-55)

SIGHTING DATA REPORT

1. DATE SIGHTED *(Day, month, year)*

TO: Commandant (C)

FROM *(Forwarding letter not necessary)*:

2. TARGET TYPE *(Check and complete)*

01 ONE MAN LIFE RAFT	06 MK-13 NIGHT SIGNAL	11 TYPE III SMALL BOAT 1/	16 MEDIUM VESSEL *(5000 to 10000 tons)*
02 SEVEN MAN LIFE RAFT	07 VERY'S PISTOL SIGNAL	12 TYPE IV SMALL BOAT 1/	17 LARGE VESSEL *(Over 10000 tons)*
03 TWENTY MAN LIFE RAFT	08 SIGNALLING MIRROR	13 TYPE V SMALL BOAT 1/	19 OTHER *(Describe)*
04 ORANGE SMOKE SIGNAL	09 TYPE I SMALL BOAT 1/	14 TYPE VI SMALL BOAT 1/	
05 SEA DYE-MARKER	10 TYPE II SMALL BOAT 1/	15 SMALL VESSEL *(500 to 5000 tons)*	

3. SIGHTING RANGE *(Naut. miles & tenths)*

METHOD *(Check)*	RANGE
ESTIMATED	
RADAR	
TIME-DISTANCE CHECK	

4. CLOCK CODE *(Relative bearing, 0-12 hours)*

5. WAKE SIZE *(Check)*
- 1 NEGLIGIBLE
- 1 ONE-HALF LENGTH OF OBJECT
- 2 ONE LENGTH OF OBJECT
- 3 TWICE LENGTH OF OBJECT
- 4 OVER TWICE THE LENGTH

6. VISUAL AID *(Check and complete)*
- 1 NONE
- 2 BINOCULARS
- 3 SUN GLASSES
- 4 OTHER *(Describe)*

7. TIME OF DAY *(Check)*
- N NIGHT
- D DAY
- T TWILIGHT *(Morning or evening)*

8. ALTITUDE (100's of ft.) FOR SIGHTINGS FROM AIRCRAFT

8a. HEIGHT OF EYE IN FEET *(For sighting from vessel)*

9. SURFACE WIND

KNOTS	FROM *(Degrees true)*

10. HEIGHT OF MAJOR SWELLS *(Feet)*

11. CLOUD COVER (%)

12. METEOROLOGICAL VISIBILITY *(Miles)* 2/

13. POSITION OF SUN

RELATIVE BEARING FROM LINE OF SIGHT *(Degrees)*	ALTITUDE *(Degrees)*

14. OBSERVER *(Check and complete)*

a. AIRCRAFT	b. VESSEL
1 PILOT	11 CO
2 CO-PILOT	12 OOD
3 BOW LOOKOUT	13 JW
4 WAIST LOOKOUT	14 BRIDGE LOOKOUT
5 TAIL LOOKOUT	15 DECK LOOKOUT
6 OTHER *(Specify)*	16 OTHER *(Specify)*

15. TYPE OF OBSERVING UNIT *(Check and complete)*

1 PATROL PLANE *(Including UF's)*	4 VESSEL OVER 200 FEET
2 UTILITY PLANE	5 VESSEL 100-200 FEET
3 HELICOPTER	6 VESSEL UNDER 100 FEET
7 OTHER *(Describe)*	

1/ Types of boats are as follows:

TYPE	LENGTH	DESCRIPTION
I	Less than 30 Feet	Bright colors such as white, orange, yellow, red. Little or no superstructure.
II	Less than 30 Feet	Dark colors such as black, blue, green, grey, offering little or no contrast with water.
III	30 to 60 Feet	Bright colors such as white, orange, yellow, red.
IV	30 to 60 Feet	Dark colors such as black, blue, green, grey.
V	60 to 100 Feet	Bright colors such as white, orange, yellow, red.
VI	60 to 100 Feet	Dark colors such as black, blue, green, grey.

2/ Meteorological visibility should be estimated by determining range at which land masses, ships, or other targets can be seen.

NOTE: *This form should be filled out using heavy, dark-colored pencil or pen and ink. Prepare original only.* **USE REVERSE FOR REMARKS.**

SIGNATURE OR INITIALS OF CO, OIC OR PLANE COMMANDER

GPO 897756

FLOW OF PROBIT CALCULATION

The notation herein is defined for this appendix only.

1. Given (x_i, n_i, r_i) , stimulus levels, number of presentations and number of responses at each level, determine frequency, $p = \frac{r}{n}$. Note: Hereafter the subscripts, i , are to be inferred.

2. Determine experimental probits, EP, such that:

$$p = \int_{-\infty}^{EP} \frac{1}{2\pi} e^{-1/2\, U^2} du$$

3. Determine best fit trial line and trial probits Y by least square method giving approximate regression of EP on x by:

$$Y = a + bx$$

4. Determine weights $w = \frac{Z^2}{PQ}$

$$Z = \frac{1}{2\pi} e^{-1/2\, Y^2}$$

$$P = \int_{-\infty}^{Y} 1/2\pi \; e^{-1/2\, U^2} du; \quad Q = 1 - P$$

5. Determine working probits $y = \frac{p - P}{Z} + Y$

6. Determine Σnw, Σnwx, Σnwy, Σnwx^2, Σnwy^2, $\Sigma nwxy$

7. Determine $\bar{x} = \frac{\sum nwx}{\sum nw}$ $\bar{y} = \frac{\sum nwy}{\sum nw}$

8. Now: $S_{xx} = \sum nwx^2 - \frac{\sum^2 nwx}{\sum nw}$

$S_{xy} = \sum nwxy - \frac{\sum nwx \sum nwy}{\sum nw}$

$S_{yy} = \sum nwy^2 - \frac{\sum^2 nwy}{\sum nw}$

9. Then: $b_1 = \frac{S_{xy}}{S_{xx}}$ and $a_1 = \bar{y} - b\bar{x}$

10. $Y_1 = a_1 + b_1 x$. The subscripts here and in 9. above indicate a next approximation.

11. The χ^2 test is applied and, if not satisfactory, recycling begins at 3. above using a_1 and b_1 in place of a and b.

12. When iteration proves satisfactory the following are determined.

Threshold, $T = \frac{-a}{b}$

Variance, $S^2 = \frac{1}{b^2}$

Variance of threshold, $S_T^2 = \frac{1}{b^2}\left[\frac{1}{\sum nw} + \frac{(m - \bar{x}^2)}{S_{xx}}\right]$

Variance of a, $S_a^2 = \frac{\sum nwx^2}{S_{xx}}$

Variance of b, $S_b^2 = \frac{1}{S_{xx}}$

Variance of standard deviation, $S_s^2 = \frac{S^4}{S_{xx}}$

NOTATION

A	Altitude, 1000's feet
B	Target bearing, degrees
C	Cloud cover, decimal fraction
$D(p)$	Normal deviate for probability p
f	Factor
$F(.)$	Factor function of . , any variable
L	Length of vessel, feet
OB	Observer
OU	Observing unit
p	Cumulative probability of sighting
$p(.)$	Probability of . , any function
r	Correlation coefficient
RD	Range determination method
S	Height of major swells, feet
s	Standard deviation
$\bar{s}$	Mean standard deviation
s_s	Standard deviation of s
$s_{\bar{s}}$	Standard deviation of $\bar{S}$
s_t	Standard deviation of T
SA	Sun altitude, degrees
SB	Sun bearing, relative to observer-target line, degrees
ST	Air station
T	Threshold, miles
T_N	Normal range, miles

APPENDIX X

T(.)	Threshold function of . , any variable, miles
TD	Time of day, general
t	Student's t function
V	Visibility, miles
VA	Visual aid
WA	Wind azimuth, degrees
WS	Wake size, proportional to length of vessel
WV	Wind velocity, knots
X^2	The accumulated value of the measure of goodness of fit and other statistical tests.

BRL

REPORT NO. 1183
DECEMBER 1962

THE SIMULATION OF INTERIOR BALLISTIC PERFORMANCE OF GUNS BY DIGITAL COMPUTER PROGRAM

Paul G. Baer
Jerome M. Frankle

RDT & E Project No. 1M010501A004

BALLISTIC RESEARCH LABORATORIES

ABERDEEN PROVING GROUND, MARYLAND

ASTIA AVAILABILITY NOTICE

Qualified requestors may obtain copies of this report from ASTIA.

The findings in this report are not to be construed as an official Department of the Army position.

BALLISTIC RESEARCH LABORATORIES

REPORT NO. 1183

DECEMBER 1962

THE SIMULATION OF INTERIOR BALLISTIC PERFORMANCE OF GUNS BY DIGITAL COMPUTE PROGRAM

Paul G. Baer

Jerome M. Frankle

Interior Ballistics Laboratory

RDT & E Project No. 1M010501A004

ABERDEEN PROVING GROUND, MARYLAND

B A L L I S T I C   R E S E A R C H   L A B O R A T O R I E S

REPORT NO. 1183

PGBaer/JMFrankle/mec
Aberdeen Proving Ground, Md.
December 1962

THE SIMULATION OF INTERIOR BALLISTIC PERFORMANCE OF GUNS BY DIGITAL COMPUTER PROGRAM

ABSTRACT

When non-conventional guns are to be considered or when detailed design information is required, interior ballistic calculations become more difficult and time-consuming. To deal with these problems, the equations which describe the interior ballistic performance of guns and gun-like weapons have been programmed for the high-speed digital computers available at the Ballistic Research Laboratories. The major innovation contained in the equations derived in this report is the provision for use of propellant charges made up of several propellants of different chemical compositions and different granulations. Results obtained by the method described in this report compare favorably with those of other interior ballistic systems. In addition, considerably more detail is obtained in far less time. A comparison with experimental data from well-instrumented gun-firings is also presented to demonstrate the validity of this method of computation.

TABLE OF CONTENTS

LIST OF SYMBOLS

a acceleration of projectile, in./sec^2

a_o constant defined by Equation (28a), dimensionless

A area of base of projectile including appropriate portion of rotating band, in.^{2}

b_i covolume of i th propellant, in.^{3}/lb

c diameter of bore, in.

c_{v_i} specific heat at constant volume of i th propellant (c_{v_i} is a function of T), in.-lb/lb-^oK

$\bar{c}_{v_i}$ mean value of specific heat at constant volume of i th propellant (over temperature range T to T_{o_i}), in.-lb/lb-^oK

$\bar{c}_{p_i}$ mean value of specific heat at constant pressure of i th propellant (over temperature range T to T_{o_i}), in.-lb/lb-^oK

C_i initial weight of i th propellant, lb

C_I initial weight of igniter, lb

d_i diameter of perforation in i th propellant grains, in.

dt incremental time, sec

dT incremental temperature, ^oK

dx incremental distance traveled by projectile, in.

$\frac{dz_i}{dt}$ mass fraction burning rate for i th propellant, sec^{-1}

D_i outside diameter of i th propellant grains, in.

E_h energy lost due to heat loss, in.-lb

E_p kinetic energy of propellant gas and unburned propellant, in.-lb

E_{pr} energy lost due to bore friction and engraving of rotating band, in.-lb

f_i functional relationship between S_i and z_i

F_a resultant axial force on projectile, lb

F_f frictional force on projectile, lb

F_i "force" of i th propellant, in.-lb/lb

F_I "force" of igniter propellant, in.-lb/lb

F_p propulsive force on base of projectile, lb

F_r gas retardation force, lb

g constant for conversion of weight units to mass units, in./sec^2

G functional relationship between p_r and x

K_v burning rate velocity coefficient, $\frac{\text{in.}}{\text{sec in./sec}}$

K_x burning rate displacement coefficient, $\frac{\text{in.}}{\text{sec-in.}}$

L_i length of i th propellant grains, in.

m_i specific mass of i th propellant, lb-mols/mol

M mass of projectile, slugs/12

n number of propellants, dimensionless

n' ratio defined by Equation (28b), dimensionless

N_i number of perforations in i th propellant grains, dimensionless

$\bar{p}$ space-mean pressure resulting from burning i propellants, psi

p_b pressure on base of projectile, psi

p_g pressure of gas or air ahead of projectile, psi

p_i space-mean pressure resulting from burning of i th propellant, psi

p_I igniter pressure, psi

p_o breech pressure, psi

p_r resistance pressure, psi

Q energy released by burning propellant, in.-lb

r_i linear burning rate of i th propellant, in./sec

r'_i adjusted linear burning rate of i th propellant, in./sec

R_i functional relationship between r_i and $\bar{p}$

S_i surface area of partially burned i th propellant grain, in.^{2}

S_{g_i} surface area of an unburned i th propellant grain, in.^{2}

t time, sec

T mean temperature of propellant gases, ^oK

T_{o_i} adiabatic flame temperature of i th propellant, ^oK

T_{o_I} adiabatic flame temperature of igniter propellant, ^oK

T_S temperature of unburned solid propellant, ^oK

u_i two times the distance each surface of i th propellant grains has receded at a given time, in.

U internal energy of propellant gases, in.-lb

v velocity of projectile, in./sec

v_m velocity of projectile at muzzle of gun, in./sec

V specific volume of propellant gas, in.^{3}/lb

V_c volume behind projectile available for propellant gas, in.^{3}

V_{g_i} volume of an unburned i th propellant grain, in.^{3}

V_o volume of empty gun chamber, in.^{3}

W external work done on projectile, in.-lb

W_p weight of projectile, lb

x travel of projectile, in.

x_m travel of projectile when base reaches muzzle, in.

z_i fraction of mass of i th propellant burned, dimensionless

z_I fraction of mass of igniter burned, dimensionless

α_i burning rate exponent for i th propellant, dimensionless

β_i burning rate coefficient for i th propellant, $\frac{in.}{sec} - \frac{1}{psi^{\alpha}}$

γ' effective ratio of specific heats as defined by Equation (27a), dimensionless

γ_i ratio of specific heats for i th propellant, dimensionless

γ_I ratio of specific heats for igniter propellant, dimensionless

δ Pidduck-Kent constant, dimensionless

ρ_i density of i th solid propellant, lb/in.^{3}

INTRODUCTION

The interior ballistician must frequently predict the interior ballistic performance of guns. In some instances, it is sufficient to calculate muzzle velocity and maximum chamber pressure for a conventional gun from a knowledge of the propellant charge, the projectile weight, and the gun characteristics. This calculation is usually referred to as the classical central problem [1]* of interior ballistics. When non-conventional guns are considered or when detailed design information is required, it is necessary to know more than these two salient values. For the more demanding problems, complete interior ballistic trajectories may have to be calculated. These trajectories consist of displacement, velocity, and acceleration of the projectile and chamber pressure, all as functions of time.

The literature of interior ballistics contains descriptions of many methods for solving the problem of predicting the performance of guns. [1] [2] Methods, varying from the purely empirical to the "exact" theoretical, have been devised in tables, graphs, nomograms, slide rules, and simplified equations solved in closed-form. Some of these methods require data from the firing of the gun being considered or from a very similar gun. All of these methods require some simplification of the basic equations of interior ballistics.

To eliminate the restrictions imposed by assumptions made only to facilitate the mathematical solution of the problem, the interior ballistic equations have been programmed for high-speed electronic computers. Both analog and digital computers have been used to calculate detailed interior ballistic trajectories. There are advantages and disadvantages associated with each type of computer. Several years ago, [3] the interior ballistic equations were programmed for the digital computers** available here at the Ballistic Research Laboratories. Since that time, considerable use has been made of this program for studying gun and gun-like systems and for routine calculations.

---

* Superscripts indicate references listed at the end of this report.

** Although the interior ballistic equations were originally programmed only for the ORDVAC, [4] they have been recently reprogrammed in more general form [5] for the ORDVAC and the newer BRLESC. [4]

The computer program described in this report has been designed to solve a set of non-linear, ordinary differential and algebraic equations which simulate the interior ballistic performance of a gun. In this method, the usual set of equations which pertains to the burning of a single propellant has been modified to account for the burning of composite charges, i.e., charges made up of several propellants of different chemical compositions and different granulations.* The computer program may be suitably modified to study non-conventional guns and gun-like systems. A number of these optional programs have been devised and used extensively.**

INTERIOR BALLISTIC THEORY

Interior Ballistic System

The basic components of the interior ballistic system for a conventional gun are shown in Figure 1. A set of equations can be formulated which mathematically describes the distribution of energy originating from the burning

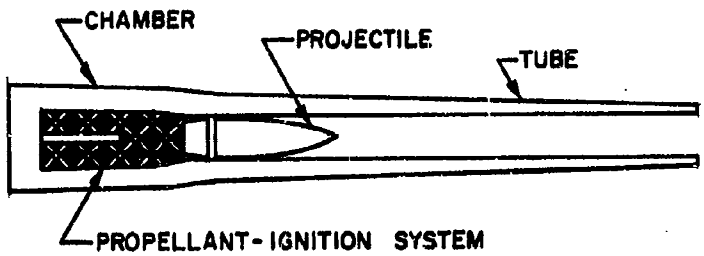

Figure 1. Basic Components of the Interior Ballistic System for a Conventional Gun

* The present program can be operated with as many as five different types of propellant charges for each problem.
** See Section entitled Options to Routine.

propellant and the subsequent motion of the components of the system. In the development which follows, two major assumptions are made to account for the behavior of composite charges:

1. The total chemical energy available is the simple sum of the chemical energies of the individual propellants.

2. The total gas pressure is the simple sum of the "partial pressures" resulting from the burning of the individual propellants.

Energy Equation

Application of the law of conservation of energy leads to the energy equation of interior ballistics. This may be written as:

$$\begin{matrix}\text{Energy Released} \\ \text{by Burning Propellant}\end{matrix} = \begin{matrix}\text{Internal Energy} \\ \text{of Propellant Gases}\end{matrix} + \begin{matrix}\text{External} \\ \text{Work Done} \\ \text{on Projectile}\end{matrix} + \begin{matrix}\text{Secondary} \\ \text{Energy Losses}\end{matrix} \tag{1}$$

or:

$$Q = U + W + \text{Losses} \tag{1a}$$

In Equation (1a) the energy released by the burning propellant (Q) is assumed to be equal to the simple sum of the energies released by the individual propellants as previously stated. Therefore:

$$Q = \sum_{i=1}^{n} \left[C_i z_i \int_0^{T_{o_i}} c_{v_i} \, dT \right] \tag{2}$$

Because of gas expansion and external work performed in a gun, the gas temperature is less than the adiabatic flame temperature (T_{o_i}). The internal energy of the gas (U) is then:

$$U = \sum_{i=1}^{n} \left[C_i z_i \int_0^{T} c_{v_i} \, dT \right] \tag{3}$$

The external work done on the projectile is given by:

$$W = A \int_0^x p_b \, dx \tag{4}$$

Substituting Equations (2), (3), and (4) into Equation (1a) gives:

$$\sum_{i=1}^{n} \left[C_i z_i \int_0^{T_{o_i}} c_{v_i} dT \right] = \sum_{i=1}^{n} \left[C_i z_i \int_0^{T} c_{v_i} dT \right] + A \int_0^x p_b \, dx + \text{Losses}$$

which may be rewritten as:

$$\sum_{i=1}^{n} \left[C_i z_i \int_T^{T_{o_i}} c_{v_i} dT \right] = A \int_0^x p_b \, dx + \text{Losses} \tag{5}$$

As the c_{v_i} do not vary greatly over the temperature ranges from T to T_{o_i}, they can be replaced with mean values ($\bar{c}_{v_i}$). Integration of Equation (5) gives:

$$\sum_{i=1}^{n} C_i z_i \bar{c}_{v_i} (T_{o_i} - T) = A \int_0^x p_b \, dx + \text{Losses} \tag{6}$$

and solving for T:

$$T = \frac{\sum_{i=1}^{n} C_i z_i \bar{c}_{v_i} T_{o_i} - A \int_0^x p_b \, dx - \text{Losses}}{\sum_{i=1}^{n} C_i z_i \bar{c}_{v_i}} \tag{7}$$

Next, the "force" of each propellant is defined by:

$$F_i = m_i R T_{o_i} \tag{8}$$

and the well-known relations:

$$\bar{c}p_i - \bar{c}v_i = m_i R \tag{9}$$

and:

$$\gamma_i = \frac{\bar{c}_{p_i}}{\bar{c}_{v_i}} \tag{10}$$

are introduced.

Combination of Equations (9) and (10) gives:

$$\bar{c}_{v_i}(\gamma_i - 1) = m_i R \tag{11}$$

Substitution of Equation (11) into Equation (8) gives:

$$T_{o_i} = \frac{F_i}{(\gamma_i - 1)\,\bar{c}_{v_i}} \tag{12}$$

Finally, substitution of Equation (12) into Equation (7) gives Rèsal's equation in the form:

$$T = \frac{\displaystyle\sum_{i=1}^{n} \frac{F_i C_i z_i}{\gamma_i - 1} - A \int_0^x p_b\, dx - \text{Losses}}{\displaystyle\sum_{i=1}^{n} \frac{F_i C_i z_i}{(\gamma_i - 1)\, T_{o_i}}} \tag{13}$$

For most problems, it is convenient to assume the igniter completely burned ($z_I = 1$) at zero-time. Equation (13) may be restated as:

$$T = \frac{\left[\displaystyle\sum_{i=1}^{n} \frac{F_i C_i z_i}{\gamma_i - 1}\right] + \frac{F_I C_I}{\gamma_I - 1} - A \int_0^x p_b\, d_x - \text{Losses}}{\left[\displaystyle\sum_{i=1}^{n} \frac{F_i C_i z_i}{(\gamma_i - 1) T_{o_i}}\right] + \frac{F_I C_I}{(\gamma_I - 1)\, T_{o_I}}} \tag{14}$$

The terms $A \int_0^x p_b\, dx$ and Losses of Equation (14) can now be considered in more detail. The work done on the projectile results in an equivalent gain in kinetic energy of the projectile except for losses. Including these losses under the general category of energy losses:

$$A \int_0^x p_b\, dx = 1/2\, \frac{W_P}{g}\, v^2 \tag{15}$$

According to Hunt,[2] the energy losses to be considered are:

(1) kinetic energy of propellant gas and unburned propellant,

(2) kinetic energy of recoiling parts of gun and carriage,

(3) heat energy lost to the gun,

(4) strain energy of the gun,

(5) energy lost in engraving the rotating band and in overcoming friction down the bore,

and

(6) rotational energy of the projectile.

For discussion of each type of secondary energy loss, see Reference (2). Types (2), (4), and (6) are estimated to be less than one percent for each category and have been neglected here.

The kinetic energy of propellant gas and unburned propellant can be represented by[6]

$$E_p = \frac{\left(\sum_{i=1}^{n} C_i\right) v^2}{2g\delta} \qquad (16)$$

The energy losses resulting from heat lost to the gun can be estimated by a semi-empirical relationship described by Hunt:[2]

$$E_h = \frac{0.38c^{1.5}\left(x_m + \frac{V_o}{A}\right)\left(\frac{\sum_{i=1}^{n} C_i T_{o_i}}{\sum_{i=1}^{n} C_i} - T_s\right) v^2}{\left[1 + \frac{0.6c^{2.175}}{\left(\sum_{i=1}^{n} C_i\right)^{0.8375}}\right] v_m^2} \qquad (17)$$

At the present time, the introduction of a more sophisticated treatment of heat loss, with its attendant complexity, does not seem to be warranted. Such a substitution can be made if and when it appears desirable.

The final energy losses to be considered here consist of those resulting from engraving of the rotating band, friction between the moving projectile and the gun tube, and acceleration of air ahead of the projectile. Individual estimates of these are difficult to make, so they have been grouped as resistive pressure in the form:

$$E_{p_r} = A \int_0^x p_r \, dx \tag{18}$$

The p_r versus x function is discussed in greater detail in the section concerning forces acting on the projectile.

Substitution of Equations (15), (16), (17), and (18) into Equation (14) results in the form of the energy equation used in this computer program:

$$T = \frac{\left[\sum_{i=1}^{n} \frac{F_i C_i z_i}{\gamma_i - 1}\right] + \frac{F_I C_I}{\gamma_I - 1} - \frac{v^2}{2g}\left(W_p + \frac{\sum_{i=1}^{n} C_i}{\delta}\right) - A\int_0^x p_r \, dx - E_h}{\left[\sum_{i=1}^{n} \frac{F_i C_i z_i}{(\gamma_i - 1)\, T_{o_i}}\right] + \frac{F_I C_I}{(\gamma_I - 1)\, T_{o_I}}} \tag{19}$$

Equation of State

The pressure acting on the base of the projectile can be calculated from a series of equations, once the temperature of the gas is determined from the energy equation. Generally, the equation of state for an ideal gas takes the form:

$$p_i V_i = m_i \, RT \tag{20}$$

where V_i = the volume per unit mass of i th propellant gas.

Now, define V_c, the volume behind the projectile which is available for propellant gas, as:

Volume Available for Propellant Gas	=	Initial Empty Chamber Volume	+	Volume Resulting from Projectile Motion
	-	Volume Occupied by Unburned Solid Propellant	-	Volume Occupied by Gas Molecules (covolume) (21)

or:

$$V_c = V_o + Ax - \sum_{i=1}^{n} \frac{C_i}{\rho_i} (1-z_i) - \sum_{i=1}^{n} C_i z_i b_i \tag{22}$$

By the definitions of Equations (20) and (21),

$$V_i = \frac{V_c}{C_i z_i} \tag{23}$$

Substituting Equations (8) and (23) into Equation (20) and rearranging gives:

$$p_i = \frac{F_i C_i z_i \; T}{V_c T_{o_i}} \tag{24}$$

If the b_i are assumed to be constants over the temperature range from T to T_{o_i}, and if the total gas pressure is taken as the simple sum of the "partial pressures" resulting from the burning of the individual propellants as previously stated, then:

$$\bar{p} = \sum_{i=1}^{n} p_i = \frac{T}{V_c} \sum_{i=1}^{n} \frac{F_i C_i z_i}{T_{o_i}} \tag{25}$$

As before, if it is assumed that the igniter is completely burned ($z_I = 1$) at zero-time, Equation (25) may be restated as:

$$\bar{p} = \frac{T}{V_c} \left[\left(\sum_{i=1}^{n} \frac{F_i C_i z_i}{T_{o_i}} \right) + \frac{F_I C_I}{T_{o_I}} \right] \tag{26}$$

The space-mean pressure, $\bar{p}$, given by Equation (26) is used in the calculation of the fraction of propellant burned at any time. This relationship is discussed in the section concerning burning rates. There is, however, a pressure gradient from the breech of the gun to the base of the projectile which must be considered in developing the equations of motion for the projectile. This pressure-gradient problem was first considered by Lagrange and is commonly referred to as the Lagrange Ballistic Problem. Later studies in this area were made by Love and Pidduck,[7] Kent,[8] and others. For this computer program, the improved Pidduck-Kent solution developed by Vinti and Kravitz[6] has been used:

$$p_b = \frac{\bar{p}}{1 + \dfrac{\sum_{i=1}^{n} C_i}{W_p \delta}} \qquad (27)^*$$

In addition the breech pressure, p_o, is calculated by the method contained in Reference (6). This is the pressure usually measured in experimental interior ballistic studies:

$$p_o = \frac{p_b}{(1-a_o)^{-n'-1}} \qquad (28)$$

$$\text{where:} \quad 1/a_o = \frac{2\,n'+3}{\delta} + \frac{2\,(n'+1)}{\sum_{i=1}^{n} C_i/W_p} \qquad (28a)$$

---

* In Reference (6), the determination of δ depends on the ratio of specific heats, γ. For composite charges, an effective value is used for this purpose.

$$\gamma' = \frac{\sum_{i=1}^{n} C_i \gamma_i}{\sum_{i=1}^{n} C_i} \qquad (27a)$$

$$\text{and } n' = \frac{1}{\gamma'-1} \tag{28b}$$

Mass-Fraction Burning Rate Equation

Both the energy equation (Equation (19)) and the equation of state (Equation (26)) are algebraic equations whose solutions depend upon the solutions of several non-linear, ordinary differential equations. The mass-fraction burning rate equation expresses the rate of consumption of solid propellant and hence the rate of evolution of propellant gas. This may be written as:

$$\frac{dz_i}{dt} = \frac{1}{V_{g_i}} S_i \; r_i \tag{29}$$

where: $$r_i = R_i \; (\bar{p}) \tag{30}$$

and: $$S_i = f_i \; (z_i) \tag{31}$$

For most gun propellants, Equation (30) may be quite satisfactorily stated as:

$$r_i = \beta_i (\bar{p})^{\alpha_i} \tag{32}$$

For certain propellants, including those plateau and mesa types used in solid-fuel rockets, Equation (32) will not suffice for gun calculations. In these cases, it is preferable to make use of a tabular listing of r_i's and corresponding $\bar{p}$'s (Equation (30)) and to interpolate for the desired r_i. The r_i's calculated by either Equation (30) or Equation (32) are closed chamber burning rates. As discussed in later sections of this report, these burning rates may be increased by addition of factors proportional to the velocity and displacement of the projectile in the following manner:

$$r_i' = r_i + K_v \, v + K_x \, x \tag{32a}$$

Similarly, the form function described by Equation (31) may be stated in one of several ways. In many interior ballistic systems, the form function is chosen for convenience of analytical solution. Where routine numerical computations are handled by use of a high-speed digital computer, the geometrical form of the propellant grain may be used to obtain the functional relationship, f_1, between S_1 and z_1. For the usual grain shapes encountered, these equations are given in Appendix A. This Appendix also contains the method for handling such equations in the computer routine. To extend these equations to include propellant slivering see Reference (9).

Equations of Projectile Motion

The translational motion of the projectile down the gun tube may be calculated from the forces acting on the projectile. Figure 2 shows the axial forces considered in determining the resultant force.

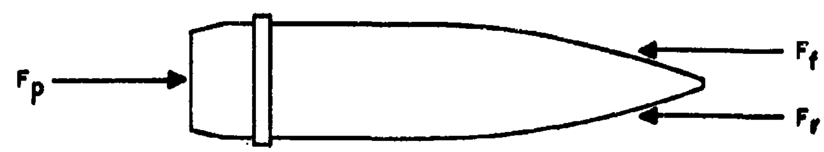

Figure 2. Axial Forces Acting on Projectile

The propulsive force, F_p, is that resulting from the pressure of the propellant gas on the base of the projectile according to:

$$F_p = p_b A \tag{33}$$

where p_b is obtained from Equation (27).

The frictional force, F_f, is the retarding force developed by resistance between the bearing surfaces of the projectile and the inside of the gun tube. This is usually the resistance between the rotating band and the rifling of the tube and includes the force required to engrave the rotating band. It may be expressed as:

$$F_f = p_r A \tag{34}$$

The determination of p_r is difficult in most cases. Many interior ballistic solutions use an increased projectile mass (approximately 5%) to account for its effect. There are several disadvantages inherent in such a treatment. Although the muzzle velocity may be calculated reasonably well, the detailed trajectory will be altered considerably. It is not possible to simulate the case where a projectile lodges in the bore (see Reference (10) for experimental trajectories for this condition). For this computer program, experimental data of the type given in Reference (11) may be used by inserting a tabulation of the function:

$$p_r = G(x) \tag{34a}$$

The gas retardation force, F_r, is that which results from the pressure of air or gas ahead of the projectile, stated as:

$$F_r = p_g A \tag{35}$$

where p_g is small enough to be neglected except for very high velocity systems, light gas guns, and other special applications. In the discussion of the Energy Equation in the Interior Ballistic Theory Section, p_g was considered a part of p_r.

The resultant force in the axial direction is then:

$$F_a = F_p - F_f - F_r \tag{36}$$

or:

$$F_a = A(p_b - p_g - p_r). \tag{37}$$

The acceleration of the projectile, by Newton's second law of motion, is:

$$a = \frac{A(p_b - p_g - p_r)}{M} \tag{38}$$

or:

$$a = \frac{Ag\,(p_b - p_g - p_r)}{W_p}. \tag{39}$$

Since $a = \frac{dv}{dt}$ and $v = \frac{dx}{dt}$, the velocity of the projectile is given by:

$$v = \int_0^t a \, dt \tag{40}$$

and the displacement of the projectile is given by:

$$x = \int_0^t v \, dt \tag{41}$$

Summary of Interior Ballistic Equations

The equations which are used in the computer program are now summarized for ease of reference.

Energy Equation

$$T = \frac{\left[\sum_{i=1}^{n} \frac{F_i C_i z_i}{\gamma_i - 1}\right] + \frac{F_I C_I}{\gamma_I - 1} - \frac{v^2}{2g}\left(W_p + \frac{\sum_{i=1}^{n} C_i}{\delta}\right) - A \int_0^x p_r \, dx - E_h}{\left[\sum_{i=1}^{n} \frac{F_i C_i z_i}{(\gamma_i - 1) T_{o_i}}\right] + \frac{F_I C_I}{(\gamma_I - 1)\, T_{o_I}}} \tag{19}$$

where:

$$E_h = \frac{0.38_c{}^{1.5}\left(x_m + \frac{V_o}{A}\right)\left(\frac{\sum_{i=1}^{n} C_i T_{o_i}}{\sum_{i=1}^{n} C_i} - T_s\right) v^2}{\left[1 + \frac{0.6c^{2.175}}{\left(\sum_{i=1}^{n} C_i\right)^{0.8375}}\right] v_m{}^2} \tag{17}$$

Equation of State

$$\bar{p} = \frac{T}{V_c}\left[\left(\sum_{i=1}^{n}\frac{F_i C_i z_i}{T_{o_i}}\right) + \frac{F_I C_I}{T_{o_I}}\right] \tag{26}$$

$$\text{where:}\quad V_c = V_o + Ax - \sum_{i=1}^{n}\frac{C_i}{\rho_i}(1-z_i) - \sum_{i=1}^{n} C_i z_i b_i \tag{22}$$

$$p_b = \frac{\bar{p}}{1+\dfrac{\sum_{i=1}^{n} C_i}{W_p \delta}} \tag{27}$$

$$p_o = \frac{p_b}{(1-a_o)^{-n'}-1} \tag{28}$$

Mass-Fraction Burning-Rate Equations

$$\frac{dz_i}{dt} = \frac{1}{V_{g_i}} S_i r_i \tag{29}$$

$$r_i = \beta_i (\bar{p})^{\alpha_i} \tag{32}$$

or:

$$r'_i = r_i + K_v v + K_x x \tag{32a}$$

Equations of Projectile Motion

$$a = \frac{Ag\,(p_b - p_g - p_r)}{W_p} \tag{39}$$

$$v = \int_0^t a\,dt \tag{40}$$

$$x = \int_0^t v\,dt \tag{41}$$

COMPUTATION ROUTINE

The set of non-linear, ordinary differential and algebraic equations, summarized at the end of the previous section, simulates the interior ballistic performance of a gun or gun-like system. A numerical computation routine has been devised for the simultaneous solution of these equations. The generalized flow-diagram for the routine is presented in Appendix B. Using the FORAST language, [5] the solution has been programmed for the ORDVAC and BRLESC computers.

Preliminary Routine

To reduce computation time and conserve memory space, a preliminary routine has been introduced. Here all data required for the computation are read into the computer, constant groupings (e.g.,

$$\frac{F_i C_i}{(\gamma_i - 1)\, T_{o_i}}, \quad \frac{F_i C_i}{(\gamma_i - 1)}, \quad \frac{C_i}{\rho_i}, \text{ etc.,}$$ are calculated and stored

for subsequent use, and data to permanently identify the computer run are printed out. A complete listing of required input data may be found in Appendix C.

Main Routine

The main computational routine is presented in the generalized flow-diagram of Appendix B. To follow the procedure, consider the three sequential phases of the problem:

Phase I - From time of ignition until the projectile starts to move.

Phase II - From time of initial projectile motion until all propellants are consumed.

Phase III - From time of propellant burnout until projectile leaves the gun muzzle.

At the time of ignition (Phase I begins), it is assumed that the igniter is completely burned ($z_I = 1$) and none of the other propellants have started to burn (all $z_i = 0$). The space-mean pressure, consisting only of the igniter pressure, is calculated from:

$$\bar{p} = p_I = \frac{F_I C_I}{V_c} \tag{42}$$

Equation (42) is derived from Equations (19) and (26) by means of the simplifying ignition assumptions stated above.

The linear burning rate for each propellant can now be determined from either Equation (30) or Equation (32) in combination with Equation (32a). If the interpolation indicated by use of Equation (30) is selected, the generalized interpolation sub-routine* is employed. The mass-fractions burned, z_i's, during a small time interval, dt, are determined by integration of Equation (29). The surface areas of the unburned propellant (see Appendix A) are used in this initial calculation. The Runga-Kutta method of numerical integration, as modified by Gill,[12] is commonly used for the solution of sets of ordinary differential equations and has been employed here.

Calculation of the temperature, T, from Equation (19) and the volume available for propellant gas, V_c, from Equation (22), will allow the calculation of the new space-mean pressure, $\bar{p}$, at time, dt, from Equation (26). The surface areas of the now partially burned propellants are computed from equations presented in Appendix A. All results of interest are printed-out at this time ** and these results used as initial conditions for calculations during

---

* See Reference (18) for interpolation by divided differences.

** See Appendix C for listing of output data.

the ensuing time-interval. Those terms in Equations (17), (19), and (22) which involve velocity or displacement are zero during this phase of the computation. This calculation-loop is continued until the space-mean pressure exceeds a pre-selected "shot-start" pressure and the projectile starts to move. Phase I, which has been arbitrarily defined, ends at this time.

Phase II requires the addition of the equations of motion to the sequence followed during Phase I. Equations (27), (39), (40), and (41) are used to calculate the values of the acceleration, velocity, and displacement of the projectile at the end of each time interval. Integration specified in Equations (40) and (41) is again performed by the Runga-Kutta-Gill method. Values of velocity and displacement are now available for use in terms of Equations (17), (19), and (22). To compute values for $E_{p_r} = A \int_0^x p_r \, dx$, which is one of the terms in Equation (19), the generalized interpolation sub-routine must be used to obtain p_r from the tabular information described by Equation (34a). This integration is performed by use of the Trapezoidal Rule.*

As time is increased by the addition of small time-intervals, calculations during Phase II are continued around this expanded loop with print-out of appropriate results at the end of each time interval. One at a time, the propellants are completely consumed and this phase is ended. A series of switches has been incorporated in the program to circumvent the necessity of introducing propellants in any special order. In fact, it may not always be possible to predict the exact order in which several different propellants will be burned out. The combination of the propellant switches and the start-of-motion switch makes it possible to handle problems where one or more propellants burn out before the projectile starts to move.

With all propellants consumed, Phase III begins. The mass-fractions burned have all become unity and the equations concerned with burning (Equations (29), (31), and (30) or (32)) are eliminated from the loop. As in the other phases,

* Although the Trapezoidal Rule is a relatively crude method for numerical integration, the accuracy of the p_r versus x data available does not warrant a more accurate and hence more complex method.

results are printed-out at the end of each time-interval. A continual check is made of the displacement of the projectile to determine whether or not it has reached the muzzle of the gun. When the projectile passes the muzzle, Phase III has ended and the program is stopped.

It is possible for the projectile to reach the muzzle (and the program stopped) before Phase II is completed. This would simulate a gun-firing in which unburned propellant is ejected from the muzzle. It is also possible for the program to simulate a firing in which the projectile becomes lodged in the tube. In this case, Phase III is not completed and the program is stopped when the projectile displacement does not increase.

At each time-interval after the beginning of Phase II, the breech pressure is determined from Equation (28) and printed out. This result is not used in the computational routine but is used to compare theoretical and experimental results. A continual check is made of the calculated pressures and the maximum breech pressure is stored with its associated time and projectile displacement. This information is printed-out at the end of the program. Calculations during the last time-interval result in a projectile displacement somewhat greater than the desired distance to the muzzle. A linear interpolation between results at the last two time-intervals is used to obtain results exactly at the muzzle. These results are also printed-out at the end of the program.

Options to Routine

A considerable number of options have been designed and coded for special problems. These include changes which enable the program to be used for guns, or gun-like weapons, which are not of conventional design (Figure 1) and changes which vary the treatment of some of the individual parameters. It is expected that the number of such options will increase as the program is used for a greater number and variety of problems.

Typical options for non-conventional guns are those for gun-boosted rockets, traveling-charge guns, and light-gas guns of the adiabatic compressor type. Examples of options for varied treatment of individual parameters are those for adjusted burning rates (previously mentioned), inhibited propellant surfaces, delayed propellant ignition, variable time-intervals, constant resistive pressure, and resistive pressure as a function of base pressure.

DISCUSSION

No attempt has been made here to present a new and different interior ballistic theory. The objective was to devise a convenient, flexible scheme for performing the tedious numerical calculations required to obtain detailed interior ballistic trajectories. The selection of a program for high-speed digital computers has made it possible to eliminate most of the simplifications of theory required to facilitate mathematical solutions by other methods.

The theory presented as the basis for the computer routine is well-known and has only been modified to account for composite charges. There are several problems present in all interior ballistic calculations and these also prove troublesome here. For example, useful propellant burning rates are not generally available. It is known that burning rates obtained from experimental firings in closed chambers are usually low. The results obtained from limited gun-firings by the authors [11] indicate gun burning rates may be twice closed chamber burning rates under certain conditions. As previously mentioned, optional methods of adjusting closed chamber burning rates have been provided for in this program. One such approach is to consider the burning rate to be a function of the projectile velocity (and possibly a function of the projectile displacement) in addition to its known dependence on pressure. This method results in the use of closed chamber burning rates when the gun chamber is practically a closed chamber (v and x are effectively zero). When the projectile is moving at higher velocities and is further down tube, reasonable increases in burning rates are obtained and used. Other equally important difficulties are associated with the determination of reasonable values for resistive pressure and shot-start pressure.

Considerable versatility has been built into the program. Instead of stopping the computation at the end of Phase III, a new problem can be automatically read into the computer and solved. This multiple-case feature can be employed to advantage for any number of additional problems during a single computer run.

Typical interior ballistic problems were used to compare results obtained from this computer routine with results from other interior ballistic schemes. (13), (14), and (15). The agreement was generally very good when the other

DISCUSSION

No attempt has been made here to present a new and different interior ballistic theory. The objective was to devise a convenient, flexible scheme for performing the tedious numerical calculations required to obtain detailed interior ballistic trajectories. The selection of a program for high-speed digital computers has made it possible to eliminate most of the simplifications of theory required to facilitate mathematical solutions by other methods.

The theory presented as the basis for the computer routine is well-known and has only been modified to account for composite charges. There are several problems present in all interior ballistic calculations and these also prove troublesome here. For example, useful propellant burning rates are not generally available. It is known that burning rates obtained from experimental firings in closed chambers are usually low. The results obtained from limited gun-firings by the authors (11) indicate gun burning rates may be twice closed chamber burning rates under certain conditions. As previously mentioned, optional methods of adjusting closed chamber burning rates have been provided for in this program. One such approach is to consider the burning rate to be a function of the projectile velocity (and possibly a function of the projectile displacement) in addition to its known dependence on pressure. This method results in the use of closed chamber burning rates when the gun chamber is practically a closed chamber (v and x are effectively zero). When the projectile is moving at higher velocities and is further down tube, reasonable increases in burning rates are obtained and used. Other equally important difficulties are associated with the determination of reasonable values for resistive pressure and shot-start pressure.

Considerable versatility has been built into the program. Instead of stopping the computation at the end of Phase III, a new problem can be automatically read into the computer and solved. This multiple-case feature can be employed to advantage for any number of additional problems during a single computer run.

Typical interior ballistic problems were used to compare results obtained from this computer routine with results from other interior ballistic schemes. (13), (14), and (15). The agreement was generally very good when the other

schemes were fairly sophisticated. In addition, detailed interior ballistic trajectories are produced in considerably less time than it takes to calculate maximum pressure and muzzle velocity by other systems. A typical computer solution for a conventional gun takes only 10 seconds if magnetic tape output is used with the BRLESC.

Results from computer simulations have also been compared to experimental data obtained from well-instrumented gun firings. To demonstrate the adequacy of the computer routine, data from a typical 105mm Howitzer firing were processed by the method described in Reference (11). In Appendix D these experimental results are compared with the predicted results obtained from a simulation of this firing.

Paul G. Baer

PAUL G. BAER

Jerome M. Frankle

JEROME M. FRANKLE

LIST OF REFERENCES

1. Corner, J. Theory of the Interior Ballistics of Guns. New York: John Wiley and Sons, Inc., 1950.

2. Hunt, F. R. W. Chairman, Editorial Panel. Internal Ballistics. New York: Philosophical Library, 1951.

3. Baer, Paul G., and Frankle, Jerome M. Digital Computer Simulation of the Interior Ballistic Performance of Guns. Ordnance Computer Research Report, VI, No. 2: 17-23, Aberdeen Proving Ground, Apr 1959.

4. Kempf, Karl, Historical Officer. Historical Monograph - Electronic Computers within the Ordnance Corps. Aberdeen Proving Ground, Nov 1961.

5. Campbell, Lloyd W., and Beck, Glenn A. The FORAST Programming Language for ORDVAC and BRLESC. Aberdeen Proving Ground: BRL R-1172, Aug 1962.

6. Vinti, John P., and Kravitz, Sidney. Tables for the Pidduck-Kent Special Solution for the Motion of the Powder Gas in a Gun. Aberdeen Proving Ground: BRL R-693, Jan 1949.

7. Love, A. E. H., and Pidduck, F. B. The Lagrange Ballistic Problem. Phil. Trans. Roy. Soc. 222: 167, London, 1923.

8. Kent, R. H. Some Special Solutions for the Motion of the Powder Gas. Physics, VII, No. 9: 319, 1936.

9. Frankle, Jerome M., and Hudson, James R. Propellant Surface Area Calculations for Interior Ballistic Systems. Aberdeen Proving Ground: BRL M-1187, Jan 1959.

10. Frankle, Jerome M. Special Interior Ballistic Tests of 115mm XM378 Slug Rounds. Aberdeen Proving Ground: BRL M-1266, May 1960 (Confidential).

11. Baer, Paul G., and Frankle, Jerome M. Reduction of Interior Ballistic Data from Artillery Weapons by High-Speed Digital Computer. Aberdeen Proving Ground: BRL M-1148, Jun 1958.

12. Gill, S. Runge-Kutta-Gill Numerical Procedure for Solving Systems of First Order Ordinary Differential Equations. Proceedings of the Cambridge Philosophical Society, 47, Part I: 96, Jan 1951.

13. Hitchcock, Henry P. Tables for Interior Ballistics. Aberdeen Proving Ground: BRL R-993, Sep 1956 and BRL TN-1298, Feb 1960.

14. Taylor, W. C., and Yagi, F. A Method for Computing Interior Ballistic Trajectories in Guns for Charges of Arbitrarily Varying Burning Surface. Aberdeen Proving Ground: BRL R-1125, Feb 1961.

15. Strittmater, R. C. A Single Chart System of Interior Ballistics. Aberdeen Proving Ground: BRL R-1126, Mar 1961.

16. Scarborough, James B. Numerical Mathematical Analysis. Baltimore: The Johns Hopkins Press, 2nd ed., 1950.

17. Baer, Paul G., and Bryson, Kenneth R. Tables of Computed Thermodynamic Properties of Military Gun Propellants. Aberdeen Proving Ground: BRL M-1338, Mar 1961.

18. Milne, William Edmund. Numerical Calculus. Princeton, New Jersey: Princeton University Press, 1949.

APPENDICES

A. FORM FUNCTION EQUATIONS

B. COMPUTATION ROUTINE

C. INPUT AND OUTPUT DATA

D. COMPARISON OF EXPERIMENTAL AND PREDICTED PERFORMANCE FOR TYPICAL 105MM HOWITZER FIRING

APPENDIX A

Form Function Equations

FORM FUNCTION EQUATIONS

Geometrical Equations

1. Initial Volume of a Propellant Grain

$$V_{g_i} = \frac{\pi}{4} \left(D_i^2 - N_i d_i^2\right) L \qquad \text{(A-1)}$$

where: V_{g_i} = volume of an unburned propellant grain, in.^{3}

D_i = outside diameter of grain, in.

N_i = number of perforations, dimensionless

d_i = diameter of perforation, in.

L_i = length of grain, in.

2. Volume of a Partially Burned Propellant Grain

$$V_{g_i}(1 - z_i) = \frac{\pi}{4} \left[(D_i - u_i)^2 - N_i (d_i + u_i)^2\right] (L_i - u_i) \qquad \text{(A-2)}$$

where: z_i = mass-fraction of i th propellant burned at a given time, dimensionless

u_i = two times the distance each surface has receded at a given time, in.

3. Initial Surface Area of a Propellant Grain

$$S_{g_i} = \pi \left[(D_i + N_i d_i)(L_i) + \frac{D_i^2 - N_i d_i^2}{2} \right] \qquad \text{(A-3)}$$

where: S_{g_i} = surface area of an unburned propellant grain, in.^{2}

4. Surface Area of a Partially Burned Propellant Grain

$$S_i = \pi \left\{ \left[(D_i - u_i) + N_i (d_i + u_i)\right]\left[L_i - u_i\right] + \frac{(D_i - u_i)^2}{2} - \frac{N_i (d_i + u_i)^2}{2} \right\} \qquad \text{(A-4)}$$

where: S_i = surface area of partially burned i th propellant grain at a given time, in.^{2}.

Equations for Newton-Raphson Method* for Finding Approximate Values of the Real Roots of a Numerical Equation

1. Rearrange Equation (A-2) to set $f(u_i) = 0$:

$$f(u_i) = \frac{\pi}{4} \left\{ (N_i - 1)\, u_i^3 - \left[L_i(N_i - 1) - 2(D_i + N_i d_i) \right] u_i^2 \right.$$

$$- \left[2L_i(D_i + N_i d_i) + (D_i^2 - N_i d_i^2) \right] u_i$$

$$\left. + L_i\, (D_i^2 - N_i d_i^2) \right\} - V_{g_i}\, (1 - z_i) \qquad \text{(A-5)}$$

2. Differentiate Equation (A-5) with respect to u_i:

$$f'(u_i) = \frac{d\left[f(u_i) \right]}{du_i} = \frac{\pi}{4} \left\{ 3(N_i - 1) u_i^2 \right.$$

$$- 2 \left[L_i(N_i - 1) - 2\,(D_i + N_i d_i) \right] u_i$$

$$\left. - \left[2L_i(D_i + N_i d_i) + (D_i^2 - N_i d_i^2) \right] \right\} \qquad \text{(A-6)}$$

3. The value of the root of Equation (A-2) is then:

$$u_{i+1} = u_i - \frac{f(u_i)}{f'(u_i)} \qquad \text{(A-7)}$$

where: u_{i+1} = the improved value of the root, where the first estimate of the root is u_i.

Procedure

1. For each propellant, determine z_i by integration of Equation (29). In the initial calculation of each z_i, Equation (A-3) is used to compute each S_i ($S_i = S_{g_i}$ when $u_i = 0$). For subsequent calculations of each z_i, Equation (A-4) is used with u_i determined as described below.

* See Reference (16) for a discussion of this method.

2. The z_i's obtained from Equation (29) are used to compute the u_i's from Equation (A-7) and then the new S_i's are computed from Equation (A-4). In the initial calculation of u_i, the first estimate of its value is zero.

Equation (A-7) is used to calculate the improved value, u_{i+1}. With u_{i+1} as the estimate, Equation (A-7) is used again to calculate a further-improved value, u_{i+2}. This procedure is continued until the improvement is less than 10^{-5} inch.

APPENDIX B

Computation Routine

1. Generalized Flow Diagram
2. FORAST Listing

INTERIOR BALLISTICS PROGRAM FOR GUNS

GENERALIZED FLOW DIAGRAM

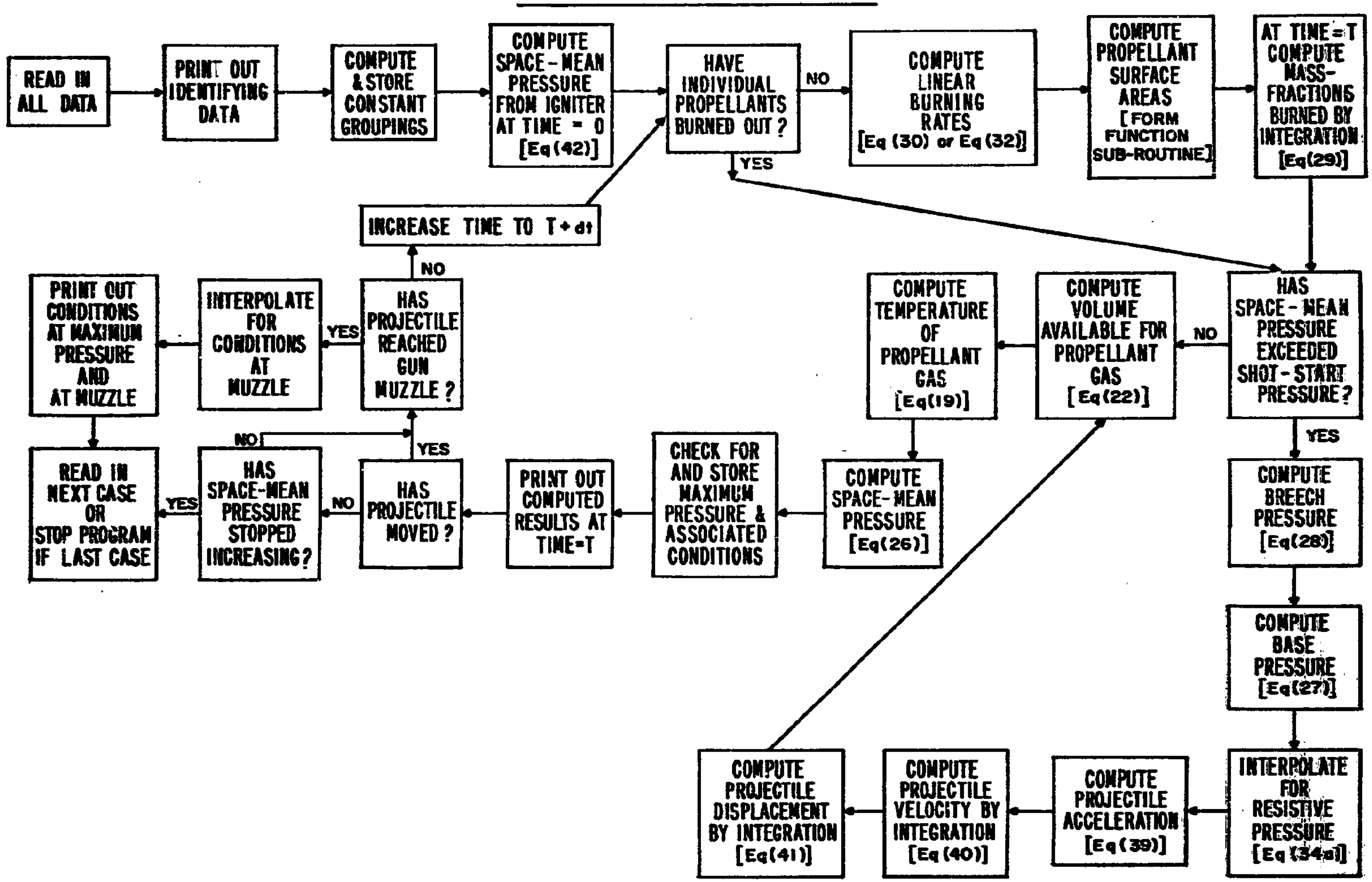

```
         PROB I 664MB  MULTI-GRAN GUN BALLISTICS
         BLOC(PR1-PR20)       AC1-AC5)K1-K7)Y1-Y7)T1-T5)U0-U5)S1-S5)R1-R5)    0003
         BLOC(BC1-BC5)CC1-CC5)DC1-DC5)EC1-EC5)GC1-GC5)IC1-IC5)JC1-JC5)FC1-FC5) 0004
         BLOC(Q1-Q7)C1-C5)F1-F5)GA1-GA5)COV1-COV5)TO1-TO5)RHO1-RHO5)BET1-BET5) 0005
         BLOC(DCZ1-DCZ5)AN1-AN104)                                           1 5
         CONTALP1-ALP5)D1-D5)(DP1-DP5)L1-L5)NP1-NP5)XC1-XC20)HC1-HC5)         0006
B1           ENTER(A,READ)AN1)13)%                                              7
             READ-FORMAT(01)-(WP)XM)VO)AP)PE)DEL)PPMAX)%                        8
             READ-FORMAT(01)-(CI)FI)GAI)TOI)%                                1008
             READ-FORMAT(01)-(DT)N1)KV)KX)D)EVP)% SET(J=0)%                     9
B1.1         READ-FORMAT(01)-(XC1,J)PR1,J)% COUNT(20)IN(J)GOTO(B1.1)%          10
             ENTER(INTEGER)N1)N)%SET( J=0)% INT(NCP=-2*N)%                   0011
B2           READ-FORMAT(01)-(C1,J)F1,J)GA1,J)COV1,J)TO1,J)RHO1,J)%            12
             READ-FORMAT(01)-(BET1,J)ALP1,J)D1,J)DP1,J)L1,J)NP1,J)%          1012
                        COUNT(,N)IN(J)GOTO(B2)%SET(J=0)%                     0013
B2.1         ENTER(A,PUNCH)AN1)1)% ENTER(A,PUNCH)AN89)1)%                      14
             ENTER(A,PUNCH)AN9)1)%                                             15
             PUNCH-FORMAT(02)-<1>(WP)XM)VO)AP)DEL)PF)PPMAX)<A>%                16
             ENTER(A,PUNCH)AN89)1)% ENTER(A,PUNCH)AN17)2)%                     17
             PUNCH-FORMAT(03)-<1>(CI)FI)GAI)TOI)<IGNITERA>%                  1017
B3           PUNCH-FORMAT(04)-<1>(C1,J)F1,J)GA1,J)COV1,J)TO1,J)RHO1,J)<A>%     18
             COUNT(,N)IN(J)GOTO(B3)% SET(J=0)% ENTER(A,PUNCH)AN89)1)%          19
             ENTER(A,PUNCH)AN33)1)%                                            20
B3.1         PUNCH-FORMAT(05)-<1>(BET1,J)ALP1,J)D1,J)DP1,J)L1,J)NP1,J)<A>%     21
             COUNT(,N)IN(J)GOTO(B3.1)% SET(J=0)% ENTER(A,PUNCH)AN89)1)%        22
             ENTER(A,PUNCH)AN41)2)%                                            23
B3.2         PUNCH-FORMAT(06)-<1>(XC1,J)PR1,J)<A>%                             24
             COUNT(20)IN(J)GOTO(B3.2)% SET(J=0)% ENTER(A,PUNCH)AN89)1)%        25
             ENTER(A,PUNCH)AN57)2)% SET(SWP=B18.1)JP=0)STUCK=B18.5)%           26
             PUNCH-FORMAT(07)-<1>(DT)N1)KV)KX)EVP)D)<A>%                       27
B4           BCI=FI*CI/(GAI-1)% ACI=BCI/TOI%CCI=FI*CI/TOI% EVM=EVP*12%       0035
B4.1         BC1,J=F1,J*C1,J/(GA1,J-1)% AC1,J=BC1,J/TO1,J% CC1,J=F1,J*C1,J/  0036
         CONTTO1,J%                                                          0037
             DC1,J=C1,J/RHO1,J% EC1,J=C1,J*COV1,J% FC1,J=NP1,J-1%            0038
             GC1,J=L1,J(NP1,J-1)-2(D1,J+NP1,J*DP1,J)%                        0039
             HC1,J=2*L1,J(D1,J+NP1,J*DP1,J)+(D1,J**2-NP1,J*DP1,J**2)%        0040
             IC1,J=L1,J(D1,J**2-NP1,J*DP1,J**2)%                             0041
             JC1,J=3.1416*IC1,J/4%COUNT(,N)IN(J)GOTO(B4.1)%SET(J=0)%         0042
B5           CT=0%TP1=0%                                                     0043
B5.1         TP1=C1,J*GA1,J+TP1% CT=C1,J+CT% COUNT(,N)IN(J)GOTO(B5.1)%       0044
             GAP=TP1/CT%SET(J=0)%GAF=GAP/(GAP-1)%EP=CT/WP%                   0045
             EP1=1+EP/DEL%TP1=1/(GAP-1)%TP2=1/((2*TP1+3)/DEL+(2*TP1+2)/EP)%  0046
             MCTD=WP*CT/DEL%TP4=0%AGW=AP*386.4/WP%                           0047
             EP2=EXP(GAF*LOG(1-TP2))% TP1=EXP(1.5*LOG(D))% TP2=EXP(2.175*LOG 0048
         CONT(D))%                                                           0049
             TP3=EXP(.8375*LOG(CT))%                                         0050
B5.2         TP4=C1,J*TO1,J+TP4% COUNT(,N)IN(J)GOTO(B5.2)% SET(J=0)%         0051
             HCL=(.38*12*TP1(XM+VO/AP)(TP4/CT-298))/((1+0.6*TP2/TP3)         0052
         CONTEVM**2)%                                                        0053
B6           CLEAR(7)NOS,AT(K1)% CLEAR(7)NOS,AT(Y1)% CLEAR(7)NOS,AT(Q1)%     0054
             PB=PR=PBR=XI=ALP=INIPR=0% T=DT%                                   55
             CLEAR(5)NOS,AT(U1)%  XLST=0%  PRLST=0%                          0056
B6.1         Y3,J=1.1% COUNT(5)IN(J)GOTO(B6.1)% SET(J=0)%                    0057
B6.2         Y3,J=0% COUNT(,N)IN(J)GOTO(B6.2)% SET(J=0)%                     0058
B7.1         IF-INT(N=1)GOTO(B7.5)%  SET(SW3=DR3.1)%                         0059
             IF-INT(N=2)GOTO(B7.6)%  SET(SW4=DR3.1)%                            6
             IF-INT(N=3)GOTO(B7.7)%  SET(SW5=DR3.1)%                         0061
             IF-INT(N=4)GOTO(B7.8)%  SET(SW6=DR3.1)% GOTO(B8)%               0062
```

```
B7.5     SET(SW3=B14)%GOTO(B8)%                                                    0063
B7.6     SET(SW4=B14)%GOTO(B8)%                                                    0064
B7.7     SET(SW5=B14)%GOTO(B8)%                                                    0065
B7.8     SET(SW6=B14)%GOTO(B8)%                                                    0066
B8       TP1=0%                                                                    0067
B8.1     TP1=DC1,J+TP1%  COUNT(,N)IN(J)GOTO(B8.1)%  SET(J=0)%                      0068
         PT=CI*FI/(V0-TP1)% SET(SW1=B15)SW8=B14.5)% PMAX=PT%                       0069
         ENTER(R,K,G,)DT)2,N)B9)Y1)K1)Q1)% GOTO(,SW1)%                             0070
B9       IF(Y3>=1)GOTO(B9.1)%SET(SW11=B10)J=0)%GOTO(DR1)%                          0071
B9.1     Y3=1%K3=0%S1=0%R1=0%U3=0%SET(SW11=B10)J=0)%GOTO(DR3.1)%                     72
B10      IF(Y4>=1)GOTO(B10.1)%SET(SW11=B11)J=1)%GOTO(DR1)%                         0073
B10.1    Y4=1%K4=0%S2=0%R2=0%U4=0%SET(SW11=B11)J=1)%GOTO(,SW3)%                      74
B11      IF(Y5>=1)GOTO(B11.1)%SET(SW11=B12)J=2)%GOTO(DR1)%                         0075
B11.1    Y5=1%K5=0%S3=0%R3=0%U5=0%SET(SW11=B12)J=2)%GOTO(,SW4)%                      76
B12      IF(Y6>=1)GOTO(B12.1)%SET(SW11=B13)J=3)%GOTO(DR1)%                         0077
B12.1    Y6=1%K6=0%S4=0%R4=0%U6=0%SET(SW11=B13)J=3)%GOTO(,SW5)%                      78
B13      IF(Y7>=1)GOTO(B13.1)%SET(SW11=B14)J=4)%GOTO(DR1)%                         0079
B13.1    Y7=1%K7=0%S5=0%R5=0%U7=0%SET(SW11=B14)J=4)%GOTO(,SW6)%                      80
B14      SET(J=0)%TP1=0%                                                           0081
B14.1    TP1=DC1,J(1-Y3,J)+EC1,J*Y3,J+TP1%COUNT(,N)IN(J)GOTO(B14.1)%               0082
         VC=V0+AP*XI-TP1%SET(J=0)%TP1=BCI%                                         0083
B14.2    TP1=BC1,J*Y3,J+TP1%COUNT(,N)IN(J)GOTO(B14.2)%                             0084
         SET(J=0)%TP2=ACI%                                                         0085
B14.3    TP2=AC1,J*Y3,J+TP2%COUNT(,N)IN(J)GOTO(B14.3)%                             0086
         SET(J=0)%TEMP=(TP1-ALP)/TP2%TP1=CCI%                                      0087
B14.4    TP1=CC1,J*Y3,J+TP1%COUNT(,N)IN(J)GOTO(B14.4)%                             0088
         SET(J=0)%PT=TEMP*TP1/VC%                            GOTO(,SW8)%           0089
B14.5    ENTER(P,K,GD)%                                                            0090
DR1      R1,J=BFT1,J*EXP(ALP1,J*LOG(PT))%U0=U1,J%H1=FC1,J%H2=GC1,J%                0092
         H3=HC1,J%H4=IC1,J%H5=JC1,J(1-Y3,J)%H6=L1,J%H7=D1,J%                       0093
         H8=DP1,J%H9=NP1,J%H10=DC1,J%H11=JC1,J%GOTO(GAM2)%                         0094
DR3      R1,J=R1,J+KV*K2+KX*XI%                                                    1094
         K3,J=S1,J*R1,J/DC1,J%                                                       95
DR3.1    GOTO(,SW11)%                                                              1095
DR4      PB=PT/EP1%PBR=PB/EP2%                                                     0096
         K1=AGW(PB-PH)%K2=Y1%XI=Y2%                                                0097
         IF(XI<XC20)GOTO(DR5)% PR=PR20% GOTO(DR9)%                                 0099
DR5      ENTER(D,D,IN)XI)PR)XC1)PR1)20)3)1)1)%                                     0100
DR9          DELX=XI-XLST%SUM1=PR+PRLST%                                           0098
         INTPR=(DELX*SUM1)/2+INTPR%XLST=XI%PRLST=PR%                               0099
         ALP=(MCTD*K2**2/772,8)+AP*INTPR+HCL*K2**2% GOTO(B14.5)%                   0100
B15      IF(PT<PE)GOTO(B15.1)% SET(SW8=DR4)SW1=B16)%                               0101
B15.1    PBR=PT% PB=PT%                                                            0102
B16      IF(Y1>0)GOTO(B17)%IF(Y3>=1)AND(Y4>=1)AND(Y5>=1)AND(Y6>=1)                  103
     CONTAND(Y7>=1)GOTO(B16.1)%GOTO(B17)%                                          1103
B16.1    SET(STUCK=B22)%                                                           2103
B17      XF=XI/12%V=Y1/12%AF=K1/12%SET(J=0)%ST=0%                                  0104
B17.1    DC71,J=K3,J*C1,J%COUNT(,N)IN(J)GOTO(B17.1)%SET(J=0)%                      0105
B17.2    ST=S1,J+ST%COUNT(,N)IN(J)GOTO(B17.2)%SET(J=0)%                            0106
         IF(PBR<PPMAX)GOTO(B17.3)% ENTER(A,PUNCH)AN73)1)% GOTO(NEWRN)%             1106
B17.3    IF(PMAX>PBR)GOTO(B18)% PMAX=PBR% XPMAX=XI% TPMAX=T%                        107
B18      GOTO(,SWP)%                                                                108
B18.1    ENTER(A,PUNCH)AN1)1)%                                                      109
B18.2    ENTER(A,PUNCH)AN89)1)% TM=T*1000%                                          110
         PUNCH-FORMAT(08)-<1>(TM)XI)PBR)PT)PB)V)AF )<A>%                            111
         PUNCH-FORMAT(09)-<1>(TM)XI)XF)TEMP)VC)PR)ST)<Δ>%                           112
B18.3    PUNCH-FORMAT(010)-<1>(TM)XI)Y3,J)DCZ1,J)R1,J)S1,J)<Δ>%                    1112
         COUNT(,N)IN(J)GOTO(B18.3)% SET(J=0)%                                      2112
```

```
          COUNT(15,NCP)IN(JP)GOTO(B18.4)% SET(SWP=B18.1)JP=0)GOTO(.STUCK)%  3112
B18.4     SET(SWP=B18.2)%GOTO(.STUCK)                                       4112
B18.5     T=T+DT%                                                            113
          IF(XI>XM)GOTO(B21)%XILST=XI%VLST=V%PBLST=PB%                      0114
          ENTER(R,K,G1)%                                                    0115
B21       VMAX=((XM-XILST)(V-VLST)/(XI-XILST))+VLST%                        0116
          PBMAX=((XM-XILST)(PB-PBLST)/(XI-XILST))+PBLST%                    0117
          TPMAX=TPMAX*1000%                                                 1117
          ENTER(A,PUNCH)AN89)1)% ENTER(A,PUNCH)AN81)1)%                      118
          PUNCH-FORMAT(O11)-<1>(VMAX)PMAX)XPMAX)TPMAX)PBMAX)<Δ>%             119
          GOTO(NEWRN)%                                                      1119
B22       ENTER(A,PUNCH)AN89)1)%ENTER(A,PUNCH)AN97)1)%ENTER(A,PUNCH)AN81)1)% 120
          VMAX=0%PBMAX=0%TPMAX=TPMAX*1000%                                   121
          PUNCH-FORMAT(O11)-<1>(VMAX)PMAX)XPMAX)TPMAX)PBMAX)<Δ>%             122
NEWRN     GOTO(B1)%                                                          123
GAM2      T1=H7-U0%T2=H8+U0                                                 0127
FF1.1     FU=.7854(U0**3+H1-U0**2*H2-U0*H3+H4)-H5%                          0128
FF2       FPU=.7854(3*U0**2*H1-2*U0*H2-H3)%                                 0129
FF2.1     U01=U0-FU/FPU%                                                    0130
FF3       IF-ABS((U01-U0)<=.00001)GOTO(FF4)%U0=U01%                         0131
FF3.1     GOTO(GAM2)%                                                       0132
FF4       SI=3.1416((H6-U0)(H7-U0+H9(H8+U0)))+.5*T1**2-.5*H9                0133
      CONT*T2**2)%S1,J=SI*H10/H11%U1,J=U0%GOTO(DR3)%                        0134
O1    FORM(10-10)1-7)                                                        132
O2    FORM(12-2-9)1-1)12-3-10)1-3)3-2)12-1-8)3-1)12-6-8)3-3)12-6-8-9)        133
O3    FORM(12-2-9)12-7-9)3-2)12-1-7)3-13)12-4-6-25)                          134
O4    FORM(12-2-9)12-7-9)3-2)12-1-7)3-4)12-2-7)3-2)12-4-6)3-4)12-0-8-20)     135
O5    FORM(12-9)3-1)12-6)3-4)12-6)3-4)12-6)3-4)12-1-7)3-5)12-1-3-23)         136
O6    FORM(3-20)12-3-8)3-11)12-5-7-32)                                       137
O7    FORM(12-7)3-5)12-1-3)3-4)12-9)3-1)12-9)3-5)12-4-6)3-5)12-1-7-17)       138
O8    FORM(12-2-8)3-1)12-3-8)3-2)12-6-10)12-6-10)12-6-10)12-5-9)3-1)         139
      CONT12-4-10-9)                                                        1139
O9    FORM(12-2-8)3-1)12-3-8)3-2)12-2-8)3-2)12-4-8)3-2)12-5-10)12-4-7)3-3)   140
      CONT12-5-9-10)                                                        1140
O10   FORM(12-2-8)3-1)12-3-8)3-2)12-1-7)3-3)12-4-9)3-1)12-3-8)3-2)12-5-9-20) 141
O11   FORM(12-5-8)3-5)12-6-8)3-4)12-3-8)3-2)12-2-7)3-3)12-6-9-24)            142
      END GOTO(B1)%                                                         0148
8                                  105 MM HOWITZER   RD 765                    Δ
1PROJ. WT.  BARREL   CHAMBER   BORE AREA    P-K    SS PRESS MAX GUN PRESSURE   Δ
1                                  M1 PROPELLANT                               Δ
1 CHARGE      FORCE      GAMMA     COVOLUME FLAME TEMP  DENSITY                Δ
1  BETA       ALPHA     O.D. GRAIN DIA. PERF GR.LENGTH NO. PERF.               Δ
1                                  RESISTANCE                                  Δ
1                     PROJ. TRAVEL            PRESSURE                         Δ
1                                  MISCELLANEOUS                               Δ
1   DI     NO. PROP.      KV          KX     EST. MUZ. VEL. DIAMETER           Δ
1                          P GREATER THAN DESIRED MAX PRESSURE                 Δ
1MUZZLE VEL. MAX. PRESSURE X AT PMAX T AT PMAX MUZ PRESSURE                    Δ
1                                                                              Δ
1                                  PROJECTILE STOPPED                          Δ
 33.        81.        153.        13.77       4600.      3.024      50000.    1
 .0429      1152000.   1.25        2000.                                       2
 1-03       2.         0           0           4.134      1500.                3
   .00      4500.                                                              4
   .10      4500.                                                              5
   .20      4500.                                                              6
   .35      4500.                                                              7
   .50      4500.                                                              8
```

1.00	4500.				
2.00	4500.				
3.50	4500.				
4.00	2800.				
4.25	2600.				
4.50	2350.				
5.00	1900.				
5.25	1650.				
5.50	1400.				
6.00	1000.				
10.00	1000.				
30.00	1000.				
40.00	1000.				
50.00	1000.				
60.00	1000.				
.0325	3670150.	1.264	31.08	2433.	.0567
.5079-03	.8497	.0478	.0194	.2453	1.
2.1356	3670150.	1.264	31.08	2433.	.0567
.5079-03	.8497	.1344	.0142	.3127	7.

PROB

APPENDIX C

Input and Output Data

1. Input Data
2. Output Data
3. Sample of Output Format

1. INPUT DATA

	Units	Program Symbol
Gun Constants		
Weight of Projectile	lb	WP
Length of Gun Tube	in.	XM
Empty Volume of Chamber	$in.^3$	VO
Cross-sectional Area of Bore	$in.^2$	AP
Shot-Start Pressure	psi	PE
Pidduck-Kent Constant	dimensionless	DEL
Resistive Pressures	psi	PR1,J
Travel of Projectile Corresponding to each of 20 Resistive Pressures	in.	XC1,J
Diameter of Bore	in.	D
Propellant Physical Constants		
Weights of Propellants	lb	C1,J
Weight of Igniter	lb	CI
Densities of Propellants	$lb/in.^3$	RHO1,J
Outside Diameter of Propellant Grains	in.	D1,J
Diameter of Propellant Perforations	in.	DP1,J
Length of Propellant Grains	in.	L1,J
Number of Perforations per Grain	dimensionless	NP1,J
Number of Propellants	dimensionless	N1
Propellant Thermodynamic Constants*		
Forces of Propellants	in.-lb/lb	F1,J
Force of Igniter	in.-lb/lb	FI

* See Reference (17) for these data.

	Units	Program Symbol
Ratios of Specific Heats of Propellants	dimensionless	GA1,J
Ratio of Specific Heats of Igniter	dimensionless	GAI
Covolumes of Propellants	$in.^3/lb$	COV1,J
Adiabatic Flame Temperatures of Propellants	^{o}K	TO1,J
Adiabatic Flame Temperature of Igniter	^{o}K	TOI
Burning Rate Coefficients	$\frac{in.}{sec} - \frac{1}{psi^{\alpha}}$	BET1,J
Burning Rate Exponents (α's)	dimensionless	ALP1,J
Burning Rate Velocity Coefficient	$\frac{in.}{sec\ in./sec}$	KV
Burning Rate Displacement Coefficient	$\frac{in.}{sec\text{-}in.}$	KX
<u>Miscellaneous Constants</u>		
Time Interval	sec	DT
Estimated Muzzle Velocity	ft /sec	EVP
Maximum Allowable Breech Pressure	psi	PPMAX

2. OUTPUT DATA

Identifying Data

The complete list of input data is printed out to permanently identify the computation.

	Units	Program Symbol
Trajectory Data		
Time	millisec	TM
Travel of Projectile	in.	XI
Travel of Projectile	ft	XF
Breech Pressure	psi	PBR
Space-mean Pressure	psi	PT
Base Pressure	psi	PB
Velocity of Projectile	ft/sec	V
Acceleration of Projectile	ft/sec^2	AF
Temperature of Propellant Gas	$^\circ$K	TEMP
Volume behind Projectile available for Propellant Gas	in.^{3}	VC
Resistive Pressure	psi	PR
Total Surface Area of Propellants	in.^{2}	ST
Mass-fractions of Propellants Burned	dimensionless	Y3,J
Mass Burning Rates of Propellants	lb/sec	DCZ1,J
Linear Burning Rates of Propellants	in./sec	R1,J
Surface Areas of Propellants	in.^{2}	S1,J

	Units	Program Symbol
Summary Data		
Muzzle Velocity	ft/sec	VMAX
Maximum Breech Pressure	psi	PMAX
Travel at Maximum Breech Pressure	in.	XPMAX
Time at Maximum Breech Pressure	sec	TPMAX
Muzzle Pressure (Base of Projectile)	psi	PBMAX

OUTPUT FORMAT

105 MM HOWITZER - RD 765

PROJ. WT.	BARREL	CHAMBER	BORE AREA	P-K	SS PRESS	MAX GUN PRESSURE
33.00000	81.00000	153.00000	13.77000	3.02400	4600.	50000.

M1 PROPELLANT

CHARGE	FORCE	GAMMA	COVOLUME	FLAME TEMP	DENSITY	
.04290	1152000.	1.2500		2000.		IGNITER
.63250	3670150.	1.2640	31.080	2433.	.056700	
2.13560	3670150.	1.2640	31.080	2433.	.056700	

BETA	ALPHA	O.D. GRAIN	DIA. PERF	GR.LENGTH	NO. PERF.
.0005079	.8497	.0478	.0194	.2453	1.
.0005079	.8497	.1344	.0142	.3127	7.

RESISTANCE

PROJ. TRAVEL	PRESSURE
.000	4500.
.100	4500.
.200	4500.
.350	4500.
.500	4500.
1.000	4500.
2.000	4500.
3.500	4500.
4.000	2800.
4.250	2600.
4.500	2350.
5.000	1900.
5.250	1650.
5.500	1400.
6.000	1000.
10.000	1000.
30.000	1000.
40.000	1000.
50.000	1000.
60.000	1000.

MISCELLANEOUS

DT	NO. PROP.	KV	KX	EST. MUZ. VEL.	DIAMETER
.00010	2.	.0000000	.0000000	1500.	4.1340

105 MM HOWITZER RD 765

*TM=.1000	XI=.000	PBR=559.30	PT=559.30	PB=559.30	V=.00	AF=.0000
TM=.1000	XI=.000	XF=.0000	TMA=2053.25	VC=104.147	PR=.0	ST=4018.93
TM=.1000	XI=.000	Y3=.0015	DCE1=9.601	R1=.102	S1=1661.83	
TM=.1000	XI=.000	Y4=.0006	DCE2=13.618	R2=.102	S2=2357.10	
.2000	.000	651.34	651.34	651.34	.00	.0000
.2000	.000	.0000	2097.81	104.112	.0	4019.58
.2000	.000	.0032	10.945	.116	1661.54	
.2000	.000	.0013	15.533	.116	2358.04	
.3000	.000	756.33	756.33	756.33	.00	.0000
.3000	.000	.0000	2137.31	104.072	.0	4020.31
.3000	.000	.0051	12.444	.132	1661.20	
.3000	.000	.0022	17.671	.132	2359.10	
.4000	.000	875.66	875.66	875.66	.00	.0000
.4000	.000	.0000	2172.18	104.026	.0	4021.14
.4000	.000	.0073	14.112	.150	1660.82	
.4000	.000	.0031	20.055	.150	2360.31	
.5000	.000	1010.97	1010.97	1010.97	.00	.0000
.5000	.000	.0000	2202.89	103.975	.0	4022.07
.5000	.000	.0098	15.963	.170	1660.39	
.5000	.000	.0041	22.706	.170	2361.68	
.6000	.000	1164.02	1164.02	1164.02	.00	.0000
.6000	.000	.0000	2229.89	103.917	.0	4023.13
.6000	.000	.0126	18.015	.191	1659.91	
.6000	.000	.0053	25.648	.191	2363.22	
.7000	.000	1336.74	1336.74	1336.74	.00	.0000
.7000	.000	.0000	2253.61	103.851	.0	4024.32
.7000	.000	.0158	20.283	.216	1659.36	
.7000	.000	.0066	28.907	.216	2364.96	
.8000	.000	1531.26	1531.26	1531.26	.00	.0000
.8000	.000	.0000	2274.43	103.777	.0	4025.66
.8000	.000	.0193	22.785	.242	1658.74	
.8000	.000	.0081	32.513	.242	2366.91	
.9000	.000	1749.89	1749.89	1749.89	.00	.0000
.9000	.000	.0000	2292.69	103.695	.0	4027.15
.9000	.000	.0233	25.542	.272	1658.05	
.9000	.000	.0098	36.496	.272	2369.10	
1.0000	.000	1995.16	1995.16	1995.16	.00	.0000
1.0000	.000	.0000	2308.72	103.602	.0	4028.83
1.0000	.000	.0278	28.574	.304	1657.28	
1.0000	.000	.0117	40.889	.304	2371.55	
1.1000	.000	2269.85	2269.85	2269.85	.00	.0000
1.1000	.000	.0000	2322.79	103.499	.0	4030.70
1.1000	.000	.0328	31.903	.340	1656.42	
1.1000	.000	.0138	45.729	.340	2374.28	

*See list of Output Data for Program Symbols and Units.

105 MM HOWITZER - RD 765

1.2000	.000	2577.01	2577.01	2577.01	.00	.0000
1.2000	.000	.0000	2335.15	103.383	.0	4032.78
1.2000	.000	.0363	35.552	.379	1655.46	
1.2000	.000	.0162	51.055	.379	2377.32	
1.3000	.000	2919.97	2919.97	2919.97	.00	.0000
1.3000	.000	.0000	2346.02	103.255	.0	4035.09
1.3000	.000	.0445	39.548	.422	1654.38	
1.3000	.000	.0188	56.911	.422	2380.70	
1.4000	.000	3302.38	3302.38	3302.38	.00	.0000
1.4000	.000	.0000	2355.58	103.112	.0	4037.66
1.4000	.000	.0514	43.918	.469	1653.19	
1.4000	.000	.0217	63.344	.469	2384.46	
1.5000	.000	3728.28	3728.28	3728.28	.00	.0000
1.5000	.000	.0000	2364.00	102.953	.0	4040.50
1.5000	.000	.0590	48.690	.520	1651.87	
1.5000	.000	.0250	70.407	.520	2388.62	
1.6000	.000	4202.09	4202.09	4202.09	.00	.0000
1.6000	.000	.0000	2371.43	102.777	.0	4043.64
1.6000	.000	.0674	53.898	.576	1650.41	
1.6000	.000	.0286	78.156	.576	2393.23	
1.7000	.000	4728.68	4728.68	4728.68	.00	.0000
1.7000	.000	.0000	2377.98	102.582	.0	4047.11
1.7000	.000	.0767	59.574	.637	1648.79	
1.7000	.000	.0326	86.655	.637	2398.32	
1.8000	.000	5384.73	5312.49	5169.10	1.49	8990.2031
1.8000	.000	.0000	2383.69	102.382	4500.0	4050.93
1.8000	.000	.0870	65.753	.704	1647.00	
1.8000	.000	.0371	95.972	.704	2403.93	
1.9000	.004	6040.79	5959.75	5798.89	2.77	17452.175
1.9000	.004	.0003	2388.72	102.162	4500.0	4055.14
1.9000	.004	.0983	72.457	.777	1645.03	
1.9000	.004	.0420	106.156	.777	2410.11	
2.0000	.009	6765.89	6675.12	6494.96	4.94	26804.618
2.0000	.009	.0007	2393.04	101.946	4500.0	4059.76
2.0000	.009	.1108	79.730	.856	1642.85	
2.0000	.009	.0474	117.296	.856	2416.91	
2.1000	.016	7565.33	7463.83	7262.38	8.08	37115.875
2.1000	.016	.0014	2396.65	101.739	4500.0	4064.83
2.1000	.016	.1245	87.594	.942	1640.46	
2.1000	.016	.0534	129.452	.942	2424.37	
2.2000	.028	8444.01	8330.73	8105.88	12.30	48449.250
2.2000	.028	.0024	2399.56	101.556	4500.0	4070.38
2.2000	.028	.1395	96.069	1.035	1637.83	
2.2000	.028	.0600	142.686	1.035	2432.55	

105 MM HOWITZER RD 765

2.3000	.046	9406.19	9280.00	9029.53	17.70	60859.566
2.3000	.046	.0039	2401.74	101.410	4500.0	4076.44
2.3000	.046	.1560	105.169	1.134	1634.94	
2.3000	.046	.0672	157.052	1.134	2441.50	
2,4000	.071	10455,21	10314,94	10036,54	24,38	74389,969
2.4000	.071	,0059	2403.13	101,320	4500.0	4083.05
2.4000	.071	.1740	114.896	1.242	1631,78	
2.4000	.071	.0752	172.598	1.242	2451,28	
2,5000	,105	11593,13	11437,59	11128,89	32,46	89066,992
2.5000	.105	.0088	2403.70	101.304	4500.0	4090.24
2.5000	.105	.1936	125.241	1.357	1628.32	
2.5000	.105	.0840	189.356	1,357	2461,92	
2.6000	.150	12820.27	12648.27	12316.89	42,05	104894.83
2.6000	.150	.0125	2403.38	101.383	4500.0	4098.04
2,6000	.150	,2150	136,177	1,478	1624,55	
2.6000	.150	.0936	207.338	1.478	2473.48	
2.7000	.207	14134.69	13945.06	13568.68	53.20	121848.41
2.7000	.207	.0172	2402.12	101.579	4500.0	4106.47
2,7000	,207	,2382	147.660	1,607	1620,45	
2.7000	.207	.1041	220.532	1.607	2486.01	
2.8000	.278	15531.68	15323.30	14919.72	66.19	139866.91
2.8000	.278	.0232	2399.83	101.916	4500.0	4115.55
2.8000	.278	.2633	159.622	1.742	1616.01	
2.8000	.278	.1155	246.895	1.742	2499.55	
2.9000	.366	17003.23	16775.11	16322.35	80.93	156847.23
2.9000	.366	.0305	2396.46	102.421	4500.0	4125.31
2,9000	.366	.2904	171.973	1,882	1611.19	
2.9000	.366	.1280	268.348	1.882	2514.12	
3.0000	.473	18537.60	18288.95	17795.33	97.58	178638.52
3.0000	.473	.0394	2391.94	103.123	4500.0	4135.75
3.0000	.473	.3196	184.593	2.027	1606.01	
3.0000	.473	.1415	290.767	2.027	2529.75	
3.1000	.601	20119.30	19849.37	19313.63	116.20	199038.66
3.1000	.601	.0501	2386.20	104.059	4500.0	4146.87
3.1000	.601	.3568	197.338	2.175	1600.43	
3.1000	.601	.1561	313.984	2.175	2546.44	
3.2000	.753	21728.45	21436.93	20858.35	136.82	219793.76
3.2000	.753	.0628	2379.19	105.235	4500.0	4158.66
3.2000	.753	.3840	210.040	2.323	1594.47	
3.2000	.753	.1719	337.780	2.323	2564.18	
3.3000	.931	23341.69	23028.53	22406.98	159.46	240601.50
3.3000	.931	.0776	2370.87	106.710	4500.0	4171.09
3.3000	.931	.4193	222.506	2.471	1588.12	
3.3000	.931	.1888	361.890	2.471	2582.96	

~~105 MM HOWITZER - RD 765~~

3.4000	1.137	24932.43	24597.93	23934.03	184.10	261119.19
3.4000	1.137	.0947	2361.21	108.510	4500.0	4184.12
3.4000	1.137	.4566	234.532	2.616	1581.39	
3.4000	1.137	.2068	386.006	2.616	2602.74	
3.5000	1.373	26471.99	26116.83	25411.94	210.69	280976.61
3.5000	1.373	.1144	2350.23	110.667	4500.0	4197.72
3.5000	1.373	.4958	245.905	2.755	1574.29	
3.5000	1.373	.2260	409.784	2.755	2623.44	
3.6000	1.643	27930.86	27556.13	26812.39	239.13	299793.28
3.6000	1.643	.1369	2337.93	113.217	4500.0	4211.82
3.6000	1.643	.5367	256.417	2.886	1566.83	
3.6000	1.643	.2464	432.862	2.886	2644.99	
3.7000	1.948	29280.32	28887.48	28107.81	269.31	317198.79
3.7000	1.948	.1625	2324.36	116.192	4500.0	4226.35
3.7000	1.948	.5792	265.874	3.008	1559.05	
3.7000	1.948	.2678	454.872	3.008	2667.31	
3.8000	2.290	30494.10	30084.98	29272.98	301.06	332854.33
3.8000	2.290	.1908	2309.60	119.625	4500.0	4241.23
3.8000	2.290	.6232	274.108	3.117	1550.97	
3.8000	2.290	.2902	475.458	3.117	2690.26	
3.9000	2.671	31549.96	31126.67	30286.56	334.20	346472.95
3.9000	2.671	.2226	2293.75	123.545	4500.0	4256.38
3.9000	2.671	.6683	280.985	3.212	1542.63	
3.9000	2.671	.3135	494.300	3.212	2713.75	
4.0000	3.092	32430.96	31995.85	31132.28	368.50	357836.18
4.0000	3.092	.2577	2276.91	127.981	4500.0	4271.70
4.0000	3.092	.7144	286.417	3.293	1534.07	
4.0000	3.092	.3377	511.126	3.293	2737.63	
4.1000	3.555	33126.32	32081.88	31799.80	403.76	366805.04
4.1000	3.555	.2963	2259.23	132.956	4353.8	4287.10
4.1000	3.555	.7612	290.358	3.357	1525.33	
4.1000	3.555	.3626	525.726	3.357	2761.77	
4.2000	4.061	33634.57	33183.32	32287.70	440.69	385840.09
4.2000	4.061	.3364	2241.04	138.493	2710.8	4302.49
4.2000	4.061	.8085	292.834	3.406	1516.45	
4.2000	4.061	.3882	538.002	3.406	2786.05	
4.3000	4.614	33945.68	33490.25	32586.35	479.72	403930.04
4.3000	4.614	.3845	2221.95	144.626	2241.9	4317.80
4.3000	4.614	.8561	293.805	3.437	1507.47	
4.3000	4.614	.4142	547.733	3.437	2810.33	
4.4000	5.213	34063.00	33605.99	32698.97	519.69	412771.20
4.4000	5.213	.4344	2202.25	151.390	1688.0	4332.93
4.4000	5.213	.9036	293.326	3.452	1498.44	
4.4000	5.213	.4406	554.862	3.452	2834.49	

105 MM HOWITZER RD 765

4.5000	5.861	33997.55	33541.42	32636.14	560.46	420082.51
4.5000	5.861	.4884	2182.08	158.810	1097.9	4347.82
4.5000	5.861	.9569	291.497	3.452	1489.41	
4.5000	5.861	.4673	559.430	3.452	2858.42	
4.6000	6.558	33762.85	33309.87	32410.84	601.73	423888.90
4.6000	6.558	.5465	2161.52	166.904	658.5	4362.40
4.6000	6.558	.9977	288.442	3.436	1480.40	
4.6000	6.558	.4941	561.529	3.436	2882.00	
4.7000	7.305	32683.86	32245.30	31375.00	642.69	414921.60
4.7000	7.305	.6087	2135.99	176.078	374.8	2904.82
4.7000	7.305	1.0000	.000	.000	.00	
4.7000	7.305	.5206	556.704	3.380	2904.82	
4.8000	8.100	31546.35	31123.11	30283.16	682.55	402787.92
4.8000	8.100	.6750	2110.52	185.947	290.7	2926.94
4.8000	8.100	1.0000	.000	.000	.00	
4.8000	8.100	.5469	544.755	3.283	2926.94	
4.9000	8.942	30382.32	29974.70	29165.68	720.95	387359.05
4.9000	8.942	.7452	2085.45	196.490	446.6	2948.17
4.9000	8.942	1.0000	.000	.000	.00	
4.9000	8.942	.5724	531.861	3.182	2948.17	
5.0000	9.829	29211.65	28819.72	28041.87	757.55	368342.90
5.0000	9.829	.8191	2060.93	207.686	883.7	2968.51
5.0000	9.829	1.0000	.000	.000	.00	
5.0000	9.829	.5973	518.326	3.086	2968.51	
5.1000	10.759	28052.88	27676.52	26929.53	792.17	348393.83
5.1000	10.759	.8966	2037.15	219.504	1000.0	2987.98
5.1000	10.759	1.0000	.000	.000	.00	
5.1000	10.759	.6215	504.441	2.977	2987.98	
5.2000	11.729	26920.30	26559.13	25842.29	825.32	333785.59
5.2000	11.729	.9774	2014.27	231.916	1000.0	3006.61
5.2000	11.729	1.0000	.000	.000	.00	
5.2000	11.729	.6451	490.446	2.877	3006.61	
5.3000	12.739	25820.59	25474.17	24786.62	857.08	319601.38
5.3000	12.739	1.0616	1992.15	244.894	1000.0	3024.42
5.3000	12.739	1.0000	.000	.000	.00	
5.3000	12.739	.6679	476.475	2.779	3024.42	
5.4000	13.785	24760.24	24428.04	23768.73	887.50	305924.79
5.4000	13.785	1.1488	1970.86	258.417	1000.0	3041.46
5.4000	13.785	1.0000	.000	.000	.00	
5.4000	13.785	.6901	462.663	2.683	3041.46	
5.5000	14.868	23745.17	23424.62	22792.39	916.62	292806.55
5.5000	14.868	1.2390	1950.39	272.461	1000.0	3057.75
5.5000	14.868	1.0000	.000	.000	.00	
5.5000	14.868	.7117	449.108	2.590	3057.75	

105 MM HOWITZER RD 765

5.6000	15.985	22771.60	22466.08	21859.72	944.52	280275.03
5.6000	15.985	1.3320	1930.73	287.005	1000.0	3073.33
5.6000	15.985	1.0000	.000	.000	.00	
5.6000	15.985	.7326	435.883	2.501	3073.33	
5.7000	17.134	21840.41	21553.31	20971.58	971.23	268341.81
5.7000	17.134	1.4278	1911.87	302.027	1000.0	3088.25
5.7000	17.134	1.0000	.000	.000	.00	
5.7000	17.134	.7529	423.041	2.416	3088.25	
5.8000	18.315	20967.52	20686.21	20127.89	996.83	257005.85
5.8000	18.315	1.5262	1893.78	317.509	1000.0	3102.53
5.8000	18.315	1.0000	.000	.000	.00	
5.8000	18.315	.7725	410.617	2.334	3102.53	
5.9000	19.526	20134.15	19864.02	19327.89	1021.37	246256.84
5.9000	19.526	1.6271	1876.45	332.431	1000.0	3116.21
5.9000	19.526	1.0000	.000	.000	.00	
5.9000	19.526	.7936	398.631	2.256	3116.21	
6.0000	20.766	19344.97	19085.43	18570.31	1044.89	236077.89
6.0000	20.766	1.7305	1859.83	349.774	1000.0	3129.33
6.0000	20.766	1.0000	.000	.000	.00	
6.0000	20.766	.8102	387.697	2.182	3129.33	
6.1000	22.033	18598.33	18348.81	17853.57	1067.47	226447.66
6.1000	22.033	1.8361	1843.90	366.521	1000.0	3141.92
6.1000	22.033	1.0000	.000	.000	.00	
6.1000	22.033	.8282	376.015	2.111	3141.92	
6.2000	23.327	17892.36	17652.31	17175.87	1089.14	217341.96
6.2000	23.327	1.9439	1828.63	383.657	1000.0	3154.01
6.2000	23.327	1.0000	.000	.000	.00	
6.2000	23.327	.8456	365.384	2.043	3154.01	
6.3000	24.646	17225.06	16993.96	16535.29	1109.95	208735.00
6.3000	24.646	2.0539	1813.99	401.165	1000.0	3165.63
6.3000	24.646	1.0000	.000	.000	.00	
6.3000	24.646	.8626	355.196	1.979	3165.63	
6.4000	25.990	16594.37	16371.73	15929.86	1129.96	200600.28
6.4000	25.990	2.1659	1799.94	419.030	1000.0	3176.79
6.4000	25.990	1.0000	.000	.000	.00	
6.4000	25.990	.8791	345.439	1.918	3176.79	
6.5000	27.358	15998.23	15783.60	15357.60	1149.21	192911.28
6.5000	27.358	2.2798	1786.45	437.239	1000.0	3187.54
6.5000	27.358	1.0000	.000	.000	.00	
6.5000	27.358	.8952	336.099	1.860	3187.54	
6.6000	28.748	15434.64	15227.56	14816.57	1167.73	185641.93
6.6000	28.748	2.3957	1773.51	455.779	1000.0	3197.89
6.6000	28.748	1.0000	.000	.000	.00	
6.6000	28.748	.9168	327.163	1.804	3197.89	

105 MM HOWITZER RD 765

6.7000	30.160	14901.62	14701.69	14304.89	1185.57	178766.96
6.7000	30.160	2.5133	1761.07	474.637	1000.0	3207.87
6.7000	30.160	1.0000	.000	.000	.00	
6.7000	30.160	.9260	318.613	1.752	3207.87	
6.8000	31.593	14397.30	14204.14	13820.77	1202.76	172262.16
6.8000	31.593	2.6327	1749.12	493.801	1000.0	3217.50
6.8000	31.593	1.0000	.000	.000	.00	
6.8000	31.593	.9408	310.434	1.702	3217.50	
6.9000	33.046	13919.88	13733.13	13362.47	1219.34	166104.36
6.9000	33.046	2.7539	1737.63	513.260	1000.0	3226.79
6.9000	33.046	1.0000	.000	.000	.00	
6.9000	33.046	.9552	302.608	1.654	3226.79	
7.0000	34.519	13467.67	13286.98	12928.37	1235.34	160271.72
7.0000	34.519	2.8766	1726.57	533.003	1000.0	3235.76
7.0000	34.519	1.0000	.000	.000	.00	
7.0000	34.519	.9693	295.119	1.609	3235.76	
7.1000	36.011	13039.07	12864.14	12516.93	1250.79	154743.60
7.1000	36.011	3.0009	1715.92	553.021	1000.0	3244.44
7.1000	36.011	1.0000	.000	.000	.00	
7.1000	36.011	.9830	287.950	1.565	3244.44	
7.2000	37.521	12632.58	12463.10	12126.72	1265.71	149500.65
7.2000	37.521	3.1267	1705.66	573.304	1000.0	3252.83
7.2000	37.521	1.0000	.000	.000	.00	
7.2000	37.521	.9964	281.086	1.524	3252.83	
7.3000	39.048	12113.37	11950.85	11628.29	1280.08	142803.69
7.3000	39.048	3.2540	1690.38	594.117	1000.0	.00
7.3000	39.048	1.0000	.000	.000	.00	
7.3000	39.048	1.0000	.000	.000	.00	
7.4000	40.592	11581.18	11425.80	11117.42	1293.77	135939.51
7.4000	40.592	3.3827	1673.65	615.268	1000.0	.00
7.4000	40.592	1.0000	.000	.000	.00	
7.4000	40.592	1.0000	.000	.000	.00	
7.5000	42.153	11084.23	10935.52	10640.37	1306.80	129529.70
7.5000	42.153	3.5127	1657.49	636.645	1000.0	.00
7.5000	42.153	1.0000	.000	.000	.00	
7.5000	42.153	1.0000	.000	.000	.00	
7.6000	43.728	10619.56	10477.09	10194.31	1319.24	123536.40
7.6000	43.728	3.6440	1641.86	658.238	1000.0	.00
7.6000	43.728	1.0000	.000	.000	.00	
7.6000	43.728	1.0000	.000	.000	.00	
7.7000	45.319	10184.55	10047.91	9776.72	1331.10	117925.56
7.7000	45.319	3.7766	1626.75	680.036	1000.0	.00
7.7000	45.319	1.0000	.000	.000	.00	
7.7000	45.319	1.0000	.000	.000	.00	

~~105 MM HOWITZER   RD 765~~

7.8000	46.923	9776.80	9645.63	9385.29	1342.44	112666.32
7.8000	46.923	3.9102	1612.13	702.030	1000.0	.00
7.8000	46.923	1.0000	.000	.000	.00	
7.8000	46.923	1.0000	.000	.000	.00	
7.9000	48.540	9394.13	9268.10	9017.95	1353.28	107730.66
7.9000	48.540	4.0450	1597.98	724.211	1000.0	.00
7.9000	48.540	1.0000	.000	.000	.00	
7.9000	48.540	1.0000	.000	.000	.00	
8.0000	50.170	9034.59	8913.38	8672.80	1363.65	103093.19
8.0000	50.170	4.1809	1584.27	746.572	1000.0	.00
8.0000	50.170	1.0000	.000	.000	.00	
8.0000	50.170	1.0000	.000	.000	.00	
8.1000	51.813	8696.37	8579.69	8348.13	1373.58	98730.794
8.1000	51.813	4.3177	1570.98	769.104	1000.0	.00
8.1000	51.813	1.0000	.000	.000	.00	
8.1000	51.813	1.0000	.000	.000	.00	
8.2000	53.467	8377.85	8265.45	8042.35	1383.09	94622.489
8.2000	53.467	4.4558	1558.10	791.800	1000.0	.00
8.2000	53.467	1.0000	.000	.000	.00	
8.2000	53.467	1.0000	.000	.000	.00	
8.3000	55.132	8077.55	7969.18	7754.09	1392.22	90749.161
8.3000	55.132	4.5943	1545.61	814.654	1000.0	.00
8.3000	55.132	1.0000	.000	.000	.00	
8.3000	55.132	1.0000	.000	.000	.00	
8.4000	56.808	7794.12	7689.55	7482.01	1400.98	87093.400
8.4000	56.808	4.7340	1533.49	837.658	1000.0	.00
8.4000	56.808	1.0000	.000	.000	.00	
8.4000	56.808	1.0000	.000	.000	.00	
8.5000	58.494	7526.32	7425.34	7224.93	1409.39	83639.325
8.5000	58.494	4.8745	1521.73	860.807	1000.0	.00
8.5000	58.494	1.0000	.000	.000	.00	
8.5000	58.494	1.0000	.000	.000	.00	
8.6000	60.190	7273.04	7175.46	6981.79	1417.47	80372.437
8.6000	60.190	5.0159	1510.30	884.096	1000.0	.00
8.6000	60.190	1.0000	.000	.000	.00	
8.6000	60.190	1.0000	.000	.000	.00	
8.7000	61.896	7033.24	6938.88	6751.60	1425.23	77279.479
8.7000	61.896	5.1580	1499.19	907.517	1000.0	.00
8.7000	61.896	1.0000	.000	.000	.00	
8.7000	61.896	1.0000	.000	.000	.00	
8.8000	63.611	6805.98	6714.67	6533.44	1432.71	74348.324
8.8000	63.611	5.3009	1488.40	931.067	1000.0	.00
8.8000	63.611	1.0000	.000	.000	.00	
8.8000	63.611	1.0000	.000	.000	.00	

105 MM HOWITZER RD 765

8.9000	65.334	6590.41	6501.97	6326.50	1439.90	71567.857
8.9000	65.334	5.4445	1477.90	954.741	1000.0	.00
8.9000	65.334	1.0000	.000	.000	.00	
8.9000	65.334	1.0000	.000	.000	.00	
9.0000	67.066	6385.73	6300.06	6130.62	1446.83	68927.685
9.0000	67.066	5.5889	1467.69	978.533	1000.0	.00
9.0000	67.066	1.0000	.000	.000	.00	
9.0000	67.066	1.0000	.000	.000	.00	
9.1000	68.807	6191.22	6108.16	5943.30	1453.50	66419.046
9.1000	68.807	5.7339	1457.75	1002.440	1000.0	.00
9.1000	68.807	1.0000	.000	.000	.00	
9.1000	68.807	1.0000	.000	.000	.00	
9.2000	70.555	6006.21	5925.63	5765.69	1459.94	64032.734
9.2000	70.555	5.8796	1448.07	1026.457	1000.0	.00
9.2000	70.555	1.0000	.000	.000	.00	
9.2000	70.555	1.0000	.000	.000	.00	
9.3000	72.310	5830.08	5751.86	5596.62	1466.14	61761.028
9.3000	72.310	6.0259	1438.64	1050.581	1000.0	.00
9.3000	72.310	1.0000	.000	.000	.00	
9.3000	72.310	1.0000	.000	.000	.00	
9.4000	74.073	5662.27	5586.31	5435.53	1472.13	59596.629
9.4000	74.073	6.1728	1429.45	1074.807	1000.0	.00
9.4000	74.073	1.0000	.000	.000	.00	
9.4000	74.073	1.0000	.000	.000	.00	
9.5000	75.843	5502.27	5428.44	5281.93	1477.91	57532.803
9.5000	75.843	6.3203	1420.49	1099.132	1000.0	.00
9.5000	75.843	1.0000	.000	.000	.00	
9.5000	75.843	1.0000	.000	.000	.00	
9.6000	77.620	5349.57	5277.80	5135.35	1483.49	55563.332
9.6000	77.620	6.4683	1411.76	1123.553	1000.0	.00
9.6000	77.620	1.0000	.000	.000	.00	
9.6000	77.620	1.0000	.000	.000	.00	
9.7000	79.404	5203.75	5133.93	4995.37	1488.89	53682.469
9.7000	79.404	6.6170	1403.24	1148.066	1000.0	.00
9.7000	79.404	1.0000	.000	.000	.00	
9.7000	79.404	1.0000	.000	.000	.00	
9.8000	81.193	5064.38	4996.43	4861.58	1494.10	51884.892
9.8000	81.193	6.7661	1394.92	1172.668	1000.0	.00
9.8000	81.193	1.0000	.000	.000	.00	
9.8000	81.193	1.0000	.000	.000	.00	

MUZZLE VEL.	MAX. PRESSURE	X AT PMAX	T AT PMAX	MUZ PRESSURE
1493.5	34063.	5.213	4.400	4876.0

APPENDIX D

Comparison of Experimental and Predicted Performance for Typical 105mm Howitzer Firing

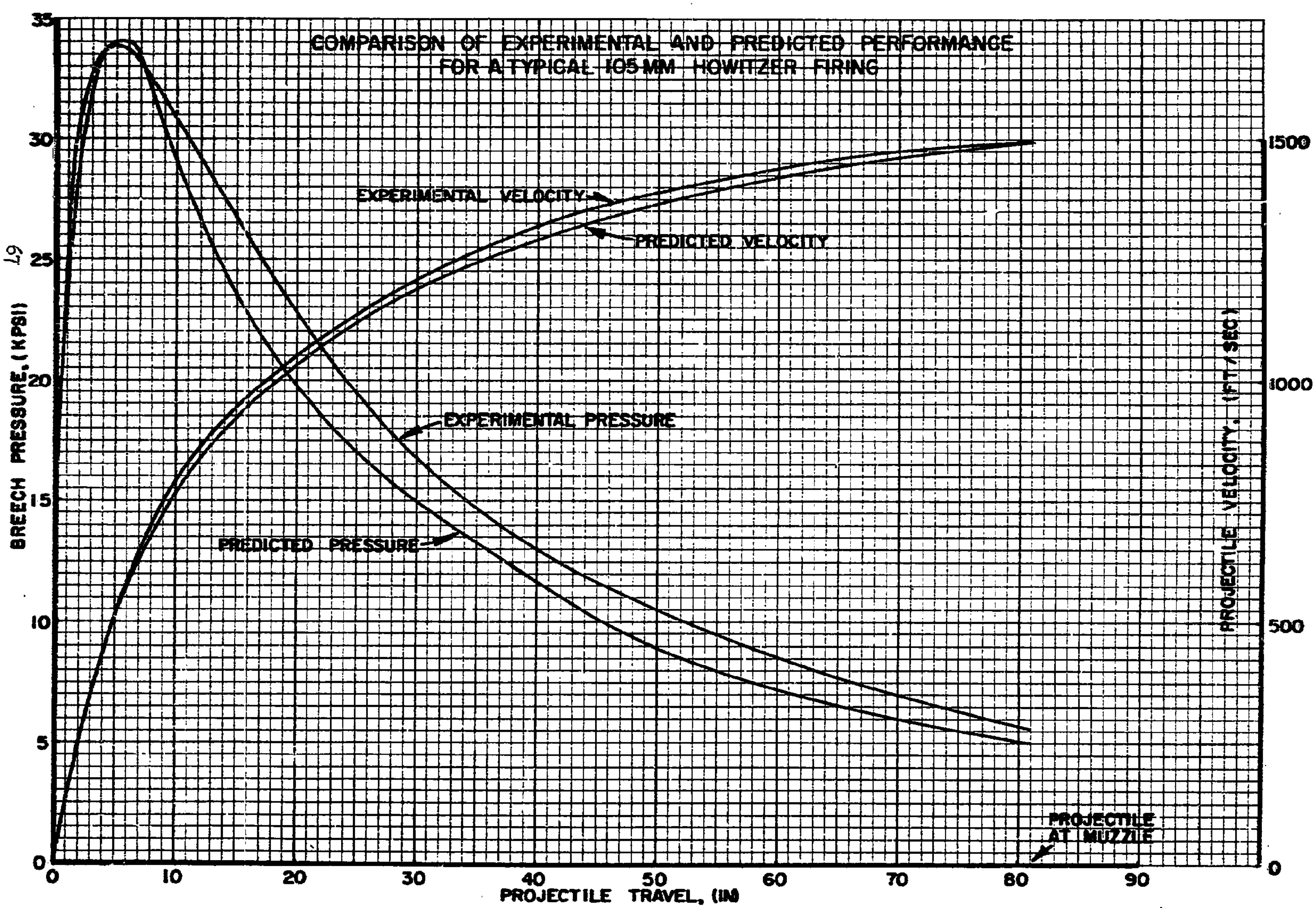
COMPARISON OF EXPERIMENTAL AND PREDICTED PERFORMANCE
FOR A TYPICAL 105 MM HOWITZER FIRING
BREECH PRESSURE, (KPSI)
PROJECTILE VELOCITY, (FT / SEC)
PROJECTILE TRAVEL, (IN)
EXPERIMENTAL VELOCITY
PREDICTED VELOCITY
EXPERIMENTAL PRESSURE
PREDICTED PRESSURE
PROJECTILE AT MUZZLE
0
5
10
15
20
25
30
35
500
1000
1500
40
50
60
70
80
90

DISTRIBUTION LIST

No. of Copies	Organization
10	Commander Armed Services Technical Information Agency ATTN: TIPCR Arlington Hall Station Arlington 12, Virginia
1	Commanding General U. S. Army Materiel Command ATTN: Mr. G. E. Stetson, AMCRD-RS-PE-Bal Research and Development Directorate Washington 25, D. C.
1	Commanding General U. S. Army Materiel Command ATTN: Mr. Stanley Swipp, AMCRD-DE-MI Research & Development Directorate Washington 25, D. C.
1	Commanding Officer Harry Diamond Laboratories ATTN: Technical Information Office, Branch 012 Washington 25, D. C.
1	Commanding General Frankford Arsenal ATTN: Propellant and Explosives Section, 1331 Philadelphia 37, Pennsylvania
1	Commanding Officer Army Research Office (Durham) Box CM, Duke Station Durham, North Carolina
3	Commanding Officer Picatinny Arsenal ATTN: Feltman Research and Engineering Laboratory Mr. Sidney Kravitz Dover, New Jersey
5	Redstone Scientific Information Center ATTN: Chief, Document Section U. S. Army Missile Command Redstone Arsenal, Alabama
1	Commanding General U. S. Army Ammunition Command ATTN: ORDLY-AREL, Engr Library Joliet, Illinois
3	Chief, Bureau of Naval Weapons ATTN: RMMP-2 RMMP-331 RRE-6 Department of the Navy Washington 25, D. C.
2	Commanding Officer U. S. Naval Propellant Plant ATTN: Technical Library Indianhead, Maryland
1	Commander U. S. Naval Weapons Laboratory ATTN: Technical Library Dahlgren, Virginia
2	Commander U. S. Naval Ordnance Laboratory ATTN: Library White Oak Silver Spring 19, Maryland
2	Commander U. S. Naval Ordnance Test Station ATTN: Technical Library Branch China Lake, California
1	Director U. S. Naval Research Laboratory ATTN: Mr. Walter Atkins Washington 20, D. C.
1	Director Special Projects Office Department of the Navy Washington 25, D. C.

DISTRIBUTION LIST

No. of Copies	Organization
1	Chief of Naval Operations ATTN: Op03EG Department of the Navy Washington 25, D. C.
1	U. S. Naval Ordnance Plant ATTN: K. L. Brown, Librarian Engineering Dept Louisville, Kentucky
1	Commander Air Proving Ground Center ATTN: PGAPI Eglin Air Force Base, Florida
2	U. S. Department of the Interior Bureau of Mines ATTN: M. M. Dolinar, Reports Librarian Explosives Research Lab 4800 Forbes Avenue Pittsburgh 13, Pennsylvania
1	National Aeronautics and Space Administration ATTN: Office of Technical Information & Educational Programs, Code ETL Washington 25, D. C.
2	Scientific and Technical Information Facility ATTN: NASA Representative P. O. Box 5700 Bethesda, Maryland
1	National Aeronautics and Space Administration Lewis Research Center ATTN: Library 21000 Brookpark Road Cleveland 35, Ohio
1	National Aeronautics and Space Administration Langley Research Center ATTN: Library Langley Air Force Center, Virginia
1	National Aeronautics and Space Administration Goddard Space Flight Center ATTN: Library Greenbelt, Maryland
1	National Aeronautics and Space Administration George C. Marshall Space Flight Center ATTN: Library Huntsville, Alabama
1	National Aeronautics and Space Administration Manned Spacecraft Center ATTN: Library P. O. Box 1537 Houston 1, Texas
2	Aerojet-General Corporation ATTN: Librarian P. O. Box 296 Azusa, California
1	American Machine and Foundry Company ATTN: Phil Rosenberg Mechanics Research Department 7501 North Natchez Avenue Niles 48, Illinois
1	Arthur D. Little, Inc. ATTN: W. H. Varley 15 Acorn Park Cambridge 40, Massachusetts

DISTRIBUTION LIST

No. of Copies	Organization
2	Armour Research Foundation of Illinois Institute of Technology Technology Center ATTN: Fluid Dynamics & Propulsion Research, Department D Chicago 16, Illinois
2	Atlantic Research Corporation Shirley Highway & Edsall Road Alexandria, Virginia
1	The Franklin Institute ATTN: Miss Marion H. Johnson, Librarian Technical Reports Library 20th and Parkway Philadelphia 3, Pennsylvania
1	Hercules Powder Company ATTN: Technical Information Division Research Center, Dr. Herman Skoinik 910 Market Street Wilmington 99, Delaware
1	Hercules Powder Company Allegheny Ballistics Laboratory ATTN: Library P. O. Box 210 Cumberland, Maryland
1	Jet Propulsion Laboratory ATTN: I. E. Newlan Chief, Reports Group 4800 Oak Grove Drive Pasadena 3, California
1	Minneapolis-Honeywell Regulator Company ATTN: Mr. Robert Gartner Ordnance Division Hopkins, Minnesota
1	Midwest Research Institute ATTN: Librarian 425 Volker Boulevard Kansas City 10, Missouri
3	Solid Propellant Information Agency Applied Physics Laboratory The Johns Hopkins University Silver Spring, Maryland
10	The Scientific Information Officer Defence Research Staff British Embassy 3100 Massachusetts Avenue, N. W. Washington 8, D. C.
4	Defence Research Member Canadian Joint Staff 2450 Massachusetts Avenue Washington 8, D. C.

AD Accession No. UNCLASSIFIED

Ballistic Research Laboratories, APG
THE SIMULATION OF INTERIOR BALLISTIC PERFORMANCE OF GUNS BY DIGITAL COMPUTER PROGRAM
Paul G. Baer and Jerome M. Frankle

Interior ballistics - Mathematical Analysis
Guns - Interior ballistics

BRL Report No. 1183 December 1962

RDT & E Project No. 1M010501A004
UNCLASSIFIED Report

When non-conventional guns are to be considered or when detailed design information is required, interior ballistic calculations become more difficult and time-consuming. To deal with these problems, the equations which describe the interior ballistic performance of guns and gun-like weapons have been programmed for the high-speed digital computers available at the Ballistic Research Laboratories. The major innovation contained in the equations derived in this report is the provision for use of propellant charges made up of several propellants of different chemical compositions and different granulations. Results obtained by the method described in this report compare favorably with those of other interior ballistic systems. In addition, considerably more detail is obtained in far less time. A comparison with experimental data from well-instrumented gun-firings is also presented to demonstrate the validity of this method of computation.

AD Accession No. UNCLASSIFIED

Ballistic Research Laboratories, APG
THE SIMULATION OF INTERIOR BALLISTIC PERFORMANCE OF GUNS BY DIGITAL COMPUTER PROGRAM
Paul G. Baer and Jerome M. Frankle

Interior ballistics - Mathematical Analysis
Guns - Interior ballistics

BRL Report No. 1183 December 1962

RDT & E Project No. 1M010501A004
UNCLASSIFIED Report

When non-conventional guns are to be considered or when detailed design information is required, interior ballistic calculations become more difficult and time-consuming. To deal with these problems, the equations which describe the interior ballistic performance of guns and gun-like weapons have been programmed for the high-speed digital computers available at the Ballistic Research Laboratories. The major innovation contained in the equations derived in this report is the provision for use of propellant charges made up of several propellants of different chemical compositions and different granulations. Results obtained by the method described in this report compare favorably with those of other interior ballistic systems. In addition, considerably more detail is obtained in far less time. A comparison with experimental data from well-instrumented gun-firings is also presented to demonstrate the validity of this method of computation.

AD Accession No. UNCLASSIFIED

Ballistic Research Laboratories, APG
THE SIMULATION OF INTERIOR BALLISTIC PERFORMANCE OF GUNS BY DIGITAL COMPUTER PROGRAM
Paul G. Baer and Jerome M. Frankle

Interior ballistics - Mathematical Analysis
Guns - Interior ballistics

BRL Report No. 1183 December 1962

RDT & E Project No. 1M010501A004
UNCLASSIFIED Report

When non-conventional guns are to be considered or when detailed design information is required, interior ballistic calculations become more difficult and time-consuming. To deal with these problems, the equations which describe the interior ballistic performance of guns and gun-like weapons have been programmed for the high-speed digital computers available at the Ballistic Research Laboratories. The major innovation contained in the equations derived in this report is the provision for use of propellant charges made up of several propellants of different chemical compositions and different granulations. Results obtained by the method described in this report compare favorably with those of other interior ballistic systems. In addition, considerably more detail is obtained in far less time. A comparison with experimental data from well-instrumented gun-firings is also presented to demonstrate the validity of this method of computation.

AD Accession No. UNCLASSIFIED

Ballistic Research Laboratories, APG
THE SIMULATION OF INTERIOR BALLISTIC PERFORMANCE OF GUNS BY DIGITAL COMPUTER PROGRAM
Paul G. Baer and Jerome M. Frankle

Interior ballistics - Mathematical Analysis
Guns - Interior ballistics

BRL Report No. 1183 December 1962

RDT & E Project No. 1M010501A004
UNCLASSIFIED Report

When non-conventional guns are to be considered or when detailed design information is required, interior ballistic calculations become more difficult and time-consuming. To deal with these problems, the equations which describe the interior ballistic performance of guns and gun-like weapons have been programmed for the high-speed digital computers available at the Ballistic Research Laboratories. The major innovation contained in the equations derived in this report is the provision for use of propellant charges made up of several propellants of different chemical compositions and different granulations. Results obtained by the method described in this report compare favorably with those of other interior ballistic systems. In addition, considerably more detail is obtained in far less time. A comparison with experimental data from well-instrumented gun-firings is also presented to demonstrate the validity of this method of computation.